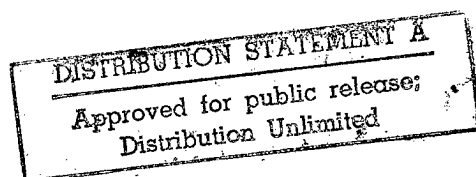FOREIGN
BROADCAST
INFORMATION
SERVICE

# JPRS Report

# Science & Technology

## Central Eurasia: Physics & Mathematics

19971229 058

DTIC QUALITY INSPECTED 2

# Science & Technology
## Central Eurasia: Physics & Mathematics

CONTENTS

## ACOUSTICS

## CRYSTALS, LASER GLASSES, SEMICONDUCTORS

## HIGH-TEMPERATURE PHYSICS

# LASERS

# MAGNETOHYDRODYNAMICS

# OPTICS, SPECTROSCOPY

## PLASMA PHYSICS

## THEORETICAL PHYSICS

## NUMERICAL ANALYSIS, ALGORITHMS

# CONTROL THEORY

# DIFFERENTIAL EQUATIONS

## Vibration Sensitivity of Rod Armored Piezoelectric Transducers

[Article by B. P. Belov, State Marine Technical University, St. Petersburg; UDC 534.83]

[Abstract] This article determines the sensitivity of armored transducers at working frequencies to vibrations, as well as the dependence of the latter on parameters of the elements of a reversible transducer, its means of attachment, and the electric load of the transducer in reception mode. The vibrations of the mechanical system of a transducer armored on one side is examined. The equations which are presented make it possible to calculate the vibration sensitivity of a transducer and provide a basis for the selection of a means of attaching the transducer to the structure of an antenna device depending on the level of vibration and the impedance properties of the surport. Analysis of various attachment schemes shows that for all examined schemes, by selecting the electric load and parameters one can obtain near minimal vibration sensitivity in the fasteners. Figures 4; reference: 1 Russian.

## Spatial Image Filtering in Ultrasonic Visualization of Large Inhomogeneities

[Article by Ye. L. Borodina, N. V. Gorskaya, S. M. Gorskiy, V. A. Zverev, T. A. Krayeva, G. N. Nikolayev, A. I. Khilko, V. N. Shirokov, Institute of Applied Physics, Russian Academy of Sciences; UDC 534.2]

[Abstract] Usually ultrasonic imaging uses the backscattered acoustic field to create an image. In the case examined here, the inhomogeneity has large wave dimensions, and the field is mainly scattered forward, so the inhomogeneity must be between the transmitter and receiver. However, the incoming initial signal can create a large disruptive background. This article studies the possibility of using spatial filtering to suppress the direct illumination of the background. One may obtain a 10-20 dB improvement in the signal to noise ratio using spatial filtering. The effective reconstruction of acoustic images depends on the amount of apriori information and the completeness of measured values of the scattered field. Numerical and model experiments were used to study this technique. Reconstruction of the parameters of inhomogeneities was studied in a nonstationary medium and under the effects of waveguide propagation. Figures 6; references 6: 5 Russian, 1 Western.

## Noise Resistance of Multipole Acoustic Receivers

[Article by A. T. Gavrilin, A. I. Grechikhin, N. I. Lobachevskiy, Nizhegorod State University; UDC 621.319]

[Abstract] Very simple three-dimensional receiving configurations are synthesized from point elementary pressure receivers which have rapidly falling dependences of the output signal on the distance to the source in all directions. There are three correct third- and fourth-order configurations: in the form of a tetrahedron, an octahedron with a central element, and a cube without a central element. These configurations are studied using statistical modeling of noise resistance to remote sources. It is shown that the advantages of third- and fourth-order receivers are realized only at very low error levels or relatively large wave dimensions of receivers. Consequently, the receiver without the central element is preferable if one considers nonideal receiving channels and errors in element location. Figures 2; table 1; references 5: 4 Russian, 1 Western.

## Excitation of a Modified Lamb Surface Wave in the Atmosphere by An Underwater Source

[Article by L. A. Gasilova, I. Yu. Gordeyeva, Yu. V. Petukhov, Institute of Applied Physics, Russian Academy of Sciences; UDC 551.596.1]

[Abstract] The effect of gravity in a compressible liquid (leading to the generation of a surface hydrodynamic wave) on the dispersion properties of a modified Lamb surface wave are studied, as well as the frequency dependence of its excitation coefficient for a point underwater mass source. The modified Lamb surface wave propagates along the interface between an isothermic atmosphere and a "heavy" compressible fluid with a density and sound velocity which is constant over depth. It is found that a resonant frequency appears equal to the ratio of gravitational acceleration to the speed of sound in air. At this frequency there is a narrow resonant maximum in the excitation coefficients of a modified Lamb wave. The frequency dependence of its phase speed intersects a similar dependence for a surface hydrohdynamic wave. The resonant frequency corresponds to the intersection of these frequency dependences. The modified Lamb surface wave propagates with a supersonic speed only for frequencies below critical and above resonant; below the resonant frequency this wave propagates at a subsonic speed (compared to air). Figures 2; references: 4 Russian.

## Modeling of Optimal Spatial Signal Processing in Underwater Sound Channels

[Article by Ye. Yu. Gorodetskaya, A. I. Malekhanov, V. I. Talanov, Institute of Applied Physics, Russian Academy of Sciences; UDC 621.372.8:621.391.26]

[Abstract] This article numerically and analytically studies the problem of optimization of spatial processing of partially coherent multi-mode signals in the horizontal plane of an underwater sound channel using a linear antenna grid. Optimization of processing is defined as maximizing the signal to noise ratio. A method for determining the

orthogonal base of amplitude-phase distribution in mode space is used to analyze the effectiveness of linear and quadratic signal processing in a field of isotropic noise depending on the number of antenna elements, the scale of intermode correlations, and mutual orthogonality of modes at the receiving aperture. It is found that apriori informaiton on the propagation of signals (mode structure and orders of intermode correlation) are fundamentally important in the analysis of the potential of processing algorithms and estimates of the effect of different "mismatching" effects of a reference mode with real fields. When one switches to vertical apertures, additional opportunities appear in connection with optimization of the placement of antenna grid elements in the region of the strongest or most correlated signal modes. Estimates are made of the maximum coefficient of amplification of processing which may be obtained when a receiving antenna is used in specific signal to noise situations which occur in oceanic waveguides. Figures 5; table 1; references: 8 Russian.

## Active Minimization of Acoustic Fields in Layered-Inhomogeneous Waveguides

[Article by G. V. Alekseyev and Ye. G. Komarov, Applied Mathematics Institute, Far Eastern Department, Russian Academy of Sciences; UDC 534.532:517.9]

[Abstract] The theory of problems in control of acoustic fields in a free space and in waveguides has continued to develop; active minimization of an acoustic field is an important representative of this class of problems. Since the total attenuation of sound by means of a discrete array is not always possible, instead of total field attenuation some researchers, such as S. J. Elliott, et al. (J. MES. THEOR. APPL., 6. Special Issue, pp 39-98, 1987), have begun to examine the problem of attenuation or minimization of noise, but using an approach based on the ideas of optimum control theory for solution of the latter problem. This approach was used in this study for solving the problem of minimizing the acoustic field formed by a noise-generating object in a layered-inhomogeneous axisymmetric waveguide simulating the ocean. A numerical algorithm is written for solving this problem which is based on the quadratic optimization method and methods for the regularization of unstable problems. The computational aspects of its application on a computer and the results of numerical experiments for suppressing the sound of a vertical array are given. The effectiveness of the method is illustrated in test examples from marine acoustics. Figures 4; references 15: 13 Russian, 2 Western.

## Increase in Longitudinal Resolution of Acoustic Systems for Visualization of Inhomogeneities With Extrapolation of Echo Pulse Spectra

[Article by Ye. G. Bazulin, EkhoTest Company; UDC 534.8+620]

[Abstract] The use of broadband converters makes it possible to obtain images of scatterers with a high longitudinal resolution. Another method for increasing resolution is the mathematical processing of the registered pulses for the purpose of broadening their spectrum by using the extrapolation of functions method for extrapolating the spectra of echo signals scattered by inhomogeneities. The presented materials demonstrate the possibility of applying the Gershberg-Papoulis algorithm for extrapolating the spectra of echo signals dispersed by inhomogeneities. The use of pulses processed in this way for obtaining and retrieving multifrequency digital holograms in a broader frequency band will make it possible to increase the longitudinal resolution of the images of models of point and extended scatterers. An increase in the spectral width of the echo pulses as a result of extrapolation results in improvement in both the longitudinal and transverse resolution of the images of scatterers in a case if the central frequency value increases. This algorithm also may be useful for increasing the longitudinal resolution of visualization systems using traditional echo monitoring methods. Figures 3; references 16: 11 Russian, 5 Western.

## Generation of Stonely-Scholte-Lamb Atmospheric Surface Wave by Acoustic Source Situated in Oceanic Waveguide

[Article by L. A. Gasilova, I. Yu. Gordeyeva and Yu. V. Petukhov, Applied Physics Institute, Russian Academy of Sciences; UDC 531.596.1]

[Abstract] This study is a continuation and generalization of earlier research (Yu. V. Petukhov, et al., AKUST. ZHURN., Vol 37, No 2, pp 405-407, 1991) and is devoted to the dispersion properties and frequency dependencies of the coefficients of generation of surface waves whose existence is possible in a more complex isothermic atmosphere system: a homogeneous layer of compressible fluid lying on a homogeneous elastic half-space, simulating the oceanic waveguide. Such a system describes the physical properties of low-frequency disturbances propagating both in the atmosphere and ocean more adequately than models proposed earlier. Specifically, a study was made of the dispersion properties of a modified Stonely-Scholte-Lamb surface wave propagating along the isothermic atmosphere-oceanic waveguide interface simulated by a layer of a homogeneous compressible fluid lying on a homogeneous elastic half-space and determined by the frequency dependence of its excitation coefficients for disturbances of pressure and velocity of medium particles in the atmosphere for the case of an underwater point source of mass. It is shown that this wave exists only at frequencies below a definite critical frequency, decreasing with an increase in the depth of the water layer, and is propagated at a supersonic (relative to the air) velocity above and at a subsonic velocity below a definite frequency (decreasing with an increase in water layer depth). Figures 4; references 7: 5 Russian, 2 Western.

## Theory of Acoustic Field Invariants in Layered Waveguides

[Article by G. A. Grachev, Hydrophysical Measurements Scientific Research Institute; UDC 551.463.21]

[Abstract] The tangents of the slopes of the lines of a constant level of sound intensity (invariants) of a multi-modal field in relative coordinate systems are determined independently of one another. There also is no unified theory making it possible to explain either the essence of already known invariants or the principal directions for further research. An attempt was therefore made to combine these invariants, $\beta$ and $\gamma$, into a single functional dependence with the eigenvalues of the Helmholtz equation and illustrate the possibility of their use for an analysis of the phase structure of the acoustic field in layered waveguides. A system of differential equations is derived showing that the existence of the known acoustic field invariants in layered waveguides is a corollary of the power-law dependence of the difference in eigenvalues of the Helmholtz equation $\Delta_{lm}$ on frequency and the waveguide variable acoustic parameter. The tangent of the slope of the lines of constant values of sound intensity, the rate of phase change along the waveguide and the group lag in the space-frequency region, is equal to the inverse value of the exponent of the $\Delta_{lm}$ frequency dependence, but in the region of the variable waveguide parameter (frequency) it is equal to the product of the acoustic parameter exponent and the space-frequency invariant. Figure 1; references 10: 7 Russian, 3 Western.

## Acoustic Fields of Spheroidal Scatterers and Emitters in Plane Waveguide

[Article by G. A. Grinblat, A. A. Kleshchev and K. V. Smirnov, St. Petersburg Marine Engineering University; UDC 534.26]

[Abstract] In AKUST. ZHURN., Vol 20, No 3, pp 470-473, 1974, A. A. Kleshchev, et al. postulated that for directional sources or scatterers situated in a stratified medium or plane waveguide the coefficients of excitation of normal modes of a point source must be further multiplied by the corresponding values of the system directivity characteristic. A study was undertaken to check this hypothesis by computing the acoustic field of a piston system situated in a plane waveguide. The vertical distribution of acoustic pressure from such a source (f = 800 Hz) was computed at a distance 500 m by the imaginary sources method and the normal waves method and applying this hypothesis. The results of computations by the two methods revealed a satisfactory consistency of the methods and confirmed the validity of the proposed hypothesis. A possibility therefore has appeared for supplementing the results of computations of the near acoustic fields of spheroidal scatterers and emitters by the imaginary sources method with the vertical and angular distributions of these same systems, but now over greater distances. The approach applied is fully explained in a recent monograph by one of the authors of this article (A. A. Kleshchev, GIDROAKUSTICHESKIYE RASSEIVATELI (Hydroacoustic Scatterers), St. Petersburg, Sudostroyeniye, 1992). This is illustrated in a specific example. Figures 4; references 13: 12 Russian, 1 Western.

## Model of Development of Acoustic Emission as Randomization of Transient Processes in Coupled Nonlinear Oscillators

[Article by V. V. Krylov, P. S. Landa and V. A. Robsman, Moscow State University imeni M. V. Lomonosov; UDC 534.222]

[Abstract] The irreversible processes involved in the failure of materials are accompanied by characteristic pulsed acoustic radiation known as acoustic emission. Growing cracks themselves are the sources of the acoustic emission signals. This article gives the results of theoretical and experimental research on the behavior of a crack as a resonator emitting pulses of acoustic emission in a jump-like growth process. Such a resonance behavior of an expanding crack is determined to a considerable degree by surface waves propagating along its sides. A crack can therefore be regarded as an acoustic resonator excited at the moment of growth at its vertex. In the spectra of acoustic emission signals transformations were observed in the form of the appearance of high-frequency harmonics and subharmonics and combination frequency components. The final stage in the development of acoustic emission was characterized by a transition to a broadband noise spectrum. These facts make it possible to postulate that in the acoustic emission phenomenon bifurcations occur similar to the bifurcations arising in the generation of dynamic chaos. Such a hypothesis served as a basis for a mathematical model of development of acoustic emission in the form of a system of related nonlinear oscillators, each of which corresponds to an individual crack. The bifurcation parameter used was the initial displacement in some one of the interacting cracks. The computed spectra, as the results of computer simulation, indicated a qualitative agreement with the evolution of spectra obtained by the processing of data from physical experiments. Figures 6; references: 6 Russian.

## Computing Acoustic Field in Coastal Region of Ocean With Complex Bottom Relief

[Article by A. N. Nekrasov, Acoustics Institute imeni N. N. Andreyev, Russian Academy of Sciences; UDC 534.231.1]

[Abstract] Procedures for computing the acoustic field in the ocean have been poorly developed, the principal difficulty being that a great volume of computations is required in order to determine the sound field. When using the ray method an enormous number of rays must emanate from the source within the limits of a given range of angles of departure in order for the adjacent rays to be of the identical type. In some cases the required density of the fan of rays is 100 rays per degree in both azimuthal and vertical angles. Millions of rays are required for studying a large water area. However, in not all cases is it necessary to compute the sound field for the entire investigated area. With a small number of detectors it is theoretically possible to simplify the problem using a priori information on the angles of departure from those rays which pass in the neighborhood of the detectors, although in actual practice this is extremely difficult to accomplish. In one case, for example, the problem can be considerably simplified. It is assumed that the source and a vertical series of detectors running from the bottom to the surface are positioned in a coastal wedge; the sound propagation path forms a relatively small angle with the general direction of the isobaths and therefore the three-dimensionality of the problem is expressed particularly strongly. The bottom relief in the wedge may be highly dissected and must be approximated by a smooth function of horizontal coordinates. The speed of sound is dependent only on depth z and there are no maxima along z. The series of detectors is continuous (there is a detector at each point on the segment). It is shown that with the proposed positioning of the detectors in a limited spatial region there is a considerable gain in computation speed. Examples of the computations are given. Figures 5; references 4: 3 Russian, 1 Western.

## Acoustic Characteristics of Water-Air Foam

[Article by Z. M. Orenbakh and G. A. Shushkov, Problems in Exploitation of North Institute, Russian Academy of Sciences; UDC 532.529:534.19:541.182.45]

[Abstract] The apparatus used in experimental study of the acoustic characteristics of liquid foam is illustrated by a block diagram (with 16 components identified) and described. With delivery of compressed air into the high-pressure chamber of a shock tube a diaphragm is ruptured and a pressure disturbance of finite duration, whose amplitude and configuration are determined by the volume of the high-pressure chamber, material and thickness of the diaphragm, is propagated through a low-pressure chamber. The low-pressure chamber is fabricated of plastic; it is a channel of square cross section in which there are six piezoelectric transducers spaced 0.05 m apart. The distance from the diaphragm to the first transducer and from the last transducer to the bottom of the chamber is more than 1 m and therefore reflected waves are not registered. The signals are fed through a six-channel commutator to an analog-to-digital converter and after quantization the data are sent to a computer and to a monitor and registered on magnetic tape for subsequent processing. Transparency of a working sector makes visual observation of the process and photographing of the foam possible. The mean size of an air bubble in the foam is determined by the processing of microphotographs. The research made it possible, by procedures jdescribed in detail, to determine the speed of sound and the acoustic attenuation coefficient in foam for the multiplicity range from 10 to 143. There is a strong dependence of the speed of sound on foam multiplicity: speed of sound increases with an increase in multiplicity. A spectral method was developed for finding the dependence of phase velocity and the acoustic attenuation coefficient on frequency. The experimental results are consistent with theoretical data in the literature. Figures 3; references: 5 Russian.

## Solitary Deformation Waves in Metals

[Article by Ye. A. Pamyatnykh and A. V. Ursulov, Ural State University imeni A. M. Gorkiy; UDC 539.2.01:548.4]

[Abstract] In the study of nonlinear acoustic waves in solids the deviation of the elastic properties of the crystal lattice from the Hooke law is usually regarded as the physical cause of the nonlinearity (this concept, strictly speaking, is applicable only to dielectrics). In metals, however, a substantial role should be played by mobile charge carriers interacting with the deformed lattice. In this study it is shown that in a case when the perturbations are formed during times greater than the time of the free path of electrons the role of conductivity electrons in nonlinear elastic phenomena can be reduced to a renormalization of the lattice moduli of elasticity of the third order and the characteristics of solitary deformation waves for this case can then be analyzed. The analysis reveals that the electrons in metals exert a considerable influence on nonlinear elastic phenomena. This influence is important when the contribution of electrons also is important for the linear characteristics. However, the contributions of electrons to the linear and nonlinear parameters are different. Stable solitons should be observed in metals with a negative dispersion of the speed of linear sound; their speed in this case is greater than the speed of linear sound. Such solitons may be both dilatation solitons and compression solitons; the conditions governing which type will be observed are discussed. References: 13 Russian.

## Screening of Internal Cavity of Cylindrical Emitter by Radial Screens

[Article by V. Ye. Glazanov and I. L. Rubanov, Morfizpribor Central Scientific Research Institute; UDC 534.232]

[Abstract] With the placement of radially positioned screens within a cylindrical emitter a possibility appears for controlling the reactive impedance of the internal cavity $Z_{in}$, as was demonstrated in two earlier studies by the authors (AKUST. ZHURN., Vol 35, No 3, pp 546-548,

1989; Vol 36, No 3, pp 366-368, 1990). Depending on the relative wave resistance of the screen and the angle between the radial screens, related to their number, $Z_{in}$ may vary in a wide range. In the earlier studies it was assumed that the length of the screen is equal to the radius of the screened surface of the emitter $H = R_0$. In this study the case $H < R_0$ is examined. The geometry of the problem and two variants of the radial screening system are illustrated and discussed. The acoustic pressure must satisfy specific boundary conditions, differing for the two proposed variants. For each variant a series of figures gives the distribution of acoustic pressure in the internal cavity of a cylindrical emitter, the dependence of the ratio of the input impedance of the investigated model to cavity impedance on frequency and the dependence of the equivalent radius of a cylindrical screen on the number of radial screens. Figure 1; references: 4 Western.

## Boundary Between Near and Distant Array Field in Waveguide

[Article by V. A. Yeliseyevnin, Acoustics Institute imeni N. N. Andreyev, Russian Academy of Sciences; UDC 534+534.231.2]

[Abstract] The acoustic field in the case of directed radiation or reception is usually divided into near (Fresnel) and distant (Fraunhofer) zones on the assumption that the radiating or receiving antennas are in a homogeneous unbounded space. The boundary between the two fields is drawn on the basis of the degree of curvature of the acoustic wave phase front at this boundary. The curvature must be such that the field phase difference in the distance between the central and extreme array elements is $\pi/8$ radian or less. The satisfaction of this condition means that the curved wave front can be considered plane. The acoustic field in the near zone has a complex interference character. Therefore, when determining the array directivity characteristics the measurements are made in the distant field of the array. A determination of the mentioned directivity characteristics also is required when the array system is in a hydroacoustic waveguide. A need arises for dividing the acoustic field of the array into near and distant zones and the boundary between them will differ from the free space condition. In the region of high acoustic frequencies, when there is the directivity necessary in practical hydroacoustics, the array aperture is usually much less than waveguide thickness and under certain assumptions this makes it possible far from the waveguide boundaries to determine the directional properties of the radiating and receiving systems in the same way as if they were situated in a homogeneous unbounded space. As a result, the array aperture may be comparable to or greater than the waveguide thickness and its directivity characteristics may differ substantially from a case when the array is in free space. It is shown that in the last analysis the problem of the near and distant fields of such a vertical array in actuality does not exist. Figure 1; references: 4 Russian.

## Sounding of Oceanic Eddy by Directed Parametric Radiation

[Article by I. B. Yesipov, S. V. Zimenkov, A. I. Kalachev and V. Ye. Nazarov, Acoustics Institute imeni N. N. Andreyev, Russian Academy of Sciences; Applied Physics Institute, Russian Academy of Sciences; UDC 534.222]

[Abstract] A merit of parametric sound emitters is a narrow directional diagram in a wide range of low frequencies, making possible their effective use in studying the ocean and its bottom structures. An earlier study (V. A. Andebura, et al., AKUST. ZHURN., Vol 36, No 3, pp 548-550, 1990) gave the results of measurements of the acoustic field of a powerful acoustic emitter operating in a parametric mode at distances up to 180 km. This article gives the results of an experimental study of the angular characteristics of the acoustic field of this same emitter obtained when sounding an oceanic eddy by directed parametric radiation. The experiments were made from two scientific research ships. The results show that the radiating antenna (whose parameters are listed) was quite effective in oceanological research using directed parametric radiation. It was therefore used in an oceanic region with well-expressed hydrological inhomogeneities, specifically, a current with characteristic eddy formations near the Kuril Islands. The results of oceanic research with the excitation and propagation of directed parametric radiation collected there show that in regions with changing spatial hydrological characteristics (such as in the form of an oceanic eddy) the angular characteristics of parametric emitters change substantially. These changes correspond to the spatial characteristics of the structure of the inhomogeneities and the shipboard emitter is an effective tool ensuring generation of highly directional LF radiation propagating well on paths of great extent. Figures 3; references 4: 3 Russian, 1 Western.

## Formation of Precursor of Acoustic Pulse Excited in Thermoelastic Generation Mode at Sea Surface

[Article by V. D. Kiselev and O. A. Maksimov, Pacific Ocean Oceanological Institute, Far Eastern Department, Russian Academy of Sciences; UDC 534.222.2]

[Abstract] In earlier studies the distortions of the leading edge of a pulse generated in an "explosive boiling" regime at the ocean surface were interpreted as a process of formation of a precursor. Arising as a result of a considerable dispersion of acoustic waves, the precursor in essence is the HF part of a signal propagating with a great velocity and therefore outpacing the main body of the pulse. It is therefore evident that such an effect also should be observed in a simpler thermoelastic generation mode. This article describes the distortions of the leading edge of an optoacoustic signal characterized by separation of a precursor in a thermoelastic excitation mode. The basis for

this work was research done earlier by O. A. Bukin, et al. (DAN SSSR, Vol 315, No 1, pp 84-86, 1990; PISMA V ZhETF, Vol 52, No 12, pp 1261-1263, 1990). The research was carried out in the near-surface layer in the presence of great concentrations of gas bubbles, resonance interaction with which results in a considerable dispersion of surface waves. A great number of factors had to be taken into account in studying this phenomenon, particularly the fact that in this layer the bubble distribution is extremely nonuniform with depth. However, the geometric dimensions of the optoacoustic pulses under these conditions are several centimeters. A method is given for describing the shape of the envelope of the optical pulse, determined by the bubble-size distribution. This distribution is quite variable since it is dependent on wind speed (wave collapse). Models of the laser pulse time envelope were analyzed. Several widely used methods are unsuitable for such an analysis, but the nature of development and characteristics of the precursor are successfully described by special procedures. References 17: 12 Russian, 5 Western.

## Experimental Research on Interaction Between Broadband High-Energy Sound and Water-Air Foam

[Article by G. S. Tolstov, Thermal Processes Scientific Research Institute; UDC 534.286.2]

[Abstract] A decrease in acoustic pressure levels to 130 db or more and the broadband character of the wave spectrum results in qualitative changes in the nature of interaction between acoustic waves and foam. This is related to activation in the energy scattering process of nonlinear dissipative mechanisms, not manifested in the interaction between foam and low-energy monochromatic sound. The research was carried out using an experimental apparatus placed within an anechoic sound chamber in which the sound source used was a supersonic hot gas jet with a Mach number 2.4 propagating in a volume bounded by a horizontally positioned cylindrical shell. This shell is adjoined by a vertically oriented cylindrical container for foam with an internal diameter 250 mm and a height 500 mm within which there is a metal grid on which there is a membrane of polyethylene film for retaining the foam in the container. Any water released from the foam escapes through a drainage hole. In the upper section of the container there is a sensor of pressure pulsations connected to an amplifier and magnetic recorder. The duration of foam irradiation in all the experiments is 7 s. Figures 1, 2, and 3 show the spectral characteristic of the background acoustic flow, spectral characteristic of the acoustic flow entering the foam layer and the spectral characteristic of the acoustic flow passing through the foam layer. The conditions under which each of these curves were registered are discussed and their significance is analyzed. Specific results are given for one such interaction experiment. Figures 3; references 3: 2 Russian, 1 Western.

## Spin Structure of Boundary States and Circular Photogalvanic Effect in Heterojunctions

[Article by M. V. Kisin, Institute of Radio Engineering and Electronics at Russian Academy of Sciences, Saratov branch; UDC 621.315.592]

[Abstract] Boundary states in heterojunctions are considered, such states being capable of strongly perturbing the energy spectrum of charge carriers even in a monotype band structure of the semiconductor pair. These states are revealed by the circular photogalvanic effect at optical transitions in the presence of nondegenerate states and most readily so in a heterojunction with a gapless semiconductor such as CdTe/HgTe or CdTe/α-Sn completely devoid of spin degeneracy, formation of nondegenerate boundary states being a manifestation of spin splitting at a given quasimomentum can take place only for one of the wave functions of a spin doublet. The remaining Kramer's degeneracy, related to symmetry with respect to time reversal, leads to a correlation between the spin state of an electron in a boundary state and the direction of its two-dimensional momentum. Only simplest boundary states and thus those near the Fermi level of such heterojunctions are considered, this level in such a system being associated with the ceiling of the valence band of HgTe or α-Sn and lying deep within the forbidden band of CdTe. An analytical model of such boundary states including their spin structure is constructed, considering that their wave function remains virtually within the gapless semiconductor and hardly passes below the barrier. The spectrum of charge carriers is, in the $\Gamma_8$ representation, described by the Lattinger-Hamiltonian and zero boundary conditions for each of the four components of the psi-function envelope. Inasmuch as the possibility of a circular photogalvanic effect at boundary states in a heterojunction here and generally depends on the probability of optical transition into states with opposing quasimomenta, the efficiency of photoexcitation is defined in terms of a parameter which quantifies the anisotropy of optical absorption. Spin polarization and the attendant circular photogalvanic effect are shown to be more pronounced in multilayer structures and in quantum wells, induced by a longitudinally flowing electric current or, in a quantum well, by a transverse electric field. Figures 1; references 17.

## Parasitic Control Through Substrate in GaAs Field-Effect Transistors

[Article by V. A. Gergel, E. A. Ilychev, A. I. Lukyanchenko, A. I. Poltoratskiy, and K. S. Shchamkhalov, Scientific Research Institute of Problems in Physics imeni F. V. Lukin, Moscow]

[Abstract] Parasitic control effects in a field-effect transistor with Schottky gate (FET-SchG) in the form of backgating through the semi-insulating substrate are analyzed on the basis of the authors' physical model (FIZIKA I TEKHNIKA POLUPROVODNIKOV, Vol 24 No 12, 1990) and an experimental study of their steady-state and transient-state characteristics. The experiment was performed with such transistors in the form of cells consisting each of uniformly doped epitaxial n-GaAs layers grown on semi-insulating GaAs:Cr³ substrates and coplanar "parasitic" either barrier-like or ohmic electrodes topologically isolated by being 20-1000 µm away from the plate. These cells were tested at temperatures covering the 300-450 K range in an electric field whose intensity was varied over the 10 V/cm to 100 kV/cm range. The test circuit had been designed to allow separate measurement of the drain current, the gate current, and the electrode current as the voltage electrode-to-gate voltage was varied. It was also designed to allow recording relaxation processes in the FET channel, but only those with a characteristic time not shorter than 100 ns. The test results reveal two kinds of parasitic control effects, those with a threshold and those without one. Those without a threshold are characterized by a monotonic dependence of the drain current in the FET-SchG channel on the voltage between the parasitic electrode and the gate. The substrate current meanwhile depends strongly on both the temperature T and the field intensity, each dependence being linearizable in the respective (log $I_s$ - $V^{1/2}$) and (log $I_s$ - $1/kT$) coordinates. Considering also the polarity of the voltage at a parasitic electrode and the linear dimensions of the active region in the FET-SchG channel, it appears that principally responsible for modulation of the electrical conductance of the FET-SchG channel during voltage variation at the parasitic electrode is accumulation of negative charge in the substrate near the substrate-channel interface following emission of holes from ≈ 0.78 eV acceptor centers therein. Relaxation of the drain current following a voltage pulse at a parasitic electrode has been found to be activation-dependent. Parasitic control effects with a threshold are characterized by changing of the drain current only when the voltage at the parasitic electrode has exceeded some threshold level in the presence of an ≈ 0.34 eV deep donor in the substrate-channel interface region. The dependence of the substrate current on the voltage at the parasitic electrode is then, in the static mode, not only different for a barrier-like electrode and for an ohmic one but also correspondingly covers two ranges: one of an ohmic and thus weak field dependence with an ≈ 0.34 eV activation energy and one of a strong field dependence with an ≈ 0.6 eV activation energy, the results of temperature measurements indicating an activation-dependent relaxation of the drain current in both ranges. The thus supplemented physical model includes the Frenkel-Poole mechanism, which raises that activation energy from 0.6 eV to 0.8 eV and by virtue of which the rate of hole emission from ≈ 0.78 eV acceptor centers increases with increasing voltage at the parasitic electrode. Figures 5; references 5.

## Effect of Dislocations Produced by Laser Radiation on Electrophysical and Luminescence Characteristics of p-CdTe

[Article by A. Baydullayeva, B. M. Bulakh, B. K. Daulemuratov, B. R. Dzhumayev, N. Ye. Korsunskaya, P. Ye. Mozol, and G. Garyagdyyev, Institute of Semiconductors at Ukrainian Academy of Sciences, Kiev]

[Abstract] An experimental study of CdTe crystals was made concerning the effect of treatment with nanosecond pulses of a ruby laser radiation on the luminescence characteristics of these crystals and on the density of dislocations in them as well as on their electrical and photoelectric properties. Intrinsic p-CdTe crystals in the form of 100 μm thick plates were grown by synthesis of Cd and Te vapors without doping, whereupon copper electrodes were deposited by a chemical process on their large surfaces. They were treated with up to four nanosecond monopulses of ruby laser radiation at an ambient temperature of 300 K, the power density being raised up to well below the crystal fracturing level and subsequent measurements being continued for a 2 h period. The density of dislocations after treatment was measured under an optical microscope, by etching and then counting the pits. Photoluminescence at 80 K and 4.2 K temperatures was then induced by excitation with a He-Ne laser and regulated by means of an MDR-23 monochromator. The characteristics of those crystals were found to begin changing, without formation of a Te film, when the power density of laser treatment had reached about 2 MW/cm². The dark current and the photocurrent as well as the photoluminescence intensity at both 300 K and 80 K were found to decrease as the number of incident radiation pulses at that power density level had increased, the dark equilibrium current at these temperatures decreasing toward respective steady threshold levels. The photocurrent spectra at both 80 K and 4.2 K temperatures were found to contain one interband-transition maximum and not to have changed upon laser treatment of the crystals. The photoluminescence spectra prior to laser treatment contained at 80 K an emission line of free excitons along with an 806 nm band and a band within the 850-950 nm range, at 4.2 K an emission line of excitons bound to neutral acceptors along with an 800-810 nm edge band and also a band within the 850-950 nm range. Laser treatment decreased the intensity of photoluminescence at 80 K across the entire spectrum but preferentially of the 800-810 nm edge band. It decreased the intensity of this photoluminescence at 4.2 K as well, but also gave rise to a new 840 nm emission band. This new emission band appeared upon treatment with the same radiation dose which began quenching the original photoluminescence. The density of dislocations prior to laser treatment was about 100 cm⁻², laser treatment not having perceptibly impaired crystal surface but subsequent selective etching having revealed a larger number of pits under the surface. Their number was, moreover, found to increase upon treatment with larger radiation doses. Inasmuch as quenching of the 800-810 nm edge band is known to be associated with recombination of excess charge carriers in donor-acceptor vapors, in which some Cd atoms are replaced by shallow $Li_{Cd}$ and $Na_{Cd}$ acceptor atoms, preferential quenching of this edge band by laser treatment may be explained by drift of acceptor atoms as well as of donor atoms with a resulting decrease of the donor-acceptor pair concentration. (Drift of only donor atoms would have increased the electrical conductivity, the donor-acceptor emission band then having been replaced by an emission band associated with capture of free acceptor electrons. Neither such an emission band nor an increase of the electrical conductivity were recorded in the experiment.) Figures 5; references 8.

## Electronic 2D-3D System—Quantum Diode, Part 1: General Properties

[Article by V. N. Kadushkin and S. I. Fomichev, Scientific Research Institute of Technology, Ryazan]

[Abstract] An experimental study of n-AlGa$_{1-x}$As/GaAs heterojunctions with x = 0.28-0.30 acting as converters of alternating voltage to static e.m.f. was made, the static e.m.f. induced in their systems of degenerate 2D-3D electrons by an alternating external electric field or by quantum "null" oscillations being measured at liquid-He temperatures. Specimens of these junctions were grown epitaxially from molecular beams. Subsequent e.m.f. measurements were first made in the presence of an uncontrollable "white" noise caused by stray pickup, using an artificial voltage signal of fixed amplitude and frequency. The heterojunctions were tested in the Van der Paw geometry of single and double Hall bridges. A magnetic field was produced by a superconducting solenoid and the induction varied from zero up to 7.4 T, its distribution deviating not more than 6.6 G/mm from a uniform one and its drift in time not exceeding 1 G/h. The temperature of specimens was monitored by means of a FeCu/C thermocouple. Measurements of both $\rho_{xx}$ and $\rho_{xy}$ tensor components of the transverse magnetoresistivity (xx - potential contacts, xy - Hall contacts) and of the static e.m.f. have revealed that this e.m.f. has not only a component appearing in a magnetic field and dependent on the induction but also a component insensitive to a magnetic field and thus existing in the absence of one as well. The component sensitive to a magnetic field was found to oscillate very asymmetrically relative to the $\rho_{xx}$ Hall component of transverse magnetoresistivity and its monotonically sensitive part to depend strongly, with inclusion of a polarity reversal, on the intensity of the magnetic field. Measurements of the static e.m.f. in the potential mode and in the Hall mode did not reveal any anomalies. Measurements of the static e.m.f. were then made upon application of controllable

alternating-voltage excitation signals of up to 400 MHz frequency, with and without the magnetic field. The dependence of the static e.m.f. on the amplitude of the alternating excitation voltage above the threshold level of the latter was recorded at various constant magnitudes of the magnetic induction B, including B = 0, and found to be steeply linear beginning not far above that threshold level. An analysis of all the data indicates that rectification of an alternating voltage is most likely effected by the barrier-layer junction in the quantum system of degenerate 2D-3D electrons forming a "quantum" double diode, due to asymmetry as well as nonlinearity of its constant-current current-voltage characteristic and depending on its resistance. This hypothesis is supported by measurements made at temperatures ranging up to 30 K, raising the temperature having lowered the diode resistance and thus diminished the rectification effect, but not changed the form of the rectification curve. Measurements made upon introduction of a constant bias voltage revealed, as expected, an increasingly more effective rectification owing to stronger asymmetry of the current-voltage characteristic as the bias voltage was raised. The authors thank A.Ya. Shik and I.I. Saydashev for helpful discussions, also S.V. Kolosova for assisting with the manuscript. Figures 7; references 6.

## Photoluminescence of Heavily Doped GaAs With Ordered Distribution of Impurity Complexes

[Article by V. A. Bogdanova and N. A. Semikolenova, Omsk State University]

[Abstract] An experimental study of heavily doped GaAs crystals was made concerning the dependence of their photoluminescence on the doping level, found not to conform to classical concepts but evidently determined by ordering of compound defects in the impurity sublattice. Specimens of GaAs crystals grown by the Czochralski method were doped with tellurium so that the concentration of free charge carriers extended over the $n = 10^{17} - 10^{19}$ cm$^{-3}$ range. Photoluminescence spectra were recorded so as to cover the edge band as well as impurity radiative-recombination bands. The peak intensity of edge photoluminescence increases, very gradually first, from its lowest level when $n = 10^{17}$ cm$^{-3}$ to a maximum when $n \approx 10^{18}$ cm$^{-3}$. It then decreases back to the same lowest level before increasing almost immediately to a second maximum when $n = (3-4) \times 10^{18}$, this maximum being almost one order of magnitude higher at 77 K and about two orders of magnitude higher at 4.5 K higher than the first one. It then decreases again to the same lowest level when $n \approx 10^{19}$ cm$^{-3}$. The impurity radiative-recombination photoluminescence covers two somewhat overlapping bands, evidently because the composition of dominant compound recombination centers changes as the carrier concentration passes through the $(2-3) \times 10^{18}$ cm$^{-3}$ range. The first band

extends over the wider $n = 10^{17} - 2.5 \times 10^{18}$ cm$^{-3}$ range with a mild peak, the intensity increasing from its lowest level when $n = 10^{17}$ cm$^{-3}$ to a maximum (hv = 1.21 - 1.22 eV) when $n \approx 10^{18}$ cm$^{-3}$ and then decreasing to the same lowest level when $n \approx 2.5 \times 10^{18}$ cm$^{-3}$. The second band extends over the narrower $n = 1.5 \times 10^{18} - 10^{19}$ cm$^{-3}$ range with a sharp peak, the intensity increasing from its lowest level (lower than the lowest level in the first band) when $n \approx 1.5 \times {}^{18}$ to a maximum (hv = 1.33-1.4 eV) when $n = 3 \times 10^{18}$ cm$^{-3}$ and then decreasing to the same lowest level already when $n \approx 6 \times 10^{18}$. The maximum-intensity wavelength in the first band was found to shift only slightly upon an increase of the carrier concentration and not to depend on the temperature within the 100-230 K range. The maximum energy $hv_{max}$ in the second band was found to increase upon an increase of the carrier concentration. The authors thank A.A. Gutkin and M.A. Reshchikov for measuring the percentage polarization of photoluminescence. Figures 3; references 8.

## Mechanism of Formation of Space-Charge Region in MODS-Transistor at 4.2 K Temperature

[Article by S. A. Okhonin and A. A. Frantsuzov, Institute of Semiconductor Physics at Siberian Department of Russian Academy of Sciences, Novosibirsk]

[Abstract] An experimental study was made concerning ionization of impurities in the substrate of an MOS-transistor and consequent formation of a space-charge region, at 4.2 K temperature. For the study were selected p-channel transistors on n-substrates doped with phosphorus to an $n = 10^{15}$ cm$^{-3}$ carrier concentration: 100 μm wide linear structures with a 10 μm long p-channel and 100 μm wide annular structures with either a 4 μm long p-channel or a 20 μm long p-channel, channel and gate in each being separated by an 800 μm thick dielectric interlayer. The threshold voltage at 4.2 K was for all transistors within the 1.2-3 V range. Application of a bias voltage pulse to the substrate was found to be followed by relaxation of the transistor channel current, indicating formation of a space-charge region under the channel. Inasmuch as enhancement of that region results in depletion of the inversion layer and thus raises the threshold voltage, there exists a correspondence between the kinetics of current decrease in the transistor channel and the kinetics of charge buildup in the substrate. The not directly measurable rate of charge buildup in the substrate was, accordingly, measured indirectly in terms of the measurable rate of current decrease in the transistor channel. Simultaneous voltage measurements revealed how the characteristic time of current relaxation in the linear transistors (to 50 percent of its initial magnitude) and the rate of change of the threshold voltage for the annular transistors (immediately after application of a bias voltage pulse to their substrate) both depend on the drain voltage. The results indicate that at

a drain voltage below 1 V the characteristic current relaxation time is almost independent of the gate voltage, though increasing the latter results in an increase of the current and thus also of the power dissipation in the transistor channel. It is not heating of the chip, therefore, that causes the rate of charge generation in the substrate to increase as the drain voltage is being raised from say 0.1 V to well below 1 V. Neither is formation of electron-hole pairs possible when the drain voltage remains so low, because then a hole cannot acquire the necessary 1.2 eV energy. (Only at a drain voltage above 5 V was the current found to rise up to about 10 pA, the transistor then operating in the cutoff mode). At a drain voltage below 1 V and 4.2 K temperature, therefore, impurity is ionized not by impact of either electrons or holes but evidently interaction with neutral particles: either photons or phonons. This was confirmed by the results of another experiment, with two annular transistors mounted on the same chip 0.4 μm apart. A drain voltage of about 0.1 V was applied to the first transistor for measurement of the rate of space-charge buildup after application of a bias voltage pulse to its substrate, the second transistor serving as a source of ionizers. The space-charge region in the first transistor was forming very slowly with the second transistor off and then increasingly fast as the drain voltage at the second transistor was being raised. As the drain voltage at each transistor was being raised at the same rate, the rate of increase of the threshold voltage was increasing faster for the second transistor than for the first one. Donor impurities were, therefore, ionized not by photons but rather by phonons. The mean life of 50 meV optical phonons is 0.001 ns on a short mean free path of about 0.1 μm. While their energy was sufficient for ionization, they decayed into acoustic phonons before reaching the ionization region in the first transistor. The mean free path for 5 meV acoustic phonons is about 1 mm long and thus longer than the distance separating the two transistors in this experiment. Such acoustic phonons thus reached the ionization region in the first transistor and the energy necessary for ionization was provided by cooperation of several of them. The authors thank S.K. Savvinikh for discussion. Figures 4; references 9.

### Effect of Radiative Defects Produced by α-Particles on Reverse Currents in Silicon P-N Junctions

[Article by O. V. Aleksandrov, B. N. Shevchenko, I. P. Matkhanova, and A. V. Kamenets, St.Peterburg Association "Svetlana" Manufacturing Electronic Devices]

[Abstract] An experimental study of $n^+$ - p junctions and $p^+$ - n junctions was made concerning the dependence of reverse currents in them on the energy spectrum of radiative defects produced in the n-Si layers and in the p-Si layers by bombardment with α particles. Silicon layers of both kinds were bombarded with a flux of 2.5

MeV mean-energy α-particles coming from a $^{210}$Po-isotope source, its fluence being $2 \times 10^{11}$ cm$^{-2}$ in a noncollimated beam and $1.3 \times 10^{11}$ cm$^{-2}$ in a beam collimated within a 43° angle. The energy spectrum of these defects was measured by transient capacitive spectroscopy of deep levels in Schottky barriers, such barriers having been formed by deposition of an aluminum layer on 300 μm thick polished plates of p-type KDB-10 silicon grown by the Czochralski method and on 4 μm thick epitaxial layers of n-type KDB-10 silicon with an electrical resistivity of 1 ohm.cm grown on p-type silicon plates. The barriers were, after bombardment with α-particles, isochronously annealed at temperatures ranging from 100°C to 340°C for 1 h at each. Junctions were formed by the diffusion process: $p^+$ - n junctions by diffusion of boron (p = $3 \times 10^{18}$ cm$^{-3}$ doping concentration at the surface) 1.3 μm deep into 10 μm thick epitaxial n-Si layers with a resistivity of 2.5 ohm.cm grown on 300 μm thick n-type substrates of KES 0.01 silicon; $n^+$ - p junctions by diffusion of phosphorus (n = $2 \times 10^{21}$ cm$^{-3}$ doping concentration at the surface) 0.75 μm deep into p-type silicon layers. Reverse currents in the junctions of both kinds were measured at temperatures covering the 20-200°C range, then again after bombardment with α-particles and after subsequent isochronous annealing at various temperatures ranging from 200°C to 500°C. The energy spectrum of radiative defects in both n-Si and p-Si was found to be similar after bombardment by noncollimated and collimated α-particle beams, but their concentration was about 1.5 times higher after bombardment by a a noncollimated one and thus with a correspondingly larger dose. Spectroscopy after bombardment and subsequent annealing revealed electron defect centers with energy $E_c$ at -0.18 eV (E1 level), -0.23 eV (E2 level), -0.30 eV (E3 level), -0.37 eV (E4 level appearing at 340°C) in n-Si and hole defect centers with energy $E_V$ at +0.20 eV (H1 level), +0.24 eV (H2 level appearing at 200°C), +0.30 eV (H3 level), +0.42 eV (H4 level) in p-Si, their cross-sections for capture ranging from $1 \times 10^{-16}$ cm$^2$ (E4) to $1 \times 10^{-14}$ cm$^2$ (H3). Their concentrations decreased, each differently, as the annealing temperature was raised. The reverse current in $p^+$ - n junctions and in $n^+$ - p junctions, while depending first on the bombardment temperature and then on the annealing temperature, is evidently determined by the generation-recombination centers bound to E3 and E1 defects in n-Si or H2 and H4 defects in p-Si respectively. Figures 4; references 18.

### Low-Temperature Electrical Conductivity of Si With Ion-Implanted P+Sb

[Article by V. V. Aleksandrov, V. A. Kulbachinskiy, V. G. Kytin, A. B. Timofeyev, and A. G. Ulyashin, Moscow State University imeni M. V. Lomonosov]

[Abstract] An experimental study of silicon with ion-implanted phosphorus and antimony was made concerning the transport of electrons in the presence of both these two donor impurities at temperatures from 300 K to 4.2 K. Silicon films were doped by heavy-dose implantation of 80 keV $P^+$ ions and 90 keV $Sb^+$ ions, $10^{16}$ $cm^{-3}$ of each. The defective layer was then annealed by laser treatment with 1.06 μm radiation in pulses of 50 ns duration, whereupon contact tabs of silver paste were deposited on the surfaces for electrical resistance measurement by the current-voltage method, covering the linear range of the current-voltage characteristic. A magnetic field of 6 T intensity was produced by a superconducting solenoid. Prior to annealing the temperature dependence was a semiconductor-like one, though not linearizable in (log R - 1/T) coordinates, addition of phosphorus to Si:Sb films decreasing the resistance and addition of antimony to Si:P films increasing the resistance. Laser annealing changed the temperature dependence of the resistance into a metal-like one, the resistance of Si:P remaining higher than the resistance of Si-Sb films and that of Si:(Sb,P) films being the lowest. Increasing the energy of incident laser radiation pulses lowered the resistance of all films. As the magnetic field of the film current was increased from zero to 60 kOe, the transverse magnetoresistance of Si:(Sb+P) films before annealing was first negative and then became positive following a crossover (at about 35 kOe at 4.2 K). Annealed films exhibited no magnetoresistance. The results indicate that laser annealing makes the distributions of implanted impurities more uniform and their wave functions to overlap so that a metal-like structure with short mean free paths is formed. The authors thank I.P. Zvyagin for helpful discussion. Figures 3; references 14.

### Effect of a Superconducting Coating on the Domain Structure of a Ferromagnetic Material

[Article by S. Yu. Bereza, Yu. I. Gorobets, A. A. Simonov, Donets State University; UDC 538.945: 537.611.44]

[Abstract] This article studies the effect of an eddy magnetic structure of a superconducting thin film on the domain structure of a ferromagnetic substance in a two-layer structure consisting of infinite ferromagnetic and superconducting films in an external homogeneous magnetic field perpendicular to the film plane. It is assumed for simplicity that the superconducting coating does not bend the domain boundaries, and eddies in the superconductor do not interact. An expression is obtained for the total energy of the two-layer structure. An equation is constructed for the dependence of the change in the period of the domains structure on the external field. It is found that the period of the domain structure of the ferromagnetic material is greatly affected by the presence of the superconducting coating, which decreases the period of the domain structure. This is due to a change in the configuration of scattering fields of the ferromagnetic film in this system. Under certain conditions the change in period is directly proportional to the thickness of the superconducting film. Figures 3; references: 8 Russian.

### Generalized Langevin Dynamics of a Soliton in a Morse Chain

[Article by I. N. Zhdanova, L. S. Zarkhin, L. I. Manevich, Scientific Research Institute of Mechanics and Applied Mathematics, Rostov on Don; UDC 541.64:539(199+3)]

[Abstract] This article examines the dynamics of a soliton in an anharmonic Morse chain in a condensed medium in the framework of generalized Langevin dynamics. In this approach, in contrast to the use of Newtonian dynamics, the stochastic dynamics of some isolated set of variables of a thermodynamic system are examined, while the effect of the remaining variables is replaced by an effective viscoelastic medium with a stochastic component satisfying the fluctuation-dissipation theorem. A numerical computer experiment for a one-dimensional model of a continuous chain of polyethylene in a viscoelastic Maxwell liquid with one relaxation time was conducted. The inertial properties of the liquid are not manifested. It is shown that the soliton becomes unstable to the effects of the medium. The "lifetime" of the soliton is found to be dependent on temperature and the viscoelastic characteristics of the medium. The results differ qualitatively from the data of computer molecular dynamics experiments for an isolated Morse chain. Results of molecular-dynamic studies and the Langevin approach are compared. Figures 9; references 12: 6 Russian, 6 Western.

### Metastable Optical Polarization of Nuclear Moments in Silicon

[Article by N. T. Bagrayev, I. S. Polovtsev, A. Yusipov, A. F. Ioffe Physicotechnical Institute, Russian Academy of Sciences, Saint Petersburg; UDC 621.315]

[Abstract] Zinc in silicon exhibits acceptor properties and forms two interrelated deep levels. An isolated zinc center is a negative-$U$ defect. Consequently, the paramagnetic $Zn^-$ state is unstable and spontaneously dissociates in the silicon lattice. The behavior of an isolated zinc center is studied using optical polarization of nuclear moments. This makes it possible to study the recharging of the point defect in the absence of an electric field. The experimental procedure is described. It is found that in weak magnetic fields ($H_0 < 10$ Oe) in silicon doped with zinc, optical polarization of nuclear

moments is caused by dipole-dipole interaction of polarized doped zinc centers with surrounding $^{29}Si$ lattice nuclei. As the magnetic field increases ($H_0 > 10$ Oe) the dominant contributor to optical polarization of nuclear moments is made by contact interaction induced by the presence of small phosphorous donors. Anomalous disappearance of optical polarization of nuclear moments is observed in prolonged optical pumping, and arises due to photodissociation of the paramagnetic state of the isolated center. Figures 3; references 11: 3 Russian, 8 Western.

## Silver Diffusion in Lead Zirconate-Titanate

[Article by R. Sh. Malkovich, Ye. A. Skoryatina, V. P. Usacheva, T. A. Shaplygina, A. F. Ioffe Physicotechnical Institute, Russian Academy of Sciences, Saint Petersburg; UDC 539.219.3]

[Abstract] Lead zirconate-titanate (LZT) is a ferrielectric material with a peroxide structure. It is a favored material for obtaining stratified structures used in memory devices and piezoelectric elements. Silver is widely used in the manufacture of these structures, and so the study of the diffusion of silver in LZT is of interest. Earlier studies of this subject are outlined. This article studies the diffusion of silver into the ceramic $PbZr_{0.54}Ti_{0.46}O_3$. The preparation of samples of this ceramic is described. Silver has a high rate of diffusion into LZT, and in a relatively short period of time penetrated tens or hundreds of microns into the material. As temperature increases, the depth of penetration increases. An expression is determined for the coefficient of diffusion as a function of temperature at 370-700°C. A change in the stoichiometry of the ceramic (addition of PbO) led to a decrease in the amount of silver which penetrated into the material. An increase in pressure during caking led to the same result. A change in the temperature of caking had no effect on silver diffusion. The high rate of diffusion and the relatively low activation energy of diffusion indicates that silver moves predominantly along intercrystalline spaces, along pores, and boundaries between ceramic grains. Divergences in the low temperature data are explained by a lack of local equilibrium (which is present at high temperatures). The process can be described with one parameter, the coefficient of diffusion. Figures 3; references 7: 5 Russian, 2 Western.

## Characteristic and Features of Conductivity of Surface δ-Doped Layers in GaAs When the Concentration of Two-Dimensional Electrons Changes

[Article by I. N. Kotelnikov, V. A. Kokin, B. K. Medvedev, V. G. Mokerov, Yu. A. Rzhanov, S. P.

Anokhina, Institute of Radio Engineering and Electronics, Russian Academy of Sciences, Moscow]

[Abstract] Magnetotransport studies are conducted at helium temperatures for two types of structures: with one δ-doped layer (Si) at a distance of 200 angstroms from the aluminum-covered GaAs surface, and with two δ-layers (L1 = 200 angstroms, L2 = 500 angstroms) containing an identical amount of donors. For the sample with one δ layer, measurements were made of the tunnel spectra and the dependence of the mobility and concentration of two-dimensional electron gas on the voltage $V$ on the gate. The data agree well with the results of self-consistent calculations of the energies and filling of subzones in a potential quantum well for a δ layer width of 50 angstroms. The behavior of mobilities in subzones with a concentration $n$ of two-dimensional electron gas makes it possible to reach a conclusion on the appearance of inter-subzone scattering effects. It has been found that the rate of growth of $n$ mobilities $\mu_1$ in an excited subzone of a potential quantum well substantially exceeds the rate of change $\mu_0(n)$. This behavior may be associated with the intensification (as $V$ increases) of the spatial separation of moving electrons of the excited subzones in the ionized doping of the δ-layer. This is characteristic of asymmetric potential quantum wells of δ layers. Data for the structure with two δ-layers qualitatively confirm this conclusion. Figures 6; table 1; references 18: 4 Russian, 14 Western.

## Electron g-Factor in Quantum Wells and Superlattices

[Article by Ye. L. Ivchenko, A. A. Kiselev, A. F. Ioffe Physicotechnical Institute, Russian Academy of Sciences, St. Petersburg]

[Abstract] This article develops a consistent kp-theory to calculate the g-factor of an electron in a structure with a single quantum well and in a superlattice. The calculation is done both in a one-zone approximation and in the Kane model, in which the kp displacement of states $c\Gamma_6$, $v\Gamma_8$, $v\Gamma_7$ is exactly considered. The dependence of the g-factor on the thickness of heterostructure layers is found. It is shown that when splitting of electron states in subzones of heavy and light holes of the valent zone is considered, due to the effects of dimensional quantization the g-factor of the electron in the conductivity zone becomes anisotropic. In a GaAs/AlGaAs structure, as the thickness of the layers changes, the longitudinal and transverse components of the g-factor pass through zero, so there exists a range of thicknesses at which these components have opposite signs. Only the one-electron g-factor is calculated here. In samples with a noticeable concentration of electrons, the g-factor may be strongly renormalized due to exchange interaction effects. Figures 3; references 13: 4 Russian, 9 Western.

## Annealing Mechanism of Divacancies in Silicon Irradiated by Protons

[Article by L. S. Berman, V. B. Voronkov, V. A. Kozlov, A. D. Remenyuk, A. F. Ioffe Physicotechnical Institute, Russian Academy of Sciences, St. Petersburg]

[Abstract] Disordered regions and divacancies are created when silicon is irradiated with high-energy heavy particles. They are the main radiation defects which determine the generation-recombination parameters of silicon devices. Irradiation by 4 MeV α particles has annealed divacancies at 150-250°C. Neutrons annealed them at 100-350°C. Irradiation with γ quanta and electrons does not form disordered regions, and divacancies are annealed at 250-350°C. The difference in temperature ranges is attributed to a difference in oxygen concentration. This article studies the dependence of the annealing of divacancies on the concentration of atomic oxygen in n-silicon irradiated by protons. The preparation of samples and the measurement method are described. The experimental results show that the state of oxygen in the silicon lattice has no substantial effect on the rate of introduction of divacancies and the temperature of their annealing. Apparently, the difference in divacancy annealing temperatures is due to a different concentration of structural defects, which are the drain for vacancies. Figure 1; references 16: 6 Russian, 10 Western.

## Photoelectron Phenomena in GaAs Layers With Quantum Heterowell Built-In on Surface

[Article by I. A. Karpovich, V. Ya. Aleshkin, A. V. Anshon, N. V. Baydus, L. M. Batukova, B. N. Zvonkov and S. M. Plankina, Nizhegorod Physical Technical Scientific Research Institute imeni N. I. Lobachevskiy]

[Abstract] The photoluminescence and capacitor photo-emf methods were used in investigating the characteristics of photoelectron phenomena in GaAs layers with an InGaAs quantum well built in on the surface in the space charge field and in a quasineutral volume. The transfer of the well to the surface results in a strong extinction of photoluminescence in the well, but exerts only a slight influence on the capacitor photo-emf. The capacitor photo-emf method is applicable for the diagnosis of quantum wells in highly defective structures. The capacitor photo-emf phenomenon is related to the emission of electron-hole pairs from a quantum well and their subsequent separation on the closest barriers. In layers with quantum wells in the space charge field there is no activation dependence of the capacitor photo-emf on temperature, such as is characteristic for layers with quantum wells in the body of the material (this is attributable to the tunneling mechanism of emission of electrons and holes from quantum wells). The principal objectives of the research were realized: development of photoelectric methods for the diagnosis of quantum wells and clarification of the influence of the electric field in the space charge region and the dielectric-semiconductor defect boundary on the characteristics of quantum wells and also the influence of the quantum well itself on photoelectron phenomena near the surface. Figures 6; references 11: 7 Russian, 4 Western.

## Long-Range Effect in GaAs Monocrystals With Different Density of Dislocations

[Article by V. P. Kladko, T. G. Kryshtab, A. V. Svitelskiy and G. N. Semenova, Semiconductors Institute, Ukrainian Academy of Sciences]

[Abstract] A study was made of the influence of the mechanical processing (polishing) of the nonworking side of monocrystalline GaAs plates alloyed with tellurium on the magnitude of deformations and spectra of photoluminescence on the working surface as a function of the density of growth dislocations. It is shown that polishing results in a decrease in the intensity of the edge emission band for plates with a cellular dislocation structure and an increase in its intensity for material without dislocations. This process results in an opposite behavior of the impurity-defect zone with an energy of the emission maximum 80 K, caused by radiative transitions in defect proper-impurity complexes, that is, ignition occurs for dislocation samples with a virtually unmodified state in GaAs without dislocations. This difference in the behavior of the photoluminescence spectra is related to the dominant role of the initial defect structure in GaAs plates. The principal result of this study was the determination of the decisive influence of the initial defect structure of GaAs plates (density of growth dislocations and the composition of point defects) on the character of subsequent defect formation and change in structurally sensitive parameters with manifestation of a long-range effect in the case of nonequilibrium operations (polishing of back side, ion implantation, etc.). It follows that in comparison of the results of study of the electro-optical characteristics of GaAs and epitaxial structures on its basis it always is necessary to investigate and thereafter take into account the initial defect structure of the object. Figures 4; references 10: 8 Russian, 2 Western.

## Mechanism of Instability of Semi-Self-Maintaining Microwave Discharge in Nitrogen

[Article by N. A. Bogatov, S. V. Golubev and S. V. Razin, Applied Physics Institute, Russian Academy of Sciences; UDC 537.32]

[Abstract] An experimental study was made of the dynamics of the electron concentration and glow of a semi-self-maintaining microwave discharge in nitrogen. The dependence of the stability of uniform combustion on the external parameters of the discharge was measured. The microwave radiation from a generator was directed through an oversize waveguide into a vacuum chamber filled with the working gas and by means of an emitter and mirror was transformed into a convergent Gaussian beam whose focus was within the vacuum chamber. The spark discharger was at a distance 3 cm from the beam focus. The UV radiation of a spark discharge ionized the gas in the focal region of the beam and the semi-self-maintaining microwave discharge transpired there. The microwave radiation source was a pulsed gyrotron with a wavelength 6.7 mm. The experiments indicated that the instability of a semi-self-maintaining microwave discharge in nitrogen, supported by UV ionizing radiation, with a small specific energy contribution to the gas, is related to accumulation in the discharge of metastable electron-induced molecules, which results in an increase in the rate of multiplication of electrons and a transition of an unstable microwave discharge into a self-maintaining discharge. An ionization mechanism through cascade excitation of high-lying electron levels is proposed: reactions were found which are capable of satisfactorily explaining the results if the jreaction rate constants are sufficiently great. Figures 7; references 22: 12 Russian, 10 Western.

## Measurement of Thermal Conductivity of Heat-Insulating Materials by Temperature Waves Method at High Temperatures

[Article by V. A. Petrov and S. Al. Ulybin, High Temperatures Institute, Novosibirsk Department, Russian Academy of Sciences; UDC 536.21]

[Abstract] A new method is described for measuring the thermal conductivity of heat-insulating materials, as well as an automated experimental apparatus based on the use of digital measuring instruments and computers for applying the traditional plane temperature waves method. A diagram of the experimental apparatus used is given; 22 components are identified and the function of each of these is described in the text. The results of study of the thermal conductivity of an especially pure quartz ceramic with a porosity 50 percent (mean pore size about 1 μm) in the temperature range 700-1400 K are given. The contribution of the radiation component of heat transfer is estimated. The availability of new equipment made it possible to reexamine the possibility of the temperature waves method applicable to heat-insulating materials. Previous difficulties have been overcome and measurement accuracy has been increased. The use of a fast Fourier transform algorithm for harmonic analysis made possible the most effective avoidance of noise and discrimination of the harmonics from the highly noise-encumbered signal at a high accuracy level and thereby increase the accuracy in phase shift determination. The total error in determining the thermal conductivity coefficient is estimated at 3 percent. The standard deviations of the results of phase shift measurements at temperatures 769 and 1431 K were 0.2 and 0.6% respectively. Figures 3; references 21: 19 Russian, 2 Western.

## Laser Heating of Carbon Particles of Cylindrical Configuration

[Article by G. P. Ledneva, Minsk Physics Institute; UDC 536.422:535.211]

[Abstract] Some estimates of heating of cylindrical particles of a carbon aerosol to the melting point in a vacuum under the influence of laser radiation are made with allowance for a nonuniform distribution of energy sources through the volume of the particles. It is assumed that heat release by a particle is described by the Stefan-Boltzmann law and the evaporation of matter can be neglected, that is, the boundary of a solid particle remains fixed. Temperature change with time within an infinite cylinder of a given radius is described by the thermal conductivity equation in a cylindrical coordinate system. In the heating of large carbon particles the decisive factor is nonuniformity in the distribution of electric field strength within them. The influence of different variables is examined. The study revealed that with laser radiation in a quite broad intensity range in a small-diameter carbon particle of cylindrical configuration the temperature distribution within it is virtually uniform, but with normal incidence of radiation the time when the melting point is reached is essentially dependent on the type of polarization. On the other hand, the heating of large-diameter particles by laser radiation of a quite high intensity results in a strongly expressed nonuniform temperature distribution and the type of polarization in actuality has no influence on when the melting point is reached. References 9: 8 Russian, 1 Western.

## Hydrodynamics of Escape of Products of Electric Detonation of Conductors. Formation of Thin Films and Ultradispersed Powders

[Article by V. P. Volkov, V. N. Gavrilov and Ye. A. Litvinov, Electrophysics Institute, Yekaterinburg; UDC 533.951]

[Abstract] The results of numerical solution of a system of equations describing the detonation of the products of electric detonation of a wire are given. The dynamics of escape of copper vapor and droplets into an inert medium was studied. It is shown that the behavior of the droplets is determined by the quantity of introduced energy, which influences the intensity of the developing shock waves. Allowance for presence of a dispersed phase exerts an influence on all the hydrodynamic parameters of escape of detonation products: on the velocity and temperature of the ambient vapor and on the intensity of the forming shock waves. However, this influence does change the qualitative picture of expansion of the products. A far greater influence is exerted not by the presence of the liquid droplets themselves, but by the evaporation and condensation transpiring at their surface. Allowance for evaporation and condensation on droplets increases the percentage of particles precipitating onto the walls of the detonation chamber. The pressure of the ambient medium exerts the greatest influence on the entire escape process: the greater the counterpressure, the fewer are the particles which are incident on the walls. In the expansion process there is partial spatial separation of particles of different sizes because at the onset of escape the large particles lag behind the small ones. However, with slowing of the products of the electric detonation of conductors by the external gas the large droplets advance farther. Moreover, large particles are incident on the chamber walls in a hotter state than small particles. Figures 4; references: 11 Russian.

## Heat Exchange in Supersonic Heterogeneous Flow

[Article by Yu. V. Polezhayev, I. V. Repin and D. S. Mikhatulin, High Temperatures Institute, Novosibirsk Department, Russian Academy of Sciences; UDC 533.6.011.55:536.25]

[Abstract] Although many studies have been devoted to research on heat exchange at the surface of bodies surrounded by a heterogeneous flow, the mechanism of this process has not been fully clarified. It has remained unclear what influence is exerted by the size and configuration of the body, the size and concentration of particles, the pressure of the slowed flow and other factors determining the degree of nonequilibrium of a heterogeneous flow. The latter circumstance has not been taken into account by some researchers, resulting in a great scatter of experimental data and even their contradictoriness. All these factors were investigated in this study. Generalization of an extensive file of experimental data made it possible to construct a physical model of heat exchange of bodies in a high-temperature heterogeneous flow. The size and concentration of a dispersed admixture were examined in the range from 20 to 250 $\mu$m and from 0 to 1 percent respectively. The test apparatus used, specially developed for studying heat exchange and erosion of bodies in heterogeneous flows, is a high-temperature gas-dynamical tube. The total enthalpy of the flow was 3700 kJ/kg and total gas pressure attained 20 MPa. The studied copper bodies were cylinders 40 or 80 mm in diameter. The research took in the range of Mach numbers j2.6-4.2 and the range of Reynolds numbers $0.4\text{-}5 \times 10^6$. The dependence for computing heat exchange in the neighborhood of the critical point of a blunted body, for example, is in satisfactory agreement with the experimentally discovered regularities and makes it possible to estimate the heat load on the frontal surfaces when there is a heterogeneous flow around a body. Figures 7; references 8: 6 Russian, 2 Western.

## Maximum Attainable Radiation Energy Parameters of Nd-Glass Laser Systems

[Article by Ye. V. Yeshmemetyeva, V. I. Korolev, Ye. P. Mesnyankin, V. V. Shashkin, and V. Ye. Yashin, All-Russian Scientific Center at State Institute of Optics imeni S. I. Vavilov, St.Peterburg; UDC 621.373.826.038.825.3]

[Abstract] An experimental study of neodymium laser glasses was made for the purpose of determining their optical breakdown threshold and their SBMS (stimulated Brillouin-Mandelshtam scattering) excitation threshold, also the gain and the energy extraction efficiency in these glasses under heavy radiation loads exceeding heretofore attainable levels. For measurement of the optical breakdown threshold was used a single-mode single-frequency master laser emitting radiation within a 0.0005 nm wide band in smooth bell-shaped pulses either 50 ns or 150 ns wide at half-amplitude level. This radiation was amplified in five stages, then passed through the 9 mm wide aperture of a diaphragm, and focused onto the glass piece by a lens with a 4379 m focal length. Two silicate neodymium glasses (GLS 1, GLS 6), two phosphate neodymium glasses (GLS 22P, OPS 117-1242), and also K 8 quartz glass were tested for this threshold. The optically toughest of these glasses was found to be OPS 117-1242 calcium-alkali-ultraphosphate neodymium glass: 232-306 $J/cm^2$ when treated with 150 ns wide laser pulses. For measurement of the SBMS threshold was used a radiation-recording calorimeter, the precision of this measurement being increased by amplification of the reflected signal prior to its subsequent reflection into the calorimeter by the polarizer in one of the two Faraday cells. This measurement yielded data on the dependence of the signal power at the SBMS-recording calorimeter on the peak energy density E in the SBMS beam, the threshold energy density being then estimated by extrapolation of this dependence to zero signal power. Two of the neodymium glasses, GLS 1 silicate glass and GLS 22P phosphate glass in the form of 630 mm long rods 45 mm in diameter, were tested for this threshold with 150 ns wide rather than 50 ns wide pulses so as to ensure steady stimulated scattering beyond the transient period. The results indicate that the SBMS threshold for 1.06 $\mu$m incident radiation threshold is higher than the optical breakdown threshold in the GLS 22P phosphate glass (47.9 $J/cm^2$) and lower than the optical breakdown threshold in the GLS 1 silicate glass (27 $J/cm^2$). For measurement of gain and energy extraction were used four rotating opaque plane mirrors, the last one leaning against a telescope so that radiation reflected by it passed through the telescope into the glass rod. Both silicate glasses (GLS 1, GLS 6) and one phosphate glass (GLS 22P), in the form of 300 mm long rods 20 mm in diameter, were so tested for performance as lasers. They were pumped by an INK-22 flash lamp with a reflective coating on the outside surface, which ensured a nearly uniform axisymmetric distribution of inverse population in the glass. The results of this test indicate that a maximum energy extraction efficiency of 95 percent and 60 percent is attainable in GLS 22P glass with a 3 x $10^{-10}$ $cm^2$ lasing cross-section and in GLS 1 glass with a 1.8 x $10^{-20}$ $cm^2$ lasing cross-section. The experimental data were collated with a theoretical evaluation of gain and energy extraction efficiency, taking into account incremental changes in both small-scale focusing and in stimulated scattering during a pulse. Calculations were based on the standard equation of energy transfer for a medium with a uniformly broadened spectral line and the derived therefrom Frantz-Nodvik formula relating the density of extracted energy to the gain and to the density of injected energy, the latter normalized to the saturation energy density. For a numerical simulation of the lasing process, the glass rod was subdivided into $\Delta l$ long elementary segments and the pump pulse was subdivided into corresponding elementary pulses of $\tau$ duration. The local dependence of the lasing cross-section on the density of energy which had passed through an elementray glass segment in the entire preceding pulse period was then used as a reference for taking nonuniform broadening of the spectral line into account. The design parameters of Nd-glass lasers for respectively maximum attainable efficiency (75.3 percent with OPS 117-1242 glass) and least likely stimulated scattering (with GLS 6 glass) have been established on this basis. Figures 3; tables 2; references 15.

## Yb₃Sc₂Ga₃O₁₂:(Cr3+,Ho3+) Crystal: Promising Active Medium for Ho³⁺-Laser in Cascade Scheme

[Article by A. L. Denisov, A. I. Zagumennyy, G. B. Lutts, V. V. Osiko, S. G. Semenkov, and A. F. Umyskov, Institute of General Physics at Russian Academy of Sciences, Moscow; UDC 621.373.826.038.825.2]

[Abstract] An experimental study was made concerning the possibility of Ho3+ ions in an optically excited $Yb_3Sc_2Ga_3O_{12}:(Cr^{3+},Ho^{3+})$ crystal lasing at room temperature according to the $^5I_6 \rightarrow {}^5I_7 \rightarrow {}^5I_8$ cascade scheme while the $Cr^{3+}$ ions absorb the pumping radiation, lasing at room temperature requiring that the $Ho^{3+}$ concentration be low. A gallium garnet has been selected on account of the easy energy transfer from $Cr^{3+}$ ions to $Yb^{3+}$ ions in it and on account of its narrow phonon spectrum. A high concentration of $Yb^{3+}$ ions ensures an effective energy transfer to $Ho^{3+}$ ions, while a narrow phonon spectrum ensures a low probability of the non-radiative $^5I_6 \rightarrow {}^5I_8$ transition in $Ho^{3+}$ ions and thus a longer life of their upper laser level. The crystal with $[Cr^{3+}] = 2$ x $10^{20}$ $cm^{-3}$ and $[Ho^{3+}] = 5$ x $10^{19}$ $cm^{-3}$ concentrations was grown by optical zone refining and the plain $Yb_3Sc_2 Ga_3O_{12}$ crystal was grown by the Czochralski method. For an analysis of the luminescence spectrum, $Cr^{3+}$ ions were excited with 694 nm radiation from a ruby laser in pulses of 150 ns duration and $Yb^{3+}$

ions were excited with 1.06 µm radiation from a YAG:Nd3+ laser in pulses of 10 ns duration. Luminescence in the three 1 µm - 2 µm - 3 µm bands was recorded with a photomultiplier, a Ge-diode, and a photoresistor respectively. The high $Yb^{3+}$ concentration almost completely quenched the luminescence of $Cr^{3+}$ ions, an indicator of an effective $Cr^{3+} \rightarrow Yb^{3+}$ energy transfer. While in the plain $Yb_3Sc_2Ga_3O_{12}$ crystal the mean life of the excited $^2F_{5/2}$ state in $Yb^{3+}$ ions was 150 µs and their luminescence in this state decayed exponentially, in the $Yb_3Sc_2Ga_3 O_{12}:(Cr^{3+},Ho^{3+})$ crystal that life was shorter and that luminescence decayed more than exponentially. The measured mean life of levels $^5I_6$ and $^5I_7$ in $Ho^{3+}$ ions 325 µs and 9.8 ms respectively, luminescence at both levels decaying exponentially. The calculated efficiency of $Cr^{3+} \rightarrow Yb^{3+} \rightarrow Ho^{3+}$ energy transfer was 60 percent. Figures 2; references 5.

## Modeling 10-Liter XeCl Electric-Discharge Laser

[Article by A. V. Demyanov, I. V. Kochetov, and A. P. Napartovich, Troitsk Institute of Innovative and Thermonuclear Research, M. Capitelli, C. Gorse, and S. Longo, Research Center for Plasma Chemistry CNR at Bari University (Italy); UDC 621.373.826.038.823]

[Abstract] Two independent models of an XeCl electric-discharge laser (1. A.V. Demyanov, Kochetov, et al.; KVANTOVAYA ELEKTRONIKA Vol 13, 1986; 2. C. Gorse, "Nonequilibrium Excimer Laser Kinetics. Non-equilibrium Processes in Partially Ionized Gases", Plenum Press, New York, 1991) are evaluated comparatively with regard to their relative agreement with the same results of an experiment involving a 10-liter laser (S. Bollanti, P.D. Larzaro, F.Flora, G. Giordano, T. Hernsen, T. Lotardi, C.E. Zheng; JOURNAL OF APPLIED PHYSICS B, Vol 50, 1990). This experiment was performed with XeCl:Xe:Ne = (0.4-5):10:2268 mm Hg mixtures and a capacitive energy storage (LC Π-circuit). Both models account for five processes: 1) $XeCl^* \rightarrow Xe + Cl + hv$, 2) $XeCl^* + HCl(v = 0) \rightarrow Xe + Cl + HCl(v = 0)$, 3) $XeCl^* + HCl(v = 1) \rightarrow XeCl + HCl(v = 1)$, 4) $XeCl^* + e \rightarrow Xe + Cl + e$, 5) $XeCl^* + Ne \rightarrow Xe + Cl + Ne$. The effect of VV and VT interactions as well as dissociation of HCl by electron impact are being evaluated separately (S. Longo, M. Capitelli, C. Gorse, A.V. Demyanov, I.V. Kochetov, A.P. Napartovich; ICPG 20, Pisa, Jul 91; JOURNAL OF PHYSICS, in print). On the basis of each model have been evaluated the dependence of the output energy and the emission time on the HCl pressure, the kinetics of XeCl, H, Cl-, Xe*, NeXe*, Xe+, $XeCl^*$ (in states B,C), $Xe_2+$, Xe**, e, and hv concentrations as well as of discharge voltage and current in HCl over the period of an emission pulse (about 900 ns wide at half-amplitude level), also the dependence of the emission power on the voltage across the storage capacitor. Both models yield only a qualitative agreement with
the experimentally determined dependence of the emission energy on the HCl pressure. Even such an agreement is lacking with respect to the duration of an emission pulse: the pulse duration was much shorter in the experiment and particularly so within the 0.5-1 mm Hg range of HCl pressure. Agreement is also lacking with respect to the dependence of the emission energy on the capacitor voltage: the emission energy in the experiment increased much less with increasing voltage over the 40-66 V range, a homogeneous discharge covering the entire electrode surface was assumed in the calculations. Quite evidently, a one-dimensional model of this laser is inadequate. Figures 6; references 22.

## Four-Pass YAG:Nd Laser Amplifier With Compensation of Wavefront Distortions Due to Aberration and Polarization

[Article by N. F. Andreyev, S. V. Kuznetsov, O. V. Palashov, G. A. Pasmanik, and Ye. A. Khazanov, Institute of Applied Physics at Russian Academy of Sciences, Nizhniy Novgorod; UDC 621.375.826.038.2]

[Abstract] An experimental study of a four-pass YAG:Nd laser amplifier with one active medium emitting pulses of 0.8-1 J energy at a repetition rate of 20-25 Hz was made, the beam with a diffractional divergence carrying an average power of 20 W. The master laser oscillator emitted $TEM_{00}$ radiation in pulses of 10 mJ energy, their repetition rate being varied up to 25 Hz with certainty of single-frequency emission. The beam of this radiation was widened by a telescope (two biconvex lenses) for passage through a soft diaphragm into a Faraday rotator (permanent magnets) with a 28 mm wide aperture. The rotator ensured retention of horizontal polarization of the radiation during forward passage of the beam and rotation of its polarization through 90° during during subsequent reverse passage of the beam. The beam then proceeded through the amplifier, another Faraday rotator (permanent magnet) with a 14 mm wide clear aperture, a 14 dB strong optical insulation, and another telescope (biconcave lens and biconvex lens) onto an opaque plane mirror. The purpose of the second telescope was to compensate the spherical lens induced in the active medium after the radiation had been reflected by that opaque plane mirror, to ensure passage of the returning beam through the active medium along approximately the same path as before. After depolarization during this second pass had been compensated, the second Faraday rotator changed the radiation polarization from horizontal to vertical. Wavefront distortion due to polarization was thus compensated by the linear optical elements and the nonreciprocal polarization rotator. A polarizer behind the active medium deflected the returning radiation into a phase-conjugating by stimulated Brillouin-Mandelshtam scattering (SBMS) $SnCl_4$ mirror. By reflecting only linearly polarized radiation, this mirror ensured compensated distortion of a plane wavefront due to aberration during

third and fourth passages through the active medium. The performance of such a four-pass laser amplifier was found to depend largely on the degree of radiation depolarization after two beam passages through the active medium. Measurements were made, therefore, for a determination of the percentage depolarization and its dependence on the pump power. Three variants of a phase-conjugating mirror were tested, the object being to maximize the ratio $\chi$ of the fraction of output energy leaving the amplifier at the diffraction angle to the fraction of input energy entering the amplifier at the diffraction angle and to minimize the dispersion of this ratio. The best scheme in this respect, yielding a ratio $\chi$ = 0.78+/-0.03 and a stable transverse structure of the reversed Stokes wave, was found to be: SBMS amplifier - attenuator - SBMS oscillator with two focusing stages. The high-gain laser amplifier was tested with the master oscillator in the free-running, to ensure reaching the SBMS threshold, as well as with Q-switching. In order not to maintain a low percentage depolarization within 10% and thus minimize the aberrations, it was necessary to limit the pump pulse energy to 0.85-0.95 J. Figures 4; references 15.

## Theoretical Basis for Reduction of "Null" Drift in Fiber-Optic Gyroscope by Means of Lyot Depolarizer

[Article by E. I. Alekseyev and Ye. N. Bazarov, Institute of Radio Engineering and Electronics at Russian Academy of Sciences, Fryazino branch; UDC 681.7.068]

[Abstract] Use of a discrete-optical Lyot (wideband) depolarizer for reduction of the "null" drift in a fiber-optic gyroscope consisting of two directional input-output couplers with an optical-fiber return loop is examined theoretically. Such a depolarizer consists of two linear phase plates, the thicker one behind the thinner one (thickness ratio 1:2) with their optical axes 45° apart. The properties of this device are described formally in the approximation of plane waves, while the polarization characteristics of incoming radiation are fully described by the coherence matrix of $E(z,t)$ times $E^+(z,t)$ cross products. The analytical signal $E(z,t)$ corresponds here to the electric component of the radiation field vector (t - time, z - space coordinate in the direction of propagation) and is expressed as twice the integral over spectral amplitudes $e(z,\omega)$ ($\omega$ - frequency) from 0 to $\infty$, these spectral amplitudes representing conventional Jones vectors. The transfer function of such a depolarizer in terms of spectral amplitudes is the Jones transfer matrix $T(\omega) = e_{out}(\omega)/e_{in}(\omega)$. The output coherence matrix is then equal to the coherence matrix of nonpolarized radiation with the Jones transfer matrix $T(\omega)$ replaced by the Jones spectral matrix $D(\omega)$, inasmuch as the spectral amplitudes of incoming radiation signals are $\delta$-correlated, and $D(\omega)$ is shown to be a unitary matrix. Only a perfect Lyot depolarizer capable of depolarizing an arbitrarily polarized radiation is selected for this gyroscope, in preference to a partial one capable of depolarizing only a specifically polarized radiation. The light source is assumed to emit time-coherent radiation, the latter thus being characterized by its spectral coherence matrix, and the photodetector diode is a assumed to be neither spectrally nor polarization sensitive. In absence of rotation the gyroscope signal may not vanish as it should, owing to presence of a polarization "pedestal." The latter can be completely eliminated by a perfect Lyot depolarizer, assuming that it is an ideal one in the sense of exactly satisfying $\delta$-correlation of elements of its Jones spectral matrix. It is further assumed that only the gyroscope itself with most of the optical fiber inside causes the "null" drift, that there are no other means of its elimination included, and that the Sagnac phase shift does not depend on the signal frequency within the radiation spectrum. Four ways of inserting a Lyot depolarizer into a fiber-optic gyroscope are evaluated: 1) behind the light source in the input branch of the first directional coupler, 2) into the fiber loop behind the second directional coupler, 3) between the two directional couplers, 4) before the photodetector diode in the output branch of the first directional coupler. A comparative performance analysis based on a "scalar" model of the input-output device and a unitary Jones spectral matrix reveals that the effectiveness of a Lyot depolarizer depends largely on whether or not it induces dichroism and birefringence in the gyroscope. When inserted into the output branch, it cannot influence the phase relations between two input components but does equalize the intensities of two orthogonally polarized output components without changing the total radiation intensity and uncorrelates them while also making each noncoherent. When inserted into the fiber loop, it eliminates neither the parasitic polarization "pedestal" nor "background" flicker and also does not eliminate fading of the interference component of the photodetector current (which takes place in the absence of dichroism but only when birefringence in the gyroscope channel is elliptic rather than purely linear). The two other schemes are equivalent but, from the standpoint of more effective "pedestal" abatement, insertion of the depolarizer between the two directional couplers is preferable to its insertion into the input branch. It is shown to be possible for the gyroscope itself to become a depolarizer, when its transfer matrix $J(\omega)$ at some mean frequency $\omega_0$ is $J_0 = E$. Figures 1; references 14.

## Nonlinear Dynamics and Generation of Nonclassical Light in Two Laser Fields

[Article by G. Yu. Kryuchkyan and K. V. Kheruntsyan, Physical Research Institute, Armenian Academy of Sciences]

[Abstract] A quantum theory of parametric four-photon mixing in a nonlinear medium under the influence of two laser fields has been formulated. The conditions for generation of three radiation field

modes in a resonator with frequencies equal to the frequencies of the perturbing laser fields and with a frequency equal to their half-sum are examined. Three types of stationary, stable solutions are found for the intensities and phases of these modes, corresponding to three lasing modes. The spectra of compression and dispersion of fluctuations of the quadrature amplitudes are computed, from which it follows that there is a new possibility for obtaining single-mode compressed light at the frequencies of each of the modes in a suprathreshold lasing mode. The effect of suppression of quantum fluctuations of the sum of intensities of the modes at the frequencies of the perturbing fields below the coherence level was discovered. An important characteristic of the considered nonlinear system is that it allows an analytic examination above the lasing threshold within the framework of linearization of the stochastic equations of motion. As a result, in a quasiclassical approximation stationary values of the filling numbers and phases of modes in the resonator were found, as well as the corresponding intensities of the radiation fields at the resonator output. A quantum analysis of the fluctuations of intensities and phases of each of the modes was made. The results confirm that the four-wave mixing process in two laser fields is extremely promising for the lasing of single-mode compressed light with suppressed quantum fluctuations of quadrature amplitudes. This process also results in the formation of a nonclassical two-mode field at the frequencies of the pumping fields, for which the fluctuations in the intensities of the two modes are reciprocally anticorrelated. Figures 7; references 28: 7 Russian, 21 Western.

## Is a Gray Soliton a Statistical Attractor of the Nonlinear Schroedinger Equation?

[Article by I. A. Ivonin and V. V. Yankov, Kurchatov Institute, Russian Scientific Center]

[Abstract] Particular solutions in the form of solitons play an important role in integrable wave systems and a still more important role in nonintegrable systems. Nonintegrable systems with wave repulsion are capable of forming gray solitons, that is, local decreases in wave intensity. In this article, on the basis of a thermodynamic analysis and the stability of gray solitons of the nonlinear Schroedinger equation the hypothesis is expressed of the possibility of an increase in their modulation amplitude and their manifestation of attractor properties. The initial conditions for the nonlinear Schrodinger equation are given, making possible experimental and numerical checking of the predicted manifestations of the attractor properties of gray solitons. An analytic description of a "gray soliton + wave" equilibrium is given for the nonintegrable Schroedinger equation with a potential of the repulsion type. This shows the thermodynamic advantageousness of an increase in the modulation amplitude of gray solitons up to some finite level. An increase in the modulation amplitude of a gray soliton, in contrast to the growth of an ordinary soliton, is accompanied by the emission of waves, not by their absorption. The simultaneous growth of all gray solitons with a low modulation amplitude is evidently difficult due to the existence of the "weak" integrals of motion in the nonlinear Schroedinger equation, real only with a low amplitude of background modulation. A number of specific cases are considered. References 23: 10 Russian, 13 Western.

## Fractal Characteristics of a Sequence of Geomagnetic Field Inversions

[Article by A. V. Yermushev, A. A. Ruzmaykin, D. D. Sokolov; UDC 550.384.3]

[Abstract] The geomagnetic field at the Earth's surface is, in the first approximation, a magnetic dipole field whose axis usually has an approximately constant direction. However, there have been periods in Earth history when the polarity of this dipole rapidly (on a geological scale) reversed. Since the rocks formed at this time "recall" the direction of the geomagnetic field, it has been possible to construct a magnetostratigraphic time scale which fixes the sequence of geomagnetic field inversions. The magneto-stratigraphic scale is very inhomogeneous. Long periods without inversions alternate with time periods where inversions occur as frequently as the method used to construct the scale can resolve. Cox was the first to note the random nature of this time series. A number of articles have studied the statistical properties of the time series of a number of geomagnetic field inversions. This article studies the time sequence of inversions from a different point of view. A similarity is noted between the graphs of the magnetostratigraphic scale and images of one-dimensional fractal sets. It is shown that the magnetostratigraphic scale can be seen as a homogeneous fractal set, and its Hausdorf dimension and measure are calculated in two ways. Results are tested for multifractality (evidence of this is not found). Results obtained in the article coincide within the margin of error with the Cox scale. It is found that the magnetostratigraphic scale is actually a fractal set of dimension 0.67. Figures 3; references 7: 3 Russian, 4 Western.

## Hydrodynamics of a Magnetically Liquified Layer in a Rotating Magnetic Field

[Article by M. K. Bologa, I. F. Marta; UDC 537.84:537.634:532.584]

[Abstract] A magnetically liquified layer is a suspended state of roughly disperse magnetized particles supported by a variable or rotating magnetic field. This mixture has features which are characteristic of magnetic liquids (internal rotation of disperse particles) and gaseous suspensions and pseudo-liquified layers (particle collisions). This article studies various prospects and applications for magnetically liquified layers in technological processes, the results of a study of the kinetics of aggregation in disperse mixtures with dipole interaction of particles in the disperse phase, and the possibility of modeling various states of media and asymmetrical hydrodynamic effects in a rotating magnetic field. The phenomenological method for the mechanics of bulk media is used to obtian a dissipative function, the Onsager equation, and hydrodynamic equations for the magnetically liquified layer. The rheological state equations are characterized by asymmetrical tensions in both phases. The average amount of energy pumped into a magnetically liquified layer in a rotating magnetic field is calculated in a linear approximation that corresponds to the case of concentrated systems. An equation is obtained to determine the average rate of chaotic forward movement of particles, and a solution is obtained for the case where viscous dissipation dominates in the system. The solution is analyzed in intermediate situations. It is shown that the phase state diagram of the magnetically liquified layer is characterized by hysteresis independent of the type of magnetic field. It is experimentally shown that there is some critical frequency of the rotating magnetic field at which the direction of rotation of the layer and the magnetic liquid changes. This process is marked by hysteresis.

## Structuring of Ferrocolloids in Rotating Magnetic Fields

[Article by A. Yu. Zubarev; UDC 537.84]

[Abstract] The behavior of magnetic liquids in rotating fields have long been of interest to researchers. It has been experimentally shown that if the strength and frequency of rotation of the field reach critical values which depend on physical properties of ferrocolloids, cylindrical domains are formed in them with an increased concentration of the disperse phase. The axes of these domains are perpendicular to the rotational plane of the field. Some authors have found that under certain conditions the homogeneous state of the magnetic liquid becomes unstable; however, it is unclear why structuring does not occur in a steady-state field. The steady-state axisymmetrical movement of the colloid inside and outside the aggregate is examined. All the equations needed to determine the radius of the stable aggregate, the concentration of the disperse phase within it, and the rate of rotation are derived. Calculated domain characteristics are shown in a figure. Figure 1; references 23: 19 Russian, 4 Western.

## Flow of a Conducting Liquid in a Rotating Magnetic Field

[Article by L. A. Gorbunov, V. L. Kolevzon; UDC 537.84]

[Abstract] The movement of a conducting liquid in a rotating magnetic field has been studied in many publications. However, they all have one substantial drawback: the induction of the magnetic field is assumed to be homogeneous over the radius, and the speed profile is assumed to be linear. But in realtiy, the magnetic field is not homogeneous, and this effects the speed profile.

The analytical model proposed in this article makes it possible to determine the $\varphi$ component of the flow rate of liquid in a rotating field when the height to radius ratio is approxiately equal to 1. The difference from experimental results is due to the fact that the flow of the r component in the boundary layer is somewhat overestimated. The structure of the boundary layer on the side wall is rather complex and is considered an inertial layer where nonlinear terms are substantially greater than viscous terms. The greatest role is played by terms with a radial shift in velocity. The model presented here may be used to approximately estimate the speed profile by height in a rotating field. Figures 6; references 10: 5 Russian, 5 Western.

### Evaluation of the Magnetic Field of Thermoelectric Currents in a Fast Neutron Reactor

*937J0066E Moscow MAGNITNAYA GIDRODINAMIKA in Russian No 4, Oct-Dec 92 pp 96-100*

[Article by A. Gaylitis, R. Freyberg; UDC 537.84]

[Abstract] The thermoelectric currents which arise in the liquid metal cooling system of a BN-600 fast neutron reactor can be evaluated from the data calculated from equivalent electric circuits. The reactor tank, including the core and the first circuit, is close in its electric properties to a bulk short-circuited conductor with inhomogeneous electric conductivity. To evaluate the bulk thermal currents in it one can use elements used in the description of bulk media. It is found that the magnetic field in the core increases linearly as one gets further from the axis of symmetry. Outside the core the magnetic field is close to the field of a current dipole and drops to zero at the outer boundary of the tank. An expression is presented for the maximum value of the magnetic field at the external boundary of the core. For the BN-600 the value is 1.78 G. The total electric current through the core is 892 A. The maximum value of the field decreases with height, but the field is significant even above the upper level of the core. The thermal currents can be identified on the background of the earth's magnetic field using the estimated values of the field in the reactor. Figures 4; references 3: Russian.

### Destruction of Aggregates by a Shear Flow of Magnetic Liquid

*937J0066A Moscow MAGNITNAYA GIDRODINAMIKA in Russian No 4, Oct-Dec 92 pp 107-109*

[Article by A. A. Kubasov; UDC 537.84]

[Abstract] Although the formation of structures in magnetic liquids has been widely studied, the breakdown of these structures has not been addressed. This article presents the results of a study of the effect of an oscillating flow created by a nonmagnetic rod vibrating in a magnetic liquid on the size of aggregates. It is found that the oscillating flow leads to a decrease in the effective size of aggregates, and the rate of change of the size of the aggregates depends on the amplitude of oscillations. Figures 3; references 8: 7 Russian, 1 Western.

### Correlation Between Normal and Tangential Components of Fluctuation Geomagnetic Field

*937J0072A Riga MAGNITNAYA GIDRODINAMIKA in Russian No 3, Jul-Sep 92 pp 3-10*

[Article by B. G. Zinchenko and D. D. Sokolov; UDC 537.84]

[Abstract] The main geomagnetic field experiences secular variations; in addition to the mean field it contains a fluctuation component. The fluctuation field in turn can be broken down into normal and tangential components. These two components are random fields and are described by a correlation function and a correlation tensor respectively. Although several hypotheses have been proposed as to origin of the fluctuation magnetic field, there is no unanimity on this matter. However, it appears that many details of the statistical picture of geomagnetic fluctuations at the earth's surface are determined by the process of transfer of fluctuations through the mantle, not by the nature of field sources. The transfer of both normal and tangential components of the fluctuation field have been studied. It has been postulated that only the normal component of the fluctuation magnetic field of the core penetrates through the core-mantle interface and the tangential component is formed from it in the mantle (O. V. Pilinenko, et al., GEOMAGNETIZM I AERONOMIYA, Vol 32, No 2, pp 140-146, 1992; D. Sokoloff, et al., ASTRONOMISCHE NACHRICHTEN, Vol 313, pp 115-123, 1992). In both studies the mantle as a simplification was approximated by a plane layer of a vacuum. These findings are explored in depth because the correlation between the normal and tangential magnetic fields has not really been fully clarified. This in-depth examination reveals that in the approximation of a plane layer of a vacuum the correlations between the normal and tangential components of the fluctuation field become equal to zero. Figures 5; references 7: 6 Russian, 1 Western.

### Determination of Properties of Magnetic Fluids From Propagation of Ultrasound. 2. Analysis of Experiments. Determination of Dependence of Characteristic Parameters of Magnetic Fluid on Temperature Change of Properties of Magnetic Fluid With Time

*937J0072B Riga MAGNITNAYA GIDRODINAMIKA in Russian No 3, Jul-Sep 92 pp 61-70*

[Article by A. N. Vinogradov, V. V. Gogosov, G. S. Nikolskiy, A. A. Usanov and S. N. Tsurikov; UDC 537.84]

[Abstract] The first part of this study (A. N. Vinogradov, et al., MAGNIT. GIDRODINAMIKA, No 2, pp 19-26,

1992) gave experimental data on the propagation of ultra-sound in a magnetic fluid. Two series of experiments were carried out with a 20-month interval (experiments I and II) using the very same sample of magnetic fluid. In this second part the method for determining the characteristic parameters of a magnetic fluid from the propagation of ultrasound, as proposed by the authors in MAGNIT. GIDRODINAMIKA, No 4, pp 29-37, 1989, is used for the processing of experiments I and II. The dependence of the volumetric concentration of the dispersed phase $\Gamma$, volumetric concentrations of magnetite $\Gamma_m$ and surface-active substance $\Gamma_s$, effective density of aggregates $\rho_a^0$, effective diameter D of aggregates and number n of aggregates per unit volume on temperature is determined. It was found that with a temperature increase the $\rho_a^0$ and n values increase, whereas $\Gamma_m$, $\Gamma_s$, $\Gamma$ and D decrease. An explanation for their dependence on temperature is proposed. The $\Gamma_m$ decrease, for example, is attributable to a weak expansion of magnetite with temperature. The change in the properties of the fluid with time can be judged from a comparison of the parameters of the magnetic fluids determined using data from experiments I and II. The nature of these and other changes is examined in detail. Both experiments indicate that with a temperature increase there is a decrease in the effective size of the aggregates and an increase in their number per unit volume of the medium. Such a process may occur as a result of decay of the aggregates. With a temperature increase Brownian motion may evidently cause such fragmentation. Figures 2; references 10: 9 Russian, 1 Western.

## Nonstationary Rotation of Conducting Fluid Under Influence of Rotating High-Frequency Field in Presence of Constant Longitudinal Magnetic Field

[Article by A. I. Karchevskiy and Ye. P. Potanin; UDC 532.526]

[Abstract] In a previous study (MAGNIT. GIDRODINAMIKA, No 3, pp 103-106, 1991) the authors examined a steady mode of rotation of a plasma column separated from the chamber walls by a vacuum gap under the influence of a HF transverse field in the presence of an external uniform longitudinal magnetic field. The relative simplicity of the stationary problem allowed a possibility for analytic solution of the system of nonlinear differential equations of motion of the medium. Continuing this work, a numerical solution has been found for a full system of nonlinear differential equations in the general case of nonstationary motion of a conducting medium under the influence of a rotating magnetic field, which in a steady state coincides with an analytic solution. A study was made of a cylindrical column of a conducting medium separated from the chamber walls by a vacuum gap and placed in an external uniform magnetic field $B_z$. Gravity is neglected. The developing radial pressure gradient of the gas (plasma) medium should result in transverse expansion of the column. An induced azimuthal electric current arises as a result of such movement of the conducting gas across the external longitudinal magnetic field. An emf preventing expansion should appear as a result of interaction between the azimuthal current and the longitudinal magnetic field. It is assumed that the longitudinal field is quite strong and therefore the radial expansion of the column can be neglected. This corresponds to the cold plasma approximation in which it is possible to neglect the radial pressure gradient. At a time t = 0 a rotating transverse magnetic field with a dipole configuration begins to act on the column of conducting gas. As a result of entrainment of the medium in an azimuthal direction and excitation of centrifugal forces a tendency to a radial expansion of the plasma column is intensified. The formulated problem is solved and validated explanations are given for the observed phenomena. Figures 2; references: 3 Russian.

## Solitons in Periodic Resonant Media

[Article by B. I. Mantsyzov, Moscow State University
imeni M. V. Lomonosov; UDC 535]

[Abstract] Evolution of solitary pulses in a one-dimensional resonant superlattice when a slight violation of the Bragg condition occurs is analyzed, considering that interaction of a coherent electromagnetic field and a one-dimensional lattice under conditions of exact resonance is described by the semiclassical Maxwell-Bloch two-wave equations for slowly varying amplitudes and that these equations reduce to the Gordon-sine equation when the Bragg condition is satisfied exactly. Next is considered coherent interaction of laser radiation and a superlattice of two-level atoms. The possibility of clearing such a medium when a slight violation of the Bragg condition occurs is examined by first space-averaging the complete system of discrete equation and then solving the thus obtained system of two nonlinear differential equations where $n(t) = -(P^*\Omega + P\Omega^*)/2$ (P - dimensionless index of atomic polarization, $\Omega^{+/-}$-soliton field). Despite their simplicity, these equations cannot be integrated exactly and thus solved analytically for just any initial conditions but only for specific ones and the condition that $n = -1$ at time $t = +/-\infty$. For various other initial conditions they must therefore be solved numerically, which has been done by the method of characteristics for also a specific set of boundary conditions. An analysis of the pulse field dynamics in a perturbed resonant medium on this basis reveals that a strong incident field induces in such a medium a two-wave soliton-like pulse, which then propagates through that medium at a relatively high velocity ($v > 0.1$) and remains stable. A weak incident field induces surprisingly a pulse which then propagates slowly ($v < 0.1$) with attendant field intensity oscillations and medium inversion so that the pulse periodically reverses its polarity and direction of motion without, however, appreciable energy losses. Nonlinear two-wave diffraction in a two-dimensional lattice (resonant medium) under the Bragg vector condition is analyzed analogously, on the basis of the corresponding Maxwell-Bloch equations. Figures 3; references 12.

## Self-Focusing and Self-Compression of Ultrashort Pulses in Planar Waveguides: Role of Group Velocity Dispersion

[Article by V. A. Vysloukh and T. A. Matveyeva,
Moscow State University imeni M. V. Lomomosov;
UDC 621.373.7]

[Abstract] Propagation of ultrashort laser beam pulses through planar optical fibers is analyzed for the effect of group velocity dispersion on their structure in both space and time, particularly on their self-focusing and self-compression. Nonlinear propagation of such pulses through an optical fiber—an inefficient waveguide—is considered and adequately described by the appropriate nonlinear Schroedinger equation for the complex amplitude of the electric field (x - transverse coordinate normalized to width of waveguide layer, z - longitudinal coordinate normalized to diffraction length, $\tau = t - z/u$, t - time, u - group velocity), with an additional term on the right-hand side representing linear refraction in the fiber ($n_0$ - refractive index of cladding, $n_c$ - maximum refractive index of core). Nonlinear group velocity dispersion and linear dispersion of higher harmonics as well as the effect of Raman scattering on the nonlinear susceptibility are disregarded here, inasmuch as they become apparent only at distances by far exceeding the diffraction length. The equation is transformed by replacement of the time coordinate $\tau$ with a third normalized space coordinate $y = \tau/\beta^{1/2}$ ($\beta = L_{diff}/L_{disp}$, $L_{diff}$ - diffraction length, $L_{disp}$ - dispersion length). The critical power for pulse self-compression is estimated by introducing the second statistical moment of radiation intensity, a function of the longitudinal z-coordinate characterizing the mean-square pulse duration and the pulse width in space. The compression length is then estimated by assuming that second moment to be a parabolic function of z: $\sigma^2(0) + H_0z^2$. Numerical integration of that Schroedinger equation upon separation of physical makes it possible to successively evaluate the role of each effect, which has been for this problem concerning the roles of diffraction, linear refraction, dispersion, and nonlinearity on each z-step of the computation grid. A numerical analysis of normal group velocity dispersion in laser pulses of $\lambda < 1.3$ $\mu$m radiation, confirms that such a dispersion competes with self-focusing and thus impedes increase of the peak radiation intensity. A numerical analysis of nonlinear wave field transformation in a planar optical fiber with anomalous group velocity dispersion in laser pulses of $\lambda > 1.3$ $\mu$m radiation indicates a possibility of appreciable pulse compression in the center section of a fiber without instability-causing modulation. Figures 3; references 6.

## Classical and Quantum States of Light During Laser Pulse Propagation Through Systems With Distributed Feedback

[Article by R. B. Alaverdyan, A. P. Alodzhants, S. M.
Arakelyan, and L. P. Gevorkyan, V. A. Makarov, and
Yu. S. Chilingaryan, Yerevan State University and
Moscow State University imeni M. V. Lomonosov;
UDC 535.42+ 535.14]

[Abstract] Dynamic scattering of ultrashort laser pulses in structures with distributed feedback such as cholesteric liquid crystals is analyzed for the first time, the problem being tackled as one involving classical pulse compression in time and quantum states of compressed light. First is considered dynamic diffraction of steady radiation in the linear and thus simplest mode in a one-dimensional sinusoidal and thus simplest kind of lattice, maximum efficiency of dynamic diffraction here corresponding to exact

Bragg resonance. Next is considered diffraction of laser pulses, namely nonsteady diffraction of frequency-modulated radiation, propagating through a structure with distributed feedback where both time lag and spatial dispersion play significant roles. A classical description of time compression of laser pulses in a transparent medium is obtained from the system of two coupled two-dimensional wave equations for two slowly varying complex amplitudes (two-wave approximation of dynamic scattering theory), for a comparative analysis of pulse compression in the symmetric Laue geometry (two waves propagating in same direction) and the symmetric Bragg geometry (two waves propagating in opposite directions) with random fluctuations in the medium disregarded. A quantum description is obtained by secondary quantization of the classical Maxwell equation for complex amplitudes of pulses nonlinearly propagating through a nonfluctuating periodic-in-space medium, with each amplitude being associated a creation operator and an annihilation operator. Time compression of pulses in a cholesteric liquid crystal has been analyzed numerically from the classical standpoint, including evaluation of the temperature dependence of the compression ratio as well as its dependence on the crystal thickness and using data from an experiment with a pulsed picosecond millijoule YAG: $Nd^3$-laser experimental data. The results indicate that compression in the Bragg geometry is less effective than it is in the Laue geometry but does not require high crystal precision, inasmuch as it tends to depend less on the thickness of thicker crystal. A description of compressed states of light in pulsed laser beams is obtained by solving from the quantum equation for long laser pulses corresponding to narrow radiation spectra, fluctuations of quadratures then being taken into account. A review of experimental studies already made indicates that nonclassical states of light in highly coherent beams of weak lasers such as a milliwatt He-Ne laser are most readily realized in a hybrid device consisting of two liquid crystals, a cholesteric one with distributed feedback behind a nematic and thus highly nonlinear one. Noteworthy is the possibility of using a polarization interferometer for heterodyning light very efficiently. Figures 6; references 42.

## Effect of Optical Nonlinearity on Field Distribution of Modes in Optical Fibers

[Article by I. A. Goncharenko, Institute of Electronics at Byelarusian Academy of Sciences; UDC 621.372.826.029.7:535.530.182]

[Abstract] The problem of optical nonlinearity in an anisotropic optical fiber is analyzed for its effect on the field distribution and parameters of guided modes, as a typical case being considered optical radiation of high intensity propagating through a circular fiber which consists of an anisotropic core and an isotropic cladding. The three nonzero diagonal components of the rank-3 permittivity tensor must in this case all be expressed as sums of linear and nonlinear dielectric permittivity. Inasmuch as a such a medium has an inversion center, its nonlinear properties depend principally on its nonlinear third-order susceptibility. Calculations are based on the displacement formula for a nonlinear fiber and the results are compared with those of analogous calculations made for a linear isotropic one serving as reference. The comparison reveals that optical nonlinearity tends to confine the guided modes within the core. In polarized light, depending on the direction of its polarization as well as on the quantitative relation between the tensor components of nonlinear susceptibity, birefringence induced by such a light in the fiber core will either amplify or attenuate birefringence due to anisotropy of its dielectric permittivity and thus correspondingly change the concentration of modes. Within a certain range of kr (k - wave number, r - radial coordinate) birefringence due anisotropy of the core and birefringence due to polarization of the light may even cancel each other out. Figures 2; references 6.

## Optical Characteristics of Laser Plasma During Initial Stage of Expansion

[Article by V. V. Kolchin, Moscow State University imeni M. V. Lomonosov; UDC 621.373.826:533.9]

[Abstract] Interaction of optical radiation and a laser plasma during the latter's initial stage of expansion is analyzed on the basis of the Born-Wolf equation for the electric field of an s-polarized wave propagating through a plane plasma layer. Incidence of a laser pulse is considered, in which case this equation must be supplemented with the equations of hydrodynamics describing the plasma expansion, the equation of heat conduction describing the temperature field, and the equation of ionization kinetics. This is done in the approximation of isothermal expansion in vacuum. A self-consistent analytical solution to the interaction problem is then obtained by the Wentzel-Kramers-Brillouin method. For a determination of the maximum duration of a laser pulse still ensuring transfer of most of its energy to the solid target material under a homogeneous plasma layer, the Born-Wolf equation was integrated numerically by the Runge Kutta method and this critical duration to be inversely proportional to the plasma temperature. Numerical estimates pertaining to a silicon plasma treated with 0.78 µm radiation and a tungsten plasma treated with 0.308 µm radiation indicate that the pulse duration should not exceed 200-100 fs when the plasma temperature is 150-300 eV. Figures 2; references 9.

## Electric Field of Laser Spark During Breakdown in Air

[Article by Ye. S. Zhivopistsev, I. V. Klimov, Ye. Yu. Markelov, V. V. Korobkin, and S. L. Motylev, Institute of General Physics at Russian Academy of Sciences; UDC 533.9]

[Abstract] An experimental study of optical breakdown in air upon incidence of a laser spark was made, of concern being the electric field induced in the process. Breakdown was initiated by means of a glass:Nd laser emitting a beam with a power density of approximately 1 TW/cm² in pulses of 0.2 J energy and 30 ns at half-amplitude level. The radiation, after passage through a substrate wedge, was focused by a lens with 5 cm focal length into a spot with a 10 μm diameter in the waist so as to form a spark there. A small segment of a 50 Ω - 1 pF coaxial cable acting as an electric probe was placed in vicinity of the breakdown region behind the spark, its output signal being boosted by a U3-33 wideband amplifier and then recorded either on an S8-14 with a 50 Ω matching load or on an S1-75 oscillograph. The wedge deflected some radiation through a focusing lens into a calorimeter and some radiation through a focusing lens into a photoelectric colorimeter. Measurement of the electric potential distribution revealed a uniform profile within the spark region between a positive jump at its near edge and a negative jump at its far edge, an electric dipole thus having formed in the breakdown region. The size of this dipole was measured by moving the spark between shots along the axis passing through the center of a small hole in a thin metal foil, the latter having been electrically connected to the grounded cable braid. For measurement of the velocity of a breakdown wave, an image of the spark was formed by an objective with x5 magnification on the photocathode of an electron-optical camera equipped with infrared filters. For measurement of the velocity of lateral plasma expansion, an image of the spark was formed in the camera by the objective in a different way: by light passing from the objective through a Love prism into a transverse slit in a screen for time analysis and from there through a second objective into that camera equipped with light filters. The data are analyzed for an evaluation of the dipole moment, considering several mechanisms involved in the action of a laser spark. The results of theoretical calculations based on a laser power of 10 MW and an electron concentration of 6 x 10²⁰ cm⁻³ in a breakdown wave of 1 TW/cm² intensity indicate that the Lorentz force induced by interaction of the electric field with the toroidal magnetic field in the laterally expanding plasma was the main contributor to the dipole moment in this experiment. An evaluation of the two dipole moments related to longitudinal polarization of the plasma, the one behind the compression peak associated with plasma polarization owing to electron temperature and concentration gradients and the oppositely oriented one at the breakdown wavefront related to plasma polarization by the axisymmetric magnetic field, reveals a high degree of compensation leaving an only small net dipole moment due to the polarization mechanism. The dipole moment related to light pressure building up during radiation absorption by the plasma

was negligible, even according to upper bound estimates. The authors thank G.A. Askaryan for helpful discussion. Figures 6; references 7.

## Generation of Steady Picosecond Pulses in Crystals of Potassium-Gadolinium Tungstate Doped With Neodymium

[Article by V. S. Gulev, K. P. Komarov, A. S. Kuchyanov, V. D. Ugozhayev, A. A. Pavlyuk, and V. F. Nesterenko, Institute of Automation and Electrometry and Institute of Inorganic Chemistry in Siberian Department of Russian Academy of Sciences; UDC 621.375.826]

[Abstract] An experimental study was made concerning the feasibility of using crystals of potassium-gadolinium tungstate doped with neodymium ions (K-Gd-W:Nd³⁺), a little known laser material, as a source of high-power picosecond light pulses. These crystals feature a larger cross-section for stimulated radiation emission (3.7 x 10⁻¹⁹ cm²) and a wider emission band (37 cm⁻¹) as well as a higher concentration of activating ions (2.2 x 10²⁰ than do YAG:Nd³⁺ crystals, their emission threshold thus being much lower under the same conditions. Their thermal conductivity is also much lower, however, which limits the maximum attainable pulse repetition rate. Another feature of these crystals is their high degree of optical homogeneity, almost approaching that of glass. The source of picosecond monopulses in the experiment was a master laser oscillator with passive mode locking provided by a cell with an ethanol solution of 3274-u dye between two 0.2 mm wide clearances and stabilized by a saturating radiation absorber. The active medium, a 90 mm long and 5 mm in diameter K-Gd-W:Nd³⁺ single crystal, was placed in a K-301V quantron and pumped by one IFP-800 flash lamp in pulses whose durations was varied as far down as about 300 σ. The about 2 m long optical cavity was formed by a spherical mirror and a plane one, an opaque plane mirror or a special total-internal-reflection prism "folding" the cavity into two arms. The intracavity radiation in the first arm was optimally focused into that absorber cell and its intensity or rather, more precisely, its average intensity over a longitudinal propagation period was stabilized by an optoelectronic negative feedback. A diaphragm with a hole about 3 mm in diameter served as selector of longitudinal modes. Into the cavity was inserted a biconvex lens with an about 7 cm focal length and with one focus at the center of curvature of the spherical mirror. The absorber cell was placed near that focus. The "folding" mirror reflected the intracavity radiation through an electrooptical quarter-wave control shutter to the plane mirror at the end of the other cavity arm. The shutter consisted of an Archard-Taylor prism with two exits, modified to serve as a polarizer, and an ML-102 modulator. Negative feedback controlling the master oscillator was provided by two photodiodes receiving a part of the radiation through the polarizer exits and sending their electric output signals to an electronic "two inputs - one output," which in turn sent its output signal to the shutter. Radiation pulses leaving the cavity through the second polarizer exit proceeded, after reflection by a plane mirror,

through two confocal biconvex to a two-pass amplifier: a 120 mm long and 10 mm in diameter K-Gd-W:Nd$^{3+}$ single crystal inside another quantron. Another cell containing an ethanol solution of 3274-u dye was inserted between the two lenses for passive mode locking. Return passage of radiation pulses through the amplifier crystal along a different but parallel path was then secured by a Porro prism placed behind on the common optical axis, the radiation pulses leaving the amplifier crystal in the reverse direction then being reflected by another Porro prism off the optical axis directly into a recording FD-10-129 photodetector diode. The output radiation was also recorded on an S1-75 oscillograph. Time sweeps of the emission spectrum having a 5 cm$^{-1}$ dispersion were obtained with the aid of a Fabry-Perot interferometer on a 1 mm long base and fixed on photographic film by a streak camera. Ultrashort radiation pulses of about 4 ps duration and with an about 2.6 cm$^{-1}$ wide spectrum were generated in this experiment at repetition rates up to 10 Hz. Their power density, estimated on the basis these data, was not higher than 0.3 GW/cm$^2$ and thus still below the not lower than 0.5 GW/cm$^2$ threshold for spontaneous stimulated Raman scattering. Figures 2; references 10.

## Generation of Intense Ultrashort Pulses With Intricate Energy Spectrum in Superradiating Systems

[Article by V. V. Zheleznyakov, V. V. Kocharovskiy, and Vl. V. Kocharovskiy, Institute of Applied Physics at Russian Academy of Sciences, Nizhniy Novgorod; UDC 539.184+621.385]

[Abstract] Superradiation as a mechanism for generating pulses of extremely short duration but high intensity is analyzed by considering spontaneous cooperative and coherent radiation emission. Each of these three radiation emission characteristics and the requirements for attaining them are defined, whereupon Diecke's two-level model is extended to superradiation emission by arbitrary oscillators in the "mean field" approximation and instability in an inverted medium is described by the the semiclassical Maxwell-Bloch equations for the simple case of exact resonance. Estimates based on quantitative relations between relevant parameters indicate that, with a given concentration N of active oscillators, superradiation of maximum intensity will be emitted by a cylindrical device having a volume $V_c = S_c L_c$ ($S_c$ - area of Fresnel surface, $L_c$ - cooperation length). With typically N = $10^{11}$ cm$^{-3}$, nanosecond pulses of 10 W/cm$^2$ intensity may be emitted at a quantum efficiency g $\approx$ 1. Shorter durations (below 100 ps) and higher intensities (above 100 MW/cm$^2$) have been attained experimentally by utilization of fast transient processes attending stimulated Raman scattering, particularly off-resonance cooperative and coherent Raman scattering of intense pumping radiation into Stokes and anti-Stokes components. Examples of Diecke superradiation with a more intricate energy spectrum are shown to be that

emitted within the ranges of anomalous and normal Doppler effects, also single-mode or multimode cyclotron emitted by an electron flux in a magnetic field. Next is considered superradiation emission by other than Diecke systems, namely a system of three-level molecules emitting "dressed" superradiation and a system of excited slightly nonlinear, thus slightly anharmonic, classical oscillators with a quasi-equidistant spectrum of energy levels. The analysis is then extended to emission of recombination superradiation during interband transitions in a semiconductor, where the oscillators are not identical nor are the spectral lines uniformly broadened, to emission of annihilation superradiation by a cluster of electrons and positrons, and to superradiation emission by a free-electron laser. Figures 7; references 59.

## Effect of Nonlinear Mode Interaction on Stability of Radiation Emission by Monoblock Ring Lasers

[Article by V. V. Dedysh, N. V. Kravtsov, V. Ye. Nadtochek, O. Ye. Naniy, and V. V. Firsov, Scientific Research Institute of Nuclear Physics and Moscow State University imeni M. V. Lomonosov; UDC 621.373.8]

[Abstract] An experimental study concerning solid-state monoblock ring lasers and causes of their instability was made, a YAG:Nd$^{3+}$-laser crystal in the form of an intricate polyhedron being for this purpose tested in a planar optical cavity and also in a nonplanar one. This laser was placed inside an thermostatic chamber controllable by an external temperature regulator and pumped either by an InGaAsP/GaAs semiconductor laser with 805-810 µm radiation or by an Ar-laser with 514.5 nm radiation through a focusing pair of biconvex lenses, the semiconductor laser having been placed inside a TEMO-9 microcooler chamber and both drawing power from a common very stable voltage supply. Radiation emitted by the solid-state laser in two directions was accordingly picked up by two photodiodes, whose electric output signals were fed into a recording and measuring apparatus: a spectrum analyzer, an oscillograph, and a microcomputer. The experiment was designed for simultaneously recording not only the optical emission spectrum and the transverse field distribution of the two counterpropagating waves but also the amplitude modulation spectrum. Measurements made in absence of an external magnetic field revealed bidirectional emission and two counterpagating waves of about the same intensity. With pump power levels only slightly above the emission threshold level, stable bidirectional single-frequency emission in the fundamental TEM$_{00}$ mode was found to be attainable by fine adjustment of the monoblock orientation relative to the pumping laser beam. A continuous variation of the monoblock and crystal temperature over the -5-(+40)°C range was found to alternate steady emission with nonsteady spike emission in equal temperature intervals. Measurements of both the optical spectra and the low-frequency noise (0.001-100 kHz) power, characterized by the amplitude of the envelope, revealed the presence of only one spectral component

within the wider temperature ranges of steady emission and two longitudinal modes within the narrower temperature ranges of nonsteady spike emission corresponding to maximum noise power. Measurements of emission in the self-modulation mode revealed that, at a pump power level below the critical, changing the temperature in one direction even over a wide range did not curtail such an emission but was attended by periodic (with respect to temperature) changes in the width of the emission line at the also changing self-modulation frequency. A strong external magnetic field of higher than 500 Oe intensity was found to suppress one of the counterpropagating waves and thus pull the laser into the traveling-wave mode with the emission spectrum shrunk into a single longitudinal mode and the emission power stability appreciably boosted. A weak external magnetic field of 100-200 Oe intensity was not capable of suppressing one wave, but was found to also appreciably attenuate irregular spikes of fluctuating radiation intensity and stabilize bidirectional radiation emission. An external magnetic field of intermediate intensity within the 200-500 Oe range was found to pull the laser into a regular self-modulation mode with two narrow-band components in the low-frequency part of the spectrum, their frequency separation being proportional to intensity of the magnetic field. Figures 3; references 4.

## Self-Modulated Radiation Emission in Diode-Pumped Ring Laser

[Article by Yu. D. Golyayev, V. V. Dedysh, V. G. Dmitriyev, N. V. Kravtsov, Ye. G. Lariontsev, A. L. Livintsev, O. Ye. Naniy, V. Ye. Nadtocheyev, T. I. Solovyeva, V. V. Firsov, and T. V. Veselovskaya, Scientific Research Institute of Nuclear Physics at Moscow State University imeni M. V. Lomonosov and Scientific Research Institute "Polyus" (Pole); UDC 621.373.8]

[Abstract] The self-modulation mode of radiation emission in very stable monolithic solid-state ring lasers is analyzed, an important factor determining the character of this emission mode being the inequality of the cavity Q-factors in the two opposite directions. It is for the first time demonstrated, by numerical simulation and with experimental data, that the inequality of Q-factors leads to several bifurcations of self-modulation modes as well as to bistability and hysteresis. The theoretical proof is based on a system of three equations for the complex amplitudes of two waves $E_{1,2}$ counterpropagating in a ring laser with a zeroth-order and two respective second-order space harmonics of inversion population. As long as the relative Q-factor difference $\delta = 2/Q_1 - Q_2/Q_1 + Q_2$ is smaller than a critical difference $\delta_0$, sinusoidal antiphase intensity self-modulation remains stable and the inversion population remains constant in time (negligibly small depth of frequency modulation). When the relative Q-factor difference exceeds that critical one, sinusoidal self-modulation becomes unstable and transition to another mode occurs with attendant doubling of the period and change of the

waveform. The waveform is then also distorted by relaxation oscillations of the population difference. The new self-modulation mode is stable as long as the absolute relative Q-factor difference $\delta$ is smaller the next higher critical one $\delta_1 > \delta_0$. The magnitudes of both critical Q-factor differences $\delta_0$ and $\delta_1$ are determined by parameters of the chip laser such as width of the resonance band and excess pump factor characterizing the pump level above the emission threshold. When the absolute relative Q-factor difference exceeds $\delta_1$, this self-modulation mode becomes replaced by one with a low-frequency envelope. The frequency of that envelope depends on the relative Q-factor difference and increases as the latter does up to the next critical one $\delta_2$, which represents the upper limit for periodic self-modulation. Above that limit self-modulation is random and remains so long as the relative Q-factor difference is smaller than the next critical one $\delta_3$, above which self-modulation has vanished and emission has become a steady unidirectional one. An experiment was performed with monolithic-chip lasers using high-quality YAG:Nd$^{3+}$ single crystals in the form of an intricate polyhedron each as the active medium, a planar or nonplanar ring cavity being established as a result of total internal reflections by the crystal facets. Such a crystal was pumped by an ILPN-112A 250 W semiconductor laser with 810 nm radiation through a spherical YAG crystal facet which had been coated with a selective mirror film reflecting 1.06 $\mu$m radiation but transmitting 0.81 $\mu$m radiation so as to let it in. Both lasers were temperature-stabilized, but each separately. Tests revealed self-modulation at temperatures from -150°C to 20°C and at pumping levels 1.1-3.5 times the emission threshold. Under optimum conditions for emission the frequency instability of self-modulation at a frequency within the 100-150 kHz range did not exceed a few hertz over an about 10 s long period of time. While rotation of the laser was found to produce an optical phase nonreciprocity of a magnitude depending on the contour area of the ring, application of an external magnetic field was found to produce optical phase and amplitude nonreciprocities of magnitudes depending principally on the cavity configuration. The results of measurements reveal the influence of the latter nonreciprocities on the self-modulation frequency in the form of its dependence on the intensity of an external magnetic field, under conditions of equal Q-factors ($\delta = 0$) as well as under conditions of Q-factor difference within the $\delta_1 < \delta < \delta_2$ range. Figures 5.

## Nonlinear Interaction of Radiation Field and Host Material in Alexandrite Lasers

[Article by V. S. Gulev, Institute of Automation and Electrometry in Siberian Department of Russian Academy of Sciences; UDC 621.373.8]

[Abstract] An experimental study of alexandrite as active laser medium was made concerning the earlier discovered reproducible and thus not accidental gaps in the luminescence spectrum of an alexandrite laser, with or without a

potassium cell inside a vacuum cavity made poorly selective by use of only one selector prism. Stability and reproducibility of these spectral gaps indicate that some radiation absorption is taking place, the experiment having been designed to locate the absorption centers responsible for those gaps. As the dispersing element for intracavity laser spectroscopy was used a 60° prism made of STF-3 glass, such a prism facilitating emission of wide-spectrum radiation and orientation of its active faces at a close to Brewster angle minimizing insertion losses in this inherently low-gain pulsed laser. Nine crystals were tested inside a vacuum cavity, all of them 5 mm in diameter and 60-70 mm long, each cut form a differently grown single crystal and some of those grown by various modifications of the Czochralski method. Their opposite end faces, either parallel or at some angle to each other, were not coated with bleaching films. Measurements were made in the free emission mode with an apparatus consisting of an STE-1 spectrograph, a prismatic deflector system, a set of lenses, and a streak camera, including also two oscillographs (S1-70 and S1-75), a set of avalanche diodes, and a calorimeter. All spectrograms were calibrated against the two 769.9 nm and 766.5 nm D-lines of the potassium atom. Without the dispersing prism inside the cavity, the emission spectrum was approximately 1-2 nm wide about the 750 nm center line. With the dispersing prism inside the cavity, the emission spectrum was 5-15 nm wide depending on the spectral band, the emission then being tunable over the 730-780 nm range. The study has confirmed the existence of two gaps in the emission spectrum of an alexandrite laser, one about the 740 nm absorption line and one about the 758.5 nm absorption line. It has also demonstrated that these gaps are due to radiation absorption not by the prism material but by the crystal in its excited state, radiation absorption by atmospheric oxygen and water vapor evidently playing no role here. The authors thank S.G. Rautian for support, V.P. Safonov, V.D. Ugozhayev, and A.M. Yurkin for helpful discussions, also A.I. Alimpiyev, V.V. Gurov, and Ye.G. Tsvetkov for supplying the alexandrite crystals. Figures 2; references 10.

## Laser With Synthetic Aperture, Phase Conjugation, and Radiation Pulse Compression

[Article by V. N. Belousov, A. M. Mamin, Yu. K. Niziyenko, and A. R. Sidorov, Institute of Atomic Energy imeni I.V. Kurchatov, branch; UDC 535.375]

[Abstract] A laser system with two amplifying stages has been designed which combines the advantages of wide apertures with those of small apertures, this being achieved by synthesizing the apertures of the wide-apertures of the first two amplifiers with loosely spaced active medium elements and pumping lamps between them. The outgoing radiation beam, though consisting of closely packed fragments, is controlled as a single solid one by means of a raster before the two-pass first amplifying stage. The
raster, which consists of nonlinear phase conjugate mirrors, splits the incoming beam on the forward pass into separate fragments corresponding to the respective active medium elements and then converge these fragments on the return pass. The scheme was tested with a master laser oscillator operating in the $TEM_{00}$ mode and emitting radiation pulses of 25 ns duration at half-amplitude level. The radiation beam carried by such a pulse, after having been widened by a x10 magnifying telescope and diffracted by a 12 mm square aperture stop, entered the first amplifying stage. This stage consisted of two amplifiers with active medium elements in the form of GLS-32 glass rods 20 mm in diameter, two Faraday rotation isolators, and a phase conjugate mirror. The mirror was a cell with $SF_6$ gas under a pressure of 15 atm, into which the radiation was focused by a lens with a 50 cm focal length. Here stimulated Brillouin-Mandelshtam scattering back-reflected about 80 percent of the radiation back without an appreciable distortion of the pulse form. After its second pass through this amplifying stage, a polarizer between the two rotation isolators extracted from it a beam with an energy of about 3 J for passage through a x3 magnifying telescope into the second amplifying stage. This one consisted of a polarizer + Fresnel rhomb decouplinng set, a raster, an amplifier, and a multichannel SBMS (stimulated Brillouin-Mandelshtam scattering) pulse compressor. The amplifier had a compound active medium consisting of nine loosely spaced elements in the form of GLS-21 glass rods 20 mm in diameter, with pumping lamps between them. The raster with a 40 mm square cross-section split the incoming beam into nine fragments with a 12 mm square cross-section each. The pulse compressor consisted of nine 300 cm long SBMS-mirror cells with $SF_6$ gas and with a 0.5 reflection coefficient, into which the radiation was focused by lenses with a 260 cm focal length each. Phase conjugation in these cells made the radiation fragments, after their two passes through the active medium elements, converge in the raster into a closely packed beam with a 40 mm square cross-section. Nine subapertures were thus formed upon diffraction in the raster with only about 1 mm wide gaps between them. The divergence of the outgoing laser beam was measured in terms of its energy distribution in the focal plane of a lens with an 8 m focal length. Through a 0.8 mm square diaphragm was extracted 70 percent of the incident energy, this corresponding to the diffraction limit for the 12 mm square aperture. Radiation emission in pulses of about 2 J energy and of an only about 2.5 ns short duration at half-amplitude level from each compressor was attainable, with all nine beams combining into one with an energy of 20 J at the exit of this laser system. Figures 2; references 2.

## Numerical Analysis of Pulse Amplification With Phase Modulation in XeCl Excimer Medium

[Article by V. P. Kandidov and A. V. Korzhonov, Moscow State University imeni M. V. Lomonosov; UDC 621.373.826]

[Abstract] The performance of an XeCl-laser amplifier is analyzed for efficiency of energy extraction from this excimer medium after subpicosecond radiation pulses with various characteristics have been amplified in it. The system of four Maxwell-Bloch equations in the two-level approximation and ignoring the coherent $j \to j+/-2$ transition is selected as the basis for a numerical analysis, this model being valid in the case of pulse durations shorter than the reciprocal of the width of the emission line and a mean life of the lower level usually being much shorter than that. Assuming here Boltzmann distributions of rotational and vibrational levels with a 300 K temperature inside XeCl(B) prior to arrival of a radiation pulse, both rotational and transverse vibrational relaxation time constants are set equal to $1/\gamma$. Calculations have been made for Gaussian radiation pulses of 10.0 ps, 1.0 ps, and 350 fs durations, the Franck-Condon factors being smaller than unity for rotational number $j < 80$. They have yielded an output energy of 4.8 mJ/cm$^2$, 5.7 mJ/cm$^2$, and 7.3 mJ/cm$^2$ respectively. The effective saturation energy was calculated using the best approximation to the Franz-Nodvik relation, which yielded 0.49 mJ/cm$^2$, 0.52 mJ/cm$^2$, and 1.0 mJ/cm$^2$ respectively. The much higher energy in a 350 fs pulse is evidently the consequence of the spectrum of such a pulse covering several vibrational bands, the two longer pulses fitting into only the one 26 cm$^{-1}$ band. Phase modulation during amplification is found to increase the output energy in a 1.0 ps pulse by making it cover more than one band, unlike a frequency-limited pulse of this duration. Phase modulation does not change the energy in a 10.0 ps pulse, because such a pulse then still does not cover more than one band. It also does change the energy of a 350 fs pulse, because the spectrum of such pulse is already wider than than the amplification line. Figures 2; references 10.

## Relation of Photoprocesses in Series of Complex Aromatic Heterocyclic Molecules to Constitution and Structure of Their Excited Electronic States

[Article by A. Ye. Obukhov, Russian University of Friendship Among Nations; UDC 621.378:535.37]

[Abstract] New aromatic polycyclic and N-, O-, S-heterocyclic oxazole and oxadiazole compounds forming a quasi-homologous series have been synthesized, the purpose being to establish how their fluorescence and lasing characteristics relate to the electronic states and the structure of their molecules. The complex molecules of these organic compounds cover a wide range of atomic orbitals and molecular orbitals so that electron-vibration and spin-orbit interactions attending excitation of electronic states and subsequent conversion of the excitation energy into radiation energy change along the series. Three mechanisms of constitutional changes along the series are identified: 1) successive monocyclic $\to$ bicyclic $\to$ tricyclic $\to$ pentacyclic polyphenyl and N-, O-, S-heptaryl transitions; 2) replacement of atoms with smaller number by atoms with larger number as, for example, -C- $\to$ -N or -O- $\to$ -S- while number of cycles and spatial configuration remain the same; 3) change of the number of molecular substructures and of their order of interlinkage in the spatial configuration as, for example, in change from saturated to unsaturated bonding or substitution of a subgroup by another one with a different electronic structure while the ratio of the number of atomic orbitals to the number of molecular ones remains the same. The radiation emission characteristics of 21 compounds optically active as vapors or in certain liquid solvents are analyzed and evaluated on the basis of available experimental data on their ultraviolet absorption, fluorescence (260-560 nm), induced singlet-singlet absorption, induced triplet-triplet absorption, and lasing (335-560 nm) spectra. These compounds include 2Me-O, PO, FO, TO, PP, PO-COOH, PO-COOMe, FOo (oxazole end cycle with saturated bonds), POO, TOO, OPO, OFO, OTO, PPP, POP, PFP, BOP, POT, POTOP, BOTOP, (O - oxazole, B - benzo or benzene, F - furyl, P - phenyl, T - thiophenyl or thienyl, furyl, Me - metal). The relevant parameters (cross-sections for and mean life of radiative state, preionization time, wavelength of maximum emission, rate constants of radiative decay and of interconversions) have been calculated by various theoretical methods (Molecular Orbitals, Linear Combinations of Atomic Orbitals, and others). The results agree with those of calculations made by semiempirical methods within the errors of the latter, which ensures their validity. They reveal a quasi-independent relaxation of excitation energy in individual molecular substructures. It is possible, therefore, to comprehensively calculate all relevant radiation emission parameters for any new complex molecule in this quasi-homologous series in this quasi-homologous series when the equilibrium configuration of nuclei in its actual or hypothetical structure is given. Figures 3; tables 3; references 20.

## Diffraction Switching Waves and Autosolitons in a Laser With a Saturable Absorbing Agent

[Article by N. N. Rozanov, S. V. Fedorov, S. I. Vavilov State Optical Institute, St. Peterburg; UDC 535.14+621.373:535]

[Abstract] A theory of spatial structures in wide-aperture lasers with a saturable absorber is proposed. The study of these spatial structures in transversely homogeneous wide-aperture lasers is of interest as it applies to digital optical computing and the control of laser radiation characteristics. Diffraction switching waves were analytically studied as well as their associated particle-like states, diffraction autosolitons. Diffraction autosolitons are steady-state islets of generation whose width is on the order of the Fresnel zone of an interferometer. The speed of a switching wave is calculated, as well as the discrete spectrum of the widths of autosolitons and their associated states. The kinetics of the formation of diffraction switching waves and autosolitons are numerically studied. The existence of diffraction switching waves and positive and negative

diffraction autosolitons is confirmed. The collision of two switching waves leads to the formation of a narrow steady-state ejection or a diffraction autosoliton in the ground state. The temporal relation between the distance between the fronts of two switching waves and the phase of the laser radiation averaged over this distance shows that the shift in the generation frequency for diffraction autosolitons occurs simultaneously with the establishment of the width of the diffraction autosoliton in the ground state. The shift in frequency is always nonzero. Figures 3; references 6: 4 Russian, 2 Western.

### Diffraction Autosolitons and Spatial Structures in Transverse Instability Conditions

[Article by N. N. Rozanov, G. V. Khodova, S. I. Vavilov State Optical Institute, St. Petersburg; UDC 535.14]

[Abstract] Diffraction autosolitons are particle-like field strucutres in wide-aperture nonlinear interferometers. They are formed due to a rather large initial field ejection on a background of "smooth" structures. High excitation of diffraction autosolitons and associated field structures are analyzed in a wide-aperture passive nonlinear interferometer excited by continuous coherent radiation in the presence of transverse radiation instabilities. The case of an interferometer with an unstable resonator is also examined. The evolution of the spatial field structure is tracked as the resonator increase coefficient rises. Figures 5; references 7: 4 Russian, 3 Western.

### New Modulation Method of Measuring Thin Film Absorption Spectra

[Article by L. M. Blinov, S. P. Palto, A. A. Udalyev, Institute of Crystallography, Moscow; UDC 535.34:539.238]

[Abstract] A new modulation method is proposed for measuring the absorption spectra of thin films. The principal feature of measurement is the use of a one-beam spectrophotometer with mechanical scanning of a beam along the surface of an immobile sample. Movement of the light source leads to the appearance of a parasite signal, but this method compensates for this by obtaining the signal at a higher modulation harmonic and filtering out the parasite singal. When the signal is recorded at one of the high modulation harmonics, this significantly improves the signal to noise ratio and makes it possible to measure the absorption of very thin films (for example, monomolecular layers) in a helium cryostat. For comparison, the absorption spectra of films obtained using another modulation method are presented, where the sample is rotated and the light beam is immobile. It is found that both sample rotation and light beam rotation can be used successfully to measure the absorption spectra of thin films. The latter

can be used to make measurements in cryostats in a wide spectral interval, especially in the infrared. Figures 4; references 5: 4 Russian, 1 Western.

### Diffraction of an Inhomogeneous Wave on a Cylinder

[Article by Ye. I. Ivlev, Scientific Research Institute of Industrial Glass, Moscow; UDC 535.42]

[Abstract] The problem of the diffraction of inhomogeneous (attenuating) waves on an infinite cylinder and the prospects for this method are shown in the study of micro-objects. The method of vector cylindrical harmonics is used to solve the problem of the diffraction of inhomogeneous waves on an infinite homogeneous right circular cylinder. Compared with homogeneous waves, the degree of inhomogeneity of a scattered wave has a substantial effect on the scattering of the radiation of an inhomogeneous wave. This makes it possible to use inhomogeneous waves to measure structural parameters of inhomogeneous waves, to measure the parameters of micro-objects with extremely high resolution, to perform local sensing of micro-objects, and to perform high-resolution tomographic study of optical fibers. To illustrate the findings, the article finds the coefficients of effectiveness of scattering for the arbitrarily polarized radiation of an inhomogeneous wave. It is found that there are substantial qualitative and quantitative differences in the scattering of inhomogeneous waves versus the scattering of homogeneous waves. Figure 1; references 8: 5 Russian, 3 Western.

### Modulation Methods in Holographic Interferometry

[Article by G. R. Lokshin, S. M. Kozel, I. S. Klimenko, and V. Ye. Belonuchkin, Moscow Physicotechnical Institute; UDC 535.317.1]

[Abstract] This article discusses the capabilities of methods of increasing the sensitivity, accuracy, and range of measurements in holographic interferometry based on spatial modulation of the illuminating laser beam. Spatial modulation of the radiation illuminating an object makes it possible to use the oscillations in visibility which arise when the object is shifted to measure small shifts with relatively high accuracy. The advantage of modulated illumination is mainly that restoration of visibility in oscillations reaches values near unity. In spatially modulated illumination, small shifts fo the object lead to a sharper change in visibility than in traditional illumination. Thus, oscillations in visiblity become a new real channel for obtaining informaiton on small shifts. Figure 1; references: 6 Russian.

## Polarization Splitting of the Propagation Plane of a Local Wave in a Step-Profile Multimode Fiber

[Article by A. V. Volyar, A. V. Gnatovskiy, S. N. Lapayeva, V. I. Myagkov, M. V Frunze Simferopol University, Institute of Physics, Ukrainian Academy of Sciences; UDC 535.2:666.130]

[Abstract] An attempt is made to examine the optical Magnus effect and the accompanying phenomena in a multi-mode step-profile fiber by considering the change in light polarization. It is assumed that the light propagates mainly along meridional ray trajectories. The original polarization is right-circular polarization. Torsion and splitting of a meridional plane in these multimode fibers is experimentally and theoretically examined. It is found that electro-refraction processes in the modulator have no effect on the excitation conditions of the fiber. The splitting of the meridional plane is thought to be associated with the expansion of the linear polarization of light into two circular polarizations. These polarizations lead to opposed twisting of the meridional planes. Figures 2; references: 13 Russian.

## Measurement of the Nonlinearity of Photochromic Media Based on Transient Polarization Transformation in Two-Beam Interaction

[Article by V. Yu. Bazhenov, O. A. Kulikovskaya, V. B. Taranenko, Ye. V. Shishkalova, Institute of Physics, Ukrainian Academy of Sciences; UDC 621.315]

[Abstract] This article presents a highly sensitive method of measuring the nonlinearity parameters of isotropic dynamic photochromic media based on transient transformation of polarization in the interaction of two continuous laser beams with undegenerated polarization. The phase of one of the beams is time modulated according to a power law. The example of an aqueous suspension of purple membranes containing photochromic molecules of natural and genetically modified bacterial rhodopsin is used to demonstrate the possibility of measuring the ratio of the real and imaginary parts of the nonlinearity coefficient, as well as its absolute value and nonlinearity realization time. Figures 8; table 1; references 10: 3 Russian, 7 Western.

## Effect of Finite Photoreceptor Aperture Dimensions on the Measured Depolarization of Scattered Radiation

[Article by V. N. Kurashov, V. V. Maryenko, T. V. Molebnaya, A. G. Chumakov, T. Shevchenko Kiev University; UDC 535.36:535.51]

[Abstract] Numerical modeling of the measurement of a scattered field is used to obtain the probability density function of the measured degree of polarization and its characteristic for different values of the relative radius of correlation of the speckle field (in units of the linear size of the photoreceptor aperture). Results of numerical and real experiments are presented which indicate a decrease in the average degree of polarization as the relative radius of correlation decreases. A possible physical cause of the existing divergence in the rate of decrease of the average degree of polarization in calculations and measurements for low values of the coefficient of correlation of the speckle field is discussed. It is proposed that one can determine the radius of correlation of the speckle structure using two measured values of the average degree of polarization or its calculated dependences on the relative correlation radius. Figures 2; references 9: 6 Russian, 3 Western.

## Parametric Formation of Transverse Surface Acoustic Waves With a SHF Electric Field

[Article by T. I. Bondarenko, G. N. Burlak, T. Shevchenko Kiev University; UDC 534.8]

[Abstract] It has been shown that transverse surface acoustic waves can be propagated in semi-bounded centrally symmetrical crystals by applying a constant electric field. The rate of propagation and the depth of penetration can be regulated by adjusting the electric field. A high-frequency electric field yields substantially better control. The most interesting area is the zone of parametric resonance of acoustic waves with a SHF field. This article studies in detail the zone of parametric resonance and demonstrates the tuning of the profile and spectrum of transverse surface acoustic waves in parametric excitation. It is found that in the case of resonance, the depth of penetration is about three orders of magnitude lower than in the nonresonant case. The mechanism of parametric excitation and formation of transverse surface acoustic waves is effective to frequencies on the order of $10^{11}$ - $10^{12}$ s$^{-1}$. References: 7 Russian.

## Generation and Transport of Solar Cosmic Rays (Survey)

[Article by L. I. Miroshnichenko, Institute of Terrestrial Magnetism, the Ionosphere, and Radio Wave Propagation, Russian Academy of Sciences; UDC 524.1.52]

[Abstract] The history and definition of solar proton events is described. Details of outstanding proton events during 1986-1991 are provided. Some of the outstanding events discussed are the series of flares in March 1989, in summer-fall 1989, and on 29 September 1989. The frequency of increases at the earth's surface and the maximum energy (rigidity) of solar cosmic rays are determined. The rigidity of solar cosmic ray spectra as determined by underground muon telescopes is discussed. Preliminary results of analysis of events on 24 May 1990, in March 1991, and in June 1991, are presented. Changes in the average energy of solar cosmic rays in the interplanetary medium are described, and the maximum frequency of increases at the earth's surface, the maximum number of relativistic particles, and the maximum energy are sought. It is found theoretically that there is a dependence of maximum energy on the acceleration model used. It is noted that increases in solar cosmic rays at the earth's surface are absent near solar maximum. It has been found that in the most intense events, the energy density of nonrelativistic protons may reach values comparable with the energy density of magnetic fields in interplanetary space and remote regions of the magnetosphere (the geomagnetic tail). The generation of turbulence in interplanetary plasma by solar cosmic ray electrons is mentioned. It is indicated that nonrelativistic solar protons may cause certain plasma effects in the interplanetary medium. Possible causes of a change in the angular distribution and energy spectra of cosmic rays in the interplanetary medium are outlined. Several models of this problem are described and analyzed. Attempts are made to describe the movement of solar cosmic rays in complex interplanetary structures (traps, loops, plasmoids). Issues not addressed in this article are outlined. Tables 2; references 85: 53 Russian, 32 Western.

## Relative Locations of a Powerful Flare, the Heliospheric Current Sheet, and the Earth Fostering the Onset of a Strong Geomagnetic Storm

[Article by K. G. Ivanov, A. F. Kharshiladze, Ye. P. Romashets, Institute of Terrestrial Magnetism, the Ionosphere, and Radio Wave Propagation, Russian Academy of Sciences; UDC 523,945:523.62]

[Abstract] The theory of the spread of magnetic clouds in a regularly inhomogeneous internal heliosphere indicates the strong dependence of their slowing, and consequently, the intensity of interplanetary and geomagnetic disturbance, on the relative positions of flares, the heliospheric current sheet, and the earth. Examples of eight solar flares are given. Four of these led to strong storms, and the other four led to weak disturbances, which agrees with the conclusions of the theory. The earth is hit by powerful geomagnetic storms when it is in the region where the magnetic cloud collides with the current sheet. The first results of theoretical calculations are presented, and they show that the dynamic pressure in the cloud in earth orbit and the value of the interplanetary and geomagnetic disturbancers depend greatly on the position of the flare relative to the heliospheric current sheet at an angle to the equator. Clouds from far flares start and propagate through relatively thin and fast solar wind plasma. When they reach earth orbit, their speed remains rather high and a high level of disturbances is generated when they encounter the heliospheric current sheet with its dense slow plasma. A cloud from a flare near the current sheet is slowed by dense slow plasma near the sun and arrives at earth with a much slower speed. Figures 3; table 1; references 7: 3 Russian, 4 Western.

## Quiet and Disturbed Heliospheric Streamers Near Earth

[Article by K. G. Ivanov, Institute of Terrestrial Magnetism, the Ionosphere, and Radio Wave Propagation, Russian Academy of Sciences; UDC 523.62.726:550.383]

[Abstract] The quiet state of a heliospheric streamer near earth is identified when there is no solar flare activity. Its properties are described, and it is shown for the first time that the current sheet associated with the streamer is comprised of a wide sheet coinciding with the streamer and a narrow sheet within it (the sector boundary). By comparing the field at the surface of the source and the field at the earth, it is shown that the widely held concept of kinematic transport of the interplanetary magnetic field from the surface of the source to the earth (along Parker spirals) leads to a 10- to 20-fold divergence of theoretical and experimental data. It is noted that this divergence can in principle be eliminated by considering the field of the heliospheric current sheet in a complete magnetohydrodynamic treatment of the current system of the solar wind. The properties of the disturbed state of the heliospheric streamer near earth are described and compared with the quiet state. For the first time a dense, fast current-carrying core and relatively diffuse, slow "wings" with a strong field in the opposite direction are identified in the macrostructure of the disturbed streamer. Figures 2; table 1; references 21: 11 Russian, 10 Western.

## Effect of Vibrationally Excited Nitrogen on the Formation of the Main Ionospheric Trough of Electron Density in the Ionospheric F Region

[Article by A. V. Pavlov, Institute of Terrestrial Magnetism, the Ionosphere, and Radio Wave Propagation, Russian Academy of Sciences; UDC 550.388.2]

[Abstract] This article studies the role of vibrationally excited nitrogen $N_2^*$ in the formation of the main ionospheric trough of electron density $N_e$ in the F region of the ionosphere. The vibration temperatures $T_v$ are calculated at altitudes of $120 \leq z \leq 500$ km in the main ionospheric trough region, considering horizontal transport by a neutral wind of $N_2^*$ from the region of outpouring of low energy electrons. It is shown that when there are small changes in the frequency W of formation of vibrational quanta in the transfer from the electron outpouring zone to the main ionospheric trough zone the effect of $N_2^*$ on $N_e$ will be about the same in a polar wall and at the main ionospheric trough minimum. Various factors affecting the shape of the trough are outlined. Figures 2; references 15: 8 Russian, 7 Western.

## Effects of Chemical Modification of the Ionosphere From Shortwave Doppler Measurements Over Oblique Radio Communication Lines

[Article by N. F. Blagoveshchenskaya, V. N. Borodkin, O. V. Kolosov, I. A. Shumilov, Arctic and Antarctic Scientific Research Institute, Russian Commission on Hydrometeorology; UDC 550.388.2]

[Abstract] This article examines and analyzes the effects of injections of plasma-forming substances (alkaline metal vapors, i.e., barium or cesium with lithium added) into the ionosphere using the data of multichannel Doppler observations in the decameter range along oblique radio communication lines. The configuration of transmitting and receiving stations and equipment are described. Paths passed directly through or near the emissions. Four types of processes were isolated: single surges, groups of quasiperiodic surtges, regular changes in spectral characteristics, and wave processes. The first effect involved a drastic short-term broadening of the Doppler spectrum at the time of injection. The second occurred 2-4 minutes after injection, involved 8-10 individual surges separated by 18-54 seconds. This effect lasted 4-6 minutes. The third effect involved a gradual shift in the frequencies of Doppler spectra maxima and spectral broadening. This effect began 3-15 minutes after injection. The fourth effect began 15-20 minutes after injection and lasted an hour or more. The probability of the appearance of any one effect is dependent on geophysical conditions at the time of injection. It was found that dispersion of injection products at 140-160 km could be accompanied by sharp changes in electron concentration in the E and F regions due to fast longitudinal induction of electric fields. Various mechanisms for the movement of charged particles in the atmosphere are outlined. Figures 2; table 1; references 6: 4 Russian, 2 Western.

## Observation of Electromagnetic VLF Radiation of Seismic Origin From Interkosmos-24

[Article by O. A. Molchanov, O. A. Mazhayeva, M. L. Protopopov, Institute of Earth Physics, Russian Academy of Sciences; UDC 550.386.550.34]

[Abstract] Interkosmos-24 observations of VLF radiation in the 8 Hz-20 kHz range associated with earthquakes were used to establish the following: 1) a burst of two-band radiation with a maximum in the ULF-ELF range (f < 1000 Hz) and in the VLF range (f = 10-14 kHz) is observed over the epicenter of an earthquake; 2) the intensity of spectral radiation in the ELF range falls with frequency; 3) far from the epicenter, but within the geomagnetic shell corresponding to it, one observes only VLF radiation; 4) the maximum probability of observing a burst occurs 12-24 hours before the main shock. Data are analyzed for 123 orbits between 16 November 1989 and 31 December 1989. In this interval there were 28 large earthquakes of magnitude 5.2-6.1. The results correspond to the concept of induced VLF burst radiation in the magnetosphere when there is a nonlinear interaction of primary ULF (0.01-10 Hz) Alfven waves from the seismic source with the energetic plasma of the magnetosphere. Figures 4; tables 2; references 19: 11 Russian, 8 Western.

## Anisotropy of Electron Distribution in Ultrastrong Microwave Field

[Article by A. T. Nayfonov and A. P. Napartovich, Troitsk Institute of Innovation and Thermonuclear Research; UDC 533.525]

[Abstract] Although the electron velocity distribution function for an ultrastrong field has been studied in various of its aspects, only the case of a not very high gas pressure was investigated, or the electron velocity distribution along the microwave field was studied analytically or numerically or the Monte Carlo method was used in finding the electron velocity distribution function and in computing the principal kinetic coefficients for such particular variants. The effect of anisotropic diffusion effect in a strong field was noted in such research. A study was therefore made in order to rectify some of the shortcomings and fill some of the gaps in this earlier work. An analytic expression is derived for the electron transverse velocity distribution function in an ultrastrong microwave field when the energy of an electron oscillating in the field is much greater than the ionization potential. The distribution of electrons by velocities transverse to the microwave field is determined by diffusion in an angular space during ionization collisions, by the ionization rate and by the energy distribution of secondary electrons. Expressions are derived in explicit form for the diffusion coefficient in the space of transverse velocities and for the spatial

transverse diffusion coefficient. The analytic for-
mulas agree well with the results of the published
numerical computations for helium. References 9: 8
Russian, 1 Western.

## Superionic Conductors. Research and Prospects

[Article by A. E. Aliyev, P. K. Khabibullayev, Thermal Physics Division, Academy of Sciences of the Republic of Uzbekistan; UDC 538.931:534.22.222:536.631]

[Abstract] Superionic conductors are a special class of solid-state substances characterized by an ion mobility on the same order as or higher than solutions of strong electrolytes. They are commonly found natural substances that are used in current sources, capacitors, displays, and other electronic equipment. To obtain detailed information on the generation of superionic phases and the effect of structural factors and kinetic parameters of the system on fast ion transfer in superionic conductors with differing degrees of conductivity, electric, acoustic, and thermal loads were placed on the superionic conductors and their relaxation mechanisms were studied theoretically and experimentally. The subjects were piezoelectric single crystals of iodate, $\alpha$ - $LiJO_3$, $Li_2B_4O_7$ and several rare earth trifluorides $LnFe_3$ (Ln = La, Ce, Pr, Nd). In the study of $Li_2B_4O_7$ an ionic conductive mechanism was found which is associated with leaping of the lithium cations along channels oriented along the polar axis. The electron components and ionic conductivity do not exceed $10^{-12} O^{-1}m^{-1}$. In a number of superionic compounds the relaxation mechanism is associated with thermal polarization. The concentration of ions participating in the polarization and the leap length of ions are obtained. It is shown that a characteristic of superionic conductors is the superposition of mechanical and electrical relaxations, which leads to a decrease in the sound absorption maximum and its shift toward lower temperatures. Peaks were observed in the temperature dependence of specific heat, which is interpreted as a transition to a disordered state. It was found that the transition to the superionic state is a "diffusive" transition and occurs in a wide range of temperatures. The mechanisms responsible for the fast radiation annealing and radiation stability of superionic conductors are determined. The deformation part of the migration activation energy of ions is studied and an analytical expression obtained to calculate conductivity activation energy. Figures 31; tables 5; references 77: 53 Russian, 24 Western.

## Thermal, Radiation, and Field Gettering in GaAs Surface Barrier Structures for Microwave Electronics

[Article by K. A. Ismaylov, R. V. Konakova, Yu. A. Tkhorik, L. S. Khazan, Nukus State University; UDC 621.382.2]

[Abstract] Stabilization of GaAs parameters is a pressing issue. This problem is mainly associated with internal mechanical stresses in device structures. The level of these stresses is determined by the intrinsic deformations and the properties of plastic relaxation in the semiconductor. Intrinsic deformations due to thermal mismatching of dislocations is discussed. Generation of undesirable dislocations is described. A mismatch accommodation model developed by Matthews, Nader, and Light is used to describe the process of thermal activation of dislocations. A simple expression is developed for the dependence of the reverse current on heating time. The model is suited to a description of processes of change in reverse current at heterojunctions when the device is affected by radiation, heat, intense light, etc. One should note the great effectiveness of athermal mechanisms of dislocation excitation (by radiation or a field) compared to thermal processes. This is due to the great amount of energy transferred to dislocations when accelerated particles scatter inelastically off them. Figures 4; references 4: 2 Russian, 2 Western.

## Localized States of Carriers in Superlattices Based on Semiconductors With a Complex Band Structure

[Article by R. Ya. Rasulov, U. G. Ganiyev, M. A. Mirzarakhimov, I. M. Kokanbayev, Fergana Polytechnical Institute; UDC 621.315.592]

[Abstract] In the quantum well of a thin semiconductor film where the thickness of the film is less than the free path length of the carrier, the component of the carrier's wave vector normal to the surface is quantized. The energy of the carrier is two-dimensional in the plane of the film. A Lattinger-Kon Hamiltonian is used to study dimensional quantization in semiconductors with a complex band structure of light and heavy holes near the point of degeneration. The quantum well is bounded by two potential walls of finite energy height. The energy spectrum of a carrier located at defects in a superlattice is studied using a composite superlattice of two semiconductor layers, one a quantum well and the other a potential barrier. A secular equation is obtained whose solution yields a dispersion equation for the energy of localized states of heavy and light holes. It is found that the energy localized states at superlattice defects corresponding to light and heavy holes may intersect. Depending on the type of intersection mini-subzones may arise which consist of localized states of carriers in the defect region. References 7: 6 Russian, 1 Western.

## Possible Role of Neutral Oxygen in Formation of Electron Spectrum of High-Temperature Superconductors

[Article by V. M. Loktev, Theoretical Physics Institute imeni N. N. Bogolyubov, Ukrainian Academy of Sciences; UDC 538.945]

[Abstract] The microscopic mechanism of the attraction observed between immediately neighboring p-holes as a result of the dynamic mixing of their states and the state of

neutral oxygen is discussed. It is shown that such attraction causes the formation of a branch of two-particle bound states of fermions in the electron spectrum of $CuO_2$ planes. The principal result of this study is a microscopic validation of the appearance of a branch of Bose excitations corresponding to bound states of Fermi particles (holes) in the electron spectrum of high-temperature superconductors (HTSC) (with a quasi-2D character of transport properties). It is not impossible that the presence of a boson branch in the spectrum of HTSC systems and the local pairs in the volume of a crystal corresponding to it requires some reexamination of the theory. Nevertheless, the theoretical model proposed here makes it possible to generalize superconductivity theory. Due to the 2D character of the electron properties of systems with high $T_c$ the bound states in the spectrum exist without a threshold and the very effect of formation of a local two-particle level, as occurs in the spectrum of a quasi-2D Lifshits model, decreases with increasing withdrawal of the crystal structure (and accordingly, the density of states) of HTSC systems from two-dimensional. The known $T_c$ decrease of a number of HTSC compounds after the number of $CuO_2$ planes in an element exceeds 3-4, when interplanar tunneling becomes increasing important and the density of states near the edge of the conductivity band becomes increasingly closer to three-dimensional, may be associated precisely with the described phenomenon. Figure 1; references 39: 15 Russian, 24 Western.

## Quasiparticle States Induced by Superconducting Current in S-I Superlattices

[Article by S. V. Kuplevakhskiy and I. I. Falko, Kharkov State University; Kharkov Polytechnic Institute; UDC 538.945]

[Abstract] Various spatial-periodic structures with regularly alternating layers of superconducting and nonconducting materials (S-I superlattice) are in wide use. Research was undertaken to clarify the spectral transformation of these structures in a current-carrying state. The problem is formulated in the following way. In a Cartesian coordinate system it is assumed that the x-axis is directed perpendicular to the interface of the layers, but in the directions y, z there is total homogeneity. A very simple case is considered in which the thickness of the S layers is great in comparison with the coherence length but the thickness of the I (dielectric) layers is small. The computations presented here show that the spectrum of I excitations in the presence of a superconducting current contains a Bloch band of quasiparticle states with energies in the gap region. The width of the Bloch band is a rapidly oscillating function of the superlattice period. The role of nonmagnetic impurities in the S regions is discussed. Scattering on impurities begins to exert an influence on the formation of Bloch states when the mean free path is less than the width of the potential wells near the S-I interfaces. References 8: 6 Russian, 2 Western.

## Inverse Population in Nonequilibrium State of Superconductors With Optical Pumping

[Article by A. M. Gulyan, Physical Research Institute, Armenian Academy of Sciences; UDC 538.945]

[Abstract] The term "inverse population" as used in this study is a state of the electron subsystem described by an $n_\varepsilon$ distribution function satisfying the condition $n_\varepsilon \geq \frac{1}{2}$ for some set of values of the energy of electron excitations falling in the supragap region $\varepsilon \geq \Delta$. One of the most practical methods for creating nonequilibrium states in superconductors is pumping with electromagnetic radiation with a frequency considerably exceeding the gap $\Delta$ in the spectrum of single-electron excitations, but despite many experiments to determine the influence of laser radiation on superconductivity states with an inverse population have never been registered. Moreover, much evidence indicates that an inverse population in superconductors cannot be attained with pumping by optical radiation (V. F. Yelesin, ZhETF, 66, 1755, 1974). The objective of this study is to demonstrate that the model used by Yelesin is oversimplified and real situations are possible when an inverse population would be observable. The analysis is made using the Yelesin method. The theoretical examination is made only for the case $T = 0$. The conclusion is drawn that inversely populated states in superconductors are possible when there is a non-Debye character of the phonon spectrum and sufficiently high values of the Cooper gap. Figure 1; references 16: 11 Russian, 5 Western.

## Josephson Current and Thermoelectric Phenomena in Superconducting Point Contacts

[Article by I. O. Kulik and A. N. Omelyanchuk, Low Temperatures Physical Technical Institute imeni B. I. Verkin, Ukrainian Academy of Sciences; UDC 538.945]

[Abstract] A study was made of the stationary Josephson effect in a nonequilibrium system—a superconducting point contact whose sides are at different temperatures. When the temperatures of the two sides differ the superconductor as a whole is in a nonequilibrium state in which heat and charge currents flow. In contrast to the nonequilibrium state arising with the imparting of a potential difference to a contact and characterized by a nonstationary phase slippage picture (nonstationary Josephson effect), in this case the system remains stationary. In particular, a superconducting Josephson current with some maximum value $J_c$ will flow between the sides of the contact; this flow is nonsinusoidally dependent on the phase difference. In addition to the Josephson current component, with a nonzero temperature difference an excitation current arises which also is dependent on the coherent phase difference. A stationary current mode

exists with currents $|J| < J_{max}$, no longer coinciding with the strength of the Josephson current $J_c$. Microscopic computations of these effects were made. The current-phase dependence and the critical Josephson current were determined. The heat flow and the thermo-emf of the contact, periodically dependent on the order parameter phase difference, were then computed. Figures 2; references: 8 Russian.

## Twenty-Ninth Conference on Low-Temperature Physics (Kazan, 30 June-4 July 1992)

*937J0058E Kharkov FIZIKA NIZKIKH*
*TEMPERATUR in Russian Vol 18 No 10, Oct 92*
*pp 1171-1176*

[Article by A. G. Anders, Ye. V. Bezugliy, N. Ye. Dyumin, V. G. Peschanskiy, S. S. Sokolov and G. Ye. Churilov]

[Abstract] The Twenty-Ninth Conference on Low-Temperature Physics was held at Kazan State University and was attended by more than 300 scientists from the CIS, Great Britain, Canada and Czechoslovakia. The key reports at the plenary sessions were centered for the most part on superconductivity and the physical properties of liquid and solid helium. A total of 216 reports were presented under the program of the section on "Fundamental Problems in Superconductivity" and 120 reports were read in the section on "Low-Temperature Solid State Physics." Many other reports were presented in the sections on "Quantum Fluids and Crystals" and "Electron Phenomena at Low Temperatures." Due to the great number of reports (over 425) this conference report gives only the names of authors and titles of a few of the most important reports and a few lines indicating their content. For example, in the field of the physics of low-temperature magnetism the following were among the subjects examined: magnetic and resonance properties of high-temperature superconducting systems and their nonsuperconducting analogues; physics of magnetics with reduced spatial dimensionality; nonlinear effects in magnetism; low-temperature spin dynamics and thermodynamics; spectra and interactions of quasiparticles; Van Vleck paramagnetism. The next 30th conference on low temperature physics will be held in late June 1994 at Dubna and a seminar on problems in low temperature physics will be held in September 1993 at Katsiveli in the Crimea.

## Superconductivity of Ultrathin Beryllium Films in Strong Localization State

*937J0079A Kharkov FIZIKA NIZKIKH*
*TEMPERATUR in Russian Vol 18 No 12, Dec 92*
*pp 1303-1308*

[Article by V. I. Tutov and Ye. Ye. Semenenko, Kharkov Physical Technical Institute; UDC 538.945]

[Abstract] The influence of a magnetic field on the resistivity of cold-precipitated beryllium films (6-10 A thick) was investigated. Local superconductivity was discovered in films with a thickness about 10 A which are in a strong localization state. The observed phenomenon is attributable to crystallites of the metastable superconducting phase of beryllium disordered to different degrees (and accordingly, with reduced $T_c$). An increase in the positive reluctance effect with a decrease in the degree of disordering (localization) corresponds to an increase in the number and size of the crystal superconducting nuclei in the condensate. The detected local superconductivity in virtually continuous ultrathin beryllium films in a strong localization state differs substantially from that known in granulated films. The local superconductivity in the latter is determined by the superconductivity of relatively large virtually undistorted (accordingly, with virtually unmodified $T_c$) granules and is manifested in the form of a minimum on the film R(T) curves at a temperature close to $T_c$ for massive metal. Localization effects in granulated films for the most part are related to the properties of an intergranular interlayer, a substance foreign relative to the granules. The total conductivity of the layer is manifested after a decrease in the resistivity of the intergranular interlayer to a level close to the threshold value. The data from this study, together with those obtained earlier, indicate that the metastable superconducting phase of beryllium arises as a result a phase dimensional effect in a narrow range of crystallite sizes (8-30 A). Figures 3; references 34: 13 Russian, 21 Western.

## Characteristics of Metal Point Contacts in Range From Acoustic to Optical Frequencies

*937J0079B Kharkov FIZIKA NIZKIKH*
*TEMPERATUR in Russian Vol 18 No 12, Dec 92*
*pp 1357-1364*

[Article by O. P. Balkashin and I. I. Kulik, Low Temperatures Physical Technical Institute imeni B. I. Verkin, Ukrainian Academy of Sciences; UDC 539.292]

[Abstract] The response of pure copper-copper point contacts to electromagnetic radiation was studied in the frequency range $10^3$ Hz - $4.75 \times 10^{14}$ Hz. Working within the framework of the theory of point contact microscopy, computations were made of the signal shaped at the contact as a function of an imparted bias. Experimental measurements were made of the dependence of constant bias for the response signal of pure copper point contacts with a ballistic mode of flowing of the transport current on electromagnetic radiation in a broad spectral range from acoustic to optical frequencies. Computations were made of the corresponding signals and the results were quite consistent with the experimental data. The principal conclusions are: at least to frequencies about $4.3 \times 10^{12}$ Hz the nature of the response signal is governed by rectification of the HF current at the nonlinear features on the contact volt-ampere characteristic; beginning from frequencies about $2.8 \times 10^{13}$ the response mechanism is related to heating of the point contact itself and its peripheral regions; a possible influence of nonequilibrium of electron-phonon system distribution functions on signal shape is operative. Figures 8; references 15: 13 Russian, 2 Western.

## New Type of Spin Waves in Normal Metals With Quasilocal Electron States

[Article by A. M. Yermolayev and N. V. Ulyanov, Kharkov State University; UDC 539.292]

[Abstract] After reviewing the causes for the generation of spin waves in nonferromagnetic metals in a magnetic field, the influence of quasilocal electron states on dynamic spin susceptibility of nonferromagnetic metals containing low concentrations of impurity atoms in a quantizing magnetic field is examined. Resonance susceptibility features were discovered. New branches of the transverse spin wave spectrum are predicted in a random phase approximation. They are detectable within narrow transparency bands in the neighborhood of the frequencies of the electron resonance spin-flip transitions between the quasilocal level and the Landau levels. These new spin waves are characterized by a definite spectrum which is defined and discussed. An example of this is the quasilocal states of electrons in the absence of a magnetic field which were discovered in bismuth with admixtures of elements of groups IV and VI. Admixtures of Sn, Pb and Se, Te resulted in quasilocal levels situated below and above the Fermi limit respectively. The values of the spectral parameters of Bi and quasilocal levels published earlier were used in computing the characteristics of the spin waves considered here. These computations revealed that several spin waves with the distinctive spectrum discussed in the article can be observed in Bi with Sn or Pb admixtures. References 10: 8 Russian, 2 Western.

## Electron-Phonon Interaction in High-Temperature Superconductors

[Article by V. M. Svistunov, M. A. Belogolovskiy and A. I. Khachaturov, Donets Physical Technical Institute, Ukrainian Academy of Sciences]

[Abstract] This comprehensive review, which gives a critical analysis of 109 recent sources, is organized as follows:

1. Introduction

2.1. Tunneling spectroscopy of phonon excitations

2.1. La-Sr-Cu-O system

2.2. R-Ba-Cu-O system

2.3. Bi-Sr-Ca-Cu-O system

2.4. Ba-K-Bi-O system

2.5. Retrieval of function of electron-phonon interaction of metal oxide compounds

3. Experimental results from study of electron-phonon interaction in metal oxides

3.1. Dependence of kinetic and thermodynamic characteristics in superconducting state on temperature

3.1.1. Density of electron states

3.1.2. London penetration depth

3.1.3. Nuclear spin relaxation factor

3.1.4. Heat capacity jump when $T = T_c$

3.2. Lattice characteristics in neighborhood of superconducting transition

3.2.1. Crystal lattice parameters

3.2.2. Phonon spectrum

3.2.3. Thermal conductivity

3.3. Properties of normal state

3.3.1. Optical conductivity

3.3.2. Resistivity

3.3.3. Electron heat capacity

3.3.4. Thermo-emf

3.4. Microcontact spectra

4. Conclusion.

The literature is reviewed under each of these headings. It is concluded that electron-phonon interaction cannot serve as a universal key to all the enigmas embodied in metal oxide superconductors. Phonon concepts are inadequate for describing the dependence of the Hall effect and magnetic susceptibility on temperature and they are entirely unsuitable for reproducing the phase diagrams of these compounds, especially transition to an antiferromagnetic state. Figures 17; references 109: 26 Russian, 83 Western.

## Quasi-Continuous Laser With Nuclear Pumping of a Ne-Xe-(He, Ar) Mixture

[Article by A. I. Konak, S. P. Melnikov, A. A. Sinyan-skiy]

[Abstract] This article presents an experimental study of the parameters of a Ne-Xe laser at atmoshperic pressures in the infrared 5d-6p transition of Xe excited by the fission products of uranium. The effect of the addition of He and Ar on laser characteristics is also considered. The dependences of the energy and threshold parameters ofthe laser on the composition of the mixture are obtained. An increase in generation power and eficiency observed when He or Ar is added to the Ne-Xe mixture is explained by an increase in the rate of collision quenching of lower laser levels. It is shown that the Ne-Xe laser operates at low specific pumping powers $q \leq 10$ W x cm$^{-3}$ in the same infrared transitions 5d-6p of Xe atoms as He-Xe and Ar-Xe lasers. At higher specific powers there is a decrease in laser energy parmaeters and a disruption in generation due to insufficiently effective collision quenching of lower laser levels. Figures 6; tables 2; references 20: 12 Russian, 8 Western.

## Characteristics of a Space Discharge Excited by a Packet of Pulses With Frequencies Up to 100 kHz

[Article by I. P. Martynov, V. N. Mekhryakov, V. V. Osipov, Institute of Electrophysics, Ukrainian Republic Diision of the Russian Academy of Sciences]

[Abstract] This article presents and studies a method of creating an active medium in a $CO_2$ laser in which the agent is pumped by a packet of excitation pulses. The interval between pulses is equal to the generation length of one pump pulse. In this case the total radiation length will be the sum of individual times, and the number of excitation pulses will be selected in accordance with the required radiation pulse length. The goal was to determine the energy characteristics of a $CO_2$ laser at atmospheric pressure with a long pulse length. The effect of the maximum energy supplied to the gas, the content and pressure of the gas mixture, the number of high-voltage pulses in the packet, and the delay time between them were studied. As hydrogen content increased, the energy supplied to the gas increased, but the effect was dependent on the number of pulses in the packet. There had to be less than three pulses in the packet for an energy increase to occur. It was found that energy decreases as the delay between pulses increased to 250 µs. Above 350 µs with pumping energy increased. This behavior is analyzed. It is shown that preliminary ionization of the medium is required for each excitation of the main space discharge. Figures 6; references 5: 3 Russian, 2 Western.

## Effect of a Rapid Increase in Plasma Concentration on the Propagation Dynamics of an Electromagneic Wave Through It

[Article by L. G. Glazov and A. A. Rykhadze, Institute of General Physics, Russian Academy of Sciences, Moscow]

[Abstract] This article examines the dynamics of a wave passing though a layer of plasma with an exponentially increasing concentration ($e^{\gamma t}$ where $\gamma$ is on the order of the wave frequency). Two simple model problems are presented which can be analytically solved, and which make it possible to study qualitative changes in the characteristics of the passage of a wave through plasma when the plasma concentration is increasing rapidly. First, the passage of a monochromatic wave through a spatially homogeneous layer with exponentially increasing concentration is examined. Then the case of a semi-infinite layer is examined. The most characteristic indicator of the effect of increasing plasma concentration is the time dependence of the reflected wave, which is calculated. Another model is examined where the ionizing capacity of particles moving into the field of a superstrong wave is independent of their speed, that is, at each point in the plasma the concentration is increasing exponentially over time. The case of VLF breakdown is examined, as is the VLF radiation cutoff mode. Figures 7; references: 9 Russian.

## Three-Dimensional Model of a $VO_2$ Memory Element

[Article by I. L. Maksimov, T. M. Muravyeva, M. Ya. Eyngorin, Nizhegorod University]

[Abstract] Most models of $VO_2$ switching elements disregard the thermal characteristics of the substrate, which is deemed important in establishing thermal balance in the system. This article presents a theoretical analysis of a three-dimensional model of a memory and information imaging element. The model considers the effect of the redistribution of heat into the substrate, finds the threshold of current crowding, calculates the volt-ampere characteristic ofthe device, and estimates its energy and dynamic parameters. The applicability of this model to the description of a new memory and information imaging element is discussed. The switch consists of a thin round $VO_2$ film on a thin insulating substrate. It is assumed that the difference in potentials between the upper and lower planes of the $VO_2$ film is constant and the current distribution in the film is homogeneous. This configuration is accompaneid by steady-state Joule dissipation into the $VO_2$ layer with subsequent redistribution of heat into the substrate. The cases of a quasi-homogeneous temperature profile and inhomogeneous distributions of temperature into the film are examined. For typical parameters it is found that the minimum switching power is 0.1 mW and the switching times $t_{on}$ and $t_{off}$ are about 0.21 and 0.8 µs

resepctively. Practical implementation of a memory element based on the model is described. Figures 5; references 17: 10 Russian, 7 Western.

## Excitation of Hollow Infrared Waveguides

[Article by V. G. Artyushenko, K. I. Kalaydzhyan, M. M. Mirakyan, Institute of Radio Physics and Electronics, Ashtarak, Reupublic of Armenia]

[Abstract] Various cases of excitation of a hollow metal waveguide are examined, in particular, excitation by a Gaussian beam and the effective connection of two waveguides. The effectiveness of excitation of waveguide modes is theoretically and experimentally determined. Details of the experimental set-up are provided. Effectiveness of mode excitation was determined from analysis of intensity distribution of output radiation in the far zone. The dependence of the effective excitation of modes on the ratio of the constriction width of the Gaussian beam to the height of the waveguide (o/a) is determined for ideal waveguide excitation (no angular or transverse displacements, and the vector of the excitation field parallel to the reflecting planes of the hollow metal waveguide). It is found that only odd modes are effectively pumped. The effectiveness of exciting even modes is 15 orders of magnitude lower. When $2o/a = 0.7$ the waveguide realizes one-mode excitation. Displacements disrupt this mode, and odd and even modes begin to be excited. Connection of two waveguides is akin to the case of excitation of a waveguide by a Gaussian beam. The effect of possible mismatches in waveguide-waveguide and laser-waveguide connections is considered. Figures 5; references: 4 Western.

## Effect of the Initial Dynamics of Formation of a Plasma Conductor on the Effective Operation of an Electrodynamic Accelerator

[Article by V. V. Zheleznyy, M. F. Zhukov, A. D. Lebedev, A. V. Plekhanov, Institute of Thermal Physics, Siberian Division, Russian Academy of Sciences, Novosibirsk]

[Abstract] Results are presented from an experimental study of the dynamics of a plasma cluster in a track accelerator. It is shown that the effectiveness of these devices is substantially affected by the initial stage of formation of the plasma conductor. The predominance of gas kinetic pressure over magnetic pressure at this stage causes free expansion of the conductivity channel. The subsequent transition to a plasma piston mode becomes problematic, predetermining a low efficiency in the track acclerator. It is shown that when this type of transition occurs, it is still possible to increase the effectiveness of the accelerator and obtain sufficiently good agreement with theoretical results. Possible reasons for divergences

between theoretical and experimental results are offered. Figures 7; table 1; references 43: 36 Russian, 7 Western.

## Spiral Dislocations as Phase Defects of the Radiation of a Production TEA $CO_2$ Laser

[Article by B. D. Bobrov and G. Yu. Snezhkov]

[Abstract] Production $CO_2$ lasers have a high radiation flux density which is the cause of many effects on the output characteristics of the laser beam. The laser beam at the resonator output has a structure similar to a speckle structure, which is acquired by the beam in the process of propagation in inhomogeneous media, the atmosphere, or reflections from objects with a coarse surface. The purpose of this article is to show that this similarity is not merely external. In addition to beam amplitude modulation, spiral dislocations of the beam may form in the resonator, that is, they are phase defects with the nontrivial topology characteristic of speckle fields. Experimental diagnosis of phase distortions was done using interferometry of a radial-azimuthal shift. Interferograms were constructed by superimposing the signal beam with a reference beam formed from the signal beam by defocusing and rotation. Interferograms of the wave front are presented and analyzed. U-shaped branching in the interferograms indicates the appearance of spiral dislocations of the wave front. The presence of these dislocations in the near zone of the laser source are experimental evidence of the similarity of the wave front topology of the laser beam and specklfe fields. It is concluded that phase distortions and amplitude modulation of the beam occur in the process of beam formation in the resonator. Consequently, there are limited possibilities of improving the quality of radiation through linear adaptive optics. Figures 2; references 10: 9 Russian, 1 Western.

## Electromagnetic Spin Waves in Structure of Hexaferrite Superconductor With Long Josephson Junction

[Article by S. V. Meriakri]

[Abstract] Slow electromagnetic waves can interact with magnetostatic waves. In a structure formed from layers of ferroelectric material and ferrite, a magnetostatic wave, propagating in the ferrite film, and a slow electromagnetic wave, propagating in the ferromagnetic layer as in a dielectric waveguide, interact with one another. The strongest interaction between the magnetostatic wave and the slow electromagnetic wave will be in the region of phase synchronism of the waves. The hybridization of the magnetostatic and electromagnetic waves occurs in the phase synchronism region. In this case hybrid electromagnetic spin waves are propagated in the structure. A study was made of the interaction of these hybrid electromagnetic spin waves in a plate of ferromagnetic material with a high

internal anisotropy and a slow Swihart electromagnetic wave in a semiconductor with a long Josephson junction in a structure made up of layers of ferromagnetic material and a semiconductor. The behavior of the interacting waves is analyzed. A wave in hexaferrite can be considered magnetostatic; the lag in the hexaferrite can be neglected. In the considered geometry a return magnetostatic body wave (RMSBW) may propagate in the ferrite; this wave may interact with a Swihart wave. Considering the interaction between the Swihart wave and the RMSBW through the interface of the media, applying the boundary conditions of electrodynamics, a law is obtained for the dispersion of hybrid electromagnetic spin waves in a hexaferrite-superconductor structure with a long Josephson junction. Figure 1; references 12: 9 Russian, 3 Western.

## Nature of 'High-Frequency Absorption Peaks' in High-Temperature Superconductors Near $T_c$

[Article by L. B. Rozenbaum]

[Abstract] A number of studies give the results of research on HF losses in ceramic and film high-temperature superconductors (HTSC) at frequencies about $10^6$ - $10^7$ Hz. This research was carried out by the induction method. The authors discovered a nonmonotonic dependence of R losses in an LC circuit (with a specific quality Q) on temperature T; near the temperature $T_c$ of the superconducting transition, usually when $T \leq T_c$, there is an "absorption peak," a maximum on the R(T) curve, or accordingly, a minimum on the Q(T) curve. At least three different authors have made attempts to explain this "absorption peak," each citing different causative factors (radio-frequency dimensional effect, granular structure of ceramic superconductors, or Beresinskii-Kosterlitz-Thouless transition). The author also observed a nonmonotonic Q(T) dependence near $T_c$ in investigations of different ceramic HTSC samples by the induction method. However, it seems that this nonmonotonic dependence is quite simple and therefore not difficult to explain. The necessary condition for observing "HF absorption peaks" is defined. The analysis indicates that the temperature "HF absorption peaks" most likely are of an instrumental origin (inherent in the induction method) and are unrelated to any physical characteristics or nonmonotonic features in the behavior of HTSC materials at high frequencies. Figures 3; references 6: 4 Russian, 2 Western.

## Interaction Between Waves and Active Periodic Structures

[Article by T. N. Verbitskaya, V. V. Demekhin and V. G. Ponomarenko]

[Abstract] A characteristic property of the process of propagation of waves of different nature in layered periodic structures (LPS) is the presence of reflection and transparency zones. Their position is determined by the LPS parameters (thicknesses of layers, density, dielectric constant, permeability, etc.). There are four principal methods for changing the LPS parameters. In such processes there is a displacement of the zones, which is used in controlling the characteristics of the wave transmitted (reflected) by the LPS in various technical devices. The magnitude of these changes is limited. The limits of change of LPS parameters are dependent on the material from which the LPS is made, on the admissible level of the controlling powers, and other factors. An effort was made to compute the magnitude of the minimum changes in LPS parameters ensuring continuous control of the intensity of the radiation transmitted (reflected) by the LPS in some wavelength range, that is, to determine the minimum adjustment of the LPS modulation coefficient which will ensure a stipulated level of the transmitted (reflected) energy for any wavelength in the investigated range. It is assumed that this range considerably exceeds the width of the allowed or forbidden zones. The analysis made it possible to determine the upward and downward limits of the possible range. References: 5 Russian.

## Resonance of Electromagnetic Absorption in Dielectric Composite Based on High-Temperature Superconductors

[Article by A. M. Grishin, V. P. Dyakonov, N. I. Mezin, V. A. Shapovalov, N. Yu. Starostyuk and G. S. Yarosh, Donets Physical Technical Institute]

[Abstract] Composites based on use of high-temperature superconducting materials are highly promising. They constitute a dielectric matrix in which there are ideal monocrystalline high-temperature superconducting (HTSC) granules. The degree of dilution of such composites can be varied in a wide range. There is no galvanic coupling among the granules. This means that there also are no hysteresis losses caused by intergranular currents. A dielectric composite based on a HTSC can serve as a model of a "soft" diamagnetic reversely magnetized by a weak magnetic field. A dielectric composite has been newly developed which has a quite high dependence of microwave properties on weak magnetic fields. This composite is produced on the basis of superconducting $YBa_2Cu_3O_{7-x}$ powder. The bonding element used is a low-temperature epoxy cement. The change in the reflection and absorption coefficients of microwave intensity in the magnetic field in the dielectric composite is essentially dependent on the technology used in preparing the powder. A virtually single-phase product was obtained. The results of research on the magnetic and microwave properties of this dielectric composite are given. The testing of the parameters and behavior of the proposed material are discussed. Particular attention is given to the electromagnetic absorption evidently caused by Fabry-Perot resonance in a plate of the new dielectric composite. Figure 1; references 11: 7 Russian, 4 Western.

## Spectra of Breakdown Electroluminescence in Silicon-Based MOS Structures

[Article by Yu. Ye. Gardin, I. V. Klimov and S. N. Kuznetsov]

[Abstract] The light radiation effect accompanying avalanche breakdown of back-biased p-n junctions in silicon has long been known, but the literature contains no data on the radiation of MOS (metal oxide superconductor) structures based on Si with avalanche breakdown of the space charge region (SCR). In this study it is shown that data on the spectra of breakdown electroluminescence (BEL) in MOS structures should be masked to a lesser degree by side effects than in the case of p-n junctions. The lack of data on spectra for MOS structures is attributable to considerable experimental difficulties in their registry. An attempt was made to fill this gap. The measurements were made in MOS structures prepared using standard industrial technology. Si backings of n- and p-types with an orientation (111) and (100) respectively were used. $SiO_2$ layers were built up on the backings by thermal oxidation in "dry" oxygen. The BEL spectra obtained in MOS structures accompanying avalanche breakdown of the space charge region characterize a radiation process with nonthermalized carriers. The data obtained within the framework of the proposed model make it possible to estimate the effective temperature of hot carriers at about 7000 K with a field strength at the silicon surface about $5 \times 10^5$ V/cm. Figure 1; references 10: 4 Russian, 6 Western.

## Resonance Anomalies in Reflection From Metal Lattice With Dielectric Coating

[Article by A. N. Dolgina and P. S. Kondratenko, Institute of Problems in Safe Development of Atomic Energy, Russian Academy of Sciences]

[Abstract] The nature of the processes transpiring during the interaction of laser radiation with condensed media in many cases is predetermined by surface excitations. This is particularly clearly manifested with the generation of surface electromagnetic waves on metal lattices, resulting in well-known reflection anomalies. The presence of a dielectric coating on the lattice adds to the surface electromagnetic waves still another type of excitation known as waveguide modes which are capable of modifying and diversifying optical effects. With these considerations taken into account this communication is devoted to theoretical research on the characteristics of reflection of coherent radiation under resonance conditions relative to surface electromagnetic waves and waveguide modes. Virtually total reflection occurs far from resonance. With approach to resonance reflection exhibits a sharp dropoff, which under definite conditions results in total suppression of mirror reflection. Under given conditions there is a

considerable distortion of the spatial and/or temporal structure of the reflected signal. A formula is given for the quantity of absorbed energy for a finite beam of pulsed radiation with the satisfaction of definite conditions. Under certain conditions energy is fully absorbed, but with violation of even one of these conditions there is only partial absorption. The behaviors examined here may be important for the theory of optical waveguides and the physics of the impact of laser radiation on the surface of metals having oxide films. References 7: 6 Russian, 1 Western.

## Surface Photo-emf of InAs-Based MDS Structures

[Article by V. M. Bazovkin and T. Ye. Kovalevskaya, Physics of Semiconductors Institute, Siberian Department, Russian Academy of Sciences, Novosibirsk; UDC 621.382]

[Abstract] InAs-based MDS structures were experimentally discovered for which the level of surface-emf, measured with inversion curvatures of zones on a semiconductor surface, has a strong dependence on electric field strength in the dielectric layer and its dependence on the intensity of illumination deviates considerably from the classical picture for surface-emf. It is shown that surface photo-emf also is dependent on the voltage across the controlling electrode. The research method is described in detail. A model is proposed which reveals that the principal characteristics of the dependency of surface photo-emf on the illumination of MDS structures can be attributed to the existence of an "anomalous" temperature field recombination process whose intensity is determined by hopping conductivity for surface states in the forbidden gap on the surface of the semiconductor and which plays the role of a shunting resistor with a conductivity dependent on the strength of the electric field in the dielectric. A precise quantitative agreement between the results of computations and experimental data is attained on the assumption that the density of the surface states has a definite dependence on electric field strength in the dielectric. Figures 4; references 9: 4 Russian, 5 Western.

## Injection-Stimulated Acceleration of Migration of Protons Along Silicon Dioxide Surface

[Article by S. N. Koslov and Ye. V. Rodionova, Physics Department, Moscow State University imeni M. V. Lomonosov; UDC 539.293]

[Abstract] The influence of photoinjection of electrons from Si into an $SiO_2$ film on the migration of protons along the surface of the oxide placed in a moist medium was investigated. The films, 1000 A thick, were obtained by thermal oxidation of the surface of p-silicon. The investigated structures were placed in an evacuated cell with a

variable water vapor pressure. Prior to measurements the structures were hydrated by holding in water vapor for 12-14 hours. The MDS structures were measured at a frequency 160 kHz. Photoinjection measurements were made using an optical system consisting of a xenon lamp and monochromator. The flux of light quanta incident on the sample surface was maintained constant in the spectral range 3.5-5.8 eV and all measurements were made at a temperature 300 K. It was established that in the studied range of relative humidities the injection of electrons into an $SiO_2$ layer is accompanied by an increase in the surface mobility of protons by a factor of about 2. This effect is associated with the excitation of vibrational modes of O-H adsorbed water molecules and O-H groups due to the energy released during the capture of injected electrons in deep traps in the oxide film near-surface region. Figures 7; references 9: 5 Russian, 4 Western.

## Angular and Energy Distribution of Ion Flux in Target During Ion Implantation

*937J0054C Moscow POVERKHNOST: FIZIKA, KHIMIYA, MEKHANIKA in Russian No 10-11, Oct-Nov 92 pp 89-94*

[Article by A. F. Burenkov, V. I. Belko, Ye. B. Boyko and I. Ye. Mozolevskiy, Belarus State University; UDC 539.12]

[Abstract] The dependence of the energy and angular distribution of moving particles on the depth of penetration of ions into a target found in this study makes it possible to compute the distributions of injected ions and defect formation during ion implantation in layered targets when the interaction sections change in a jump at the interface of the studied materials. Total information on the ion flux in a target makes it possible to investigate surface effects, such as the reflection coefficient and the angular and energy distribution of ions reflected from a surface. With these considerations taken into account, an algorithm is proposed for numerical solution of the boundary value problem for the transfer equation which is based on partial discretization of the transfer equation using angular and energy variables and applying the Galerkin method. This makes it possible to simulate ion implantation. The proposed algorithm is easily applied using such computers as the IBM PC AT, has a high speed in comparison with the Monte Carlo method and makes it possible to compute the distribution function for the ion flux in a target for different implantation conditions. Examples are given of the energy and angular distribution of the flux of $As^+$ and $P^+$ ions in a silicon target with an implantation energy 50 keV. Figures 3; references 5: 3 Russian, 2 Western.

## Grain Boundary and Bulk Diffusion in Thin Films in Gold-Copper System

*937J0054D Moscow POVERKHNOST: FIZIKA, KHIMIYA, MEKHANIKA in Russian No 10-11, Oct-Nov 92 pp 111-117*

[Article by A. N. Aleshin, B. S. Bokshteyn, V. K. Yegorov and P. V. Kurkin, Institute of Problems in Technology of Microelectronics and Ultrapure Materials, Russian Academy of Sciences, Chernogolovka; UDC 539.216.2:539.219.3]

[Abstract] The Rutherford $He^+$ ion backscattering method was used in studying diffusion in thin films of an Au-Cu system. This system was selected because Au and Cu are metals in which diffusion has been studied quite well for massive samples. Although many studies have been made of diffusion in thin films of this system, it has been the "effective" diffusion coefficients which have been computed, that is, the bulk and grain boundary components of diffusion were not discriminated in the Cu film. In an earlier article by the authors (POVERKHNOST, No 5, p 157, 1991) grain boundary diffusion of Au in a Cu film were obtained; the bulk and grain boundary diffusion coefficients are determined in this article for Au in Cu and Cu in Au in a somewhat broader temperature range than in the earlier study. It is shown that the activation energies of bulk and grain boundary diffusion are close in value, being about 1 eV. A comparison of the diffusion parameters in thin films of the Au-Cu system with the diffusion parameters in massive samples was made. It was found that the activation energy of bulk diffusion in thin films is about half as great as the activation energy of bulk diffusion in massive samples. Figures 6; references 29: 5 Russian, 24 Western.

## Deposition of Thin Dielectric Film on Metal Surface in Strong Electric Film

*937J0054E Moscow POVERKHNOST: FIZIKA, KHIMIYA, MEKHANIKA in Russian No 10-11, Oct-Nov 92 pp 118-120*

[Article by S. V. Zaytsev; UDC 621.319.7]

[Abstract] A microscopic study was made of regularities in the deposition of a dielectric film and the change in its structure in a strong electric field. Condensation of the liquid film occurred in a vacuum chamber at a water vapor pressure $10^{-7}$ mm Hg and with a field strength at the surface of a pointed metal sample $10^8$ V/m. An increase in field strength to $5 \times 10^8$ V/m results in the development of a characteristic microgranular structure on the surface. It is postulated that the reason for the appearance of this structure is that each granule contains a unit electric charge. Granule equilibrium is governed by a balance of surface tension and ponderomotive forces. Under the influence of force fields processes of elementary ordering begin to occur with the appearance of stable structures in the form of concentric rings which may be the consequence of the Coulomb interaction of microgranules. The results indicate that a nonuniform electric field makes it possible to deposit a film on metal from a gaseous state even if the concentration of this matter is extremely small. By changing temperature and field strength it is possible to control structure in a wide range. The appearance of granulation and ordering elements on the surface of the liquid film makes it possible to regard this system as a convenient experimental model for research on the processes of self-organization of matter. Figures 2; references: 2 Russian.

## Ultraviolet Silicon Carbide Photodetectors

[Article by R. G. Verenchikova, Yu. A. Vodakov, D. P. Litvin, Ye. N. Mokhov, A. D. Royenkov and V. I. Sankin, Physical Technical Institute imeni A. F. Ioffe, Russian Academy of Sciences, St. Petersburg]

[Abstract] There is a serious need for solid-state photodetectors (PD) with a high response and speed useable in the UV spectral region. The semiconductor materials presently used do not fully ensure efficient operation of these PD in the wavelength region 200-300 nm. With respect to a number of properties silicon carbide in a hexagonal modification differs advantageously from other materials which have been used. The characteristics of different silicon carbide photodetectors are therefore examined in depth: 1) a PD based on a Schottky barrier; 2) a PD based on p-n junctions obtained by epitaxy and diffusion of aluminum and boron; 3) avalanche photodiodes. It is shown that they have a high efficiency in the ultraviolet spectral region with a response maximum at 250-300 nm and retain operability to temperatures 500°C. The review shows that silicon carbide PD are efficient detectors of UV radiation. With an adequately high response they have a number of unique merits such as insensitivity to the entire range of visible light, absence of degradation under the influence of UV irradiation, resistance to radiation and thermal factors and stability with time. These considerations support the conclusion that they are promising and preferable among the considered PD types for a wide range of applications. Figures 5; references ·14: 9 Russian, 5 Western.

## Influence of Strong Microwave Field on Photoelectric Characteristics of Silicon p-n Junctions

[Article by N. A. Ablyazimova, A. I. Veynger and V. S. Pitanov, Physical Technical Institute imeni A. F. Ioffe, Russian Academy of Sciences, St. Petersburg]

[Abstract] In an earlier study by the authors (FTP, Vol 22 No 11, pp 2001-2007, 1988) it was demonstrated that there is no satisfactory explanation of the influence of a microwave field on the volt-ampere characteristic (VAC) for silicon p-n junctions; the change in the slope of the VAC in the microwave field is anomalously great. Research was therefore carried out for explaining the mechanism of interaction between the microwave field and silicon p-n junctions. Results were obtained showing the influence of a strong microwave field on the photoelectric characteristics of p-n junctions. It is shown that the height of the barrier of the p-n junction in a strong microwave field and the decrease in the barrier with illumination of the p-n junction are proportional to the height of the initial barrier if the latter is lowered by direct displacement. Near zero

displacement and with retrograde displacement this proportionality is impaired due to the influence of the return current through the p-n junction. A mechanism is proposed for increasing the barrier of the p-n junction which is based on allowance for generation-recombination processes in the space charge layer. Figures 4; references 7: 6 Russian, 1 Western.

## Influence of Laser Annealing on Electric Characteristics of GaAs-Based MDS Structures

[Article by V. P. Voronkov, V. M. Kalygina, S. Yu. Mulenkov, Ye. I. Oborina, Ye. G. Salman and T. P. Smirnova, Siberian Physical Technical Institute imeni V. D. Kuznetsov at Tomsk State University, Tomsk]

[Abstract] The influence of pulsed laser annealing on the electric characteristics of $Si_3N_4$-BN-GaAs metal structures was investigated. The work was carried out for clarifying the possibility of controlling the properties of the dielectric-GaAs interface. Boron nitride and silicon nitride films were applied in high-frequency plasma at backing temperatures 200 and 400° respectively. The thicknesses of the dielectric layers were 500 A for both BN and $Si_3N_4$. The laser radiation wavelength was 0.69 μm and was selected taking into account dielectric transparency and surface absorption in GaAs, making it possible to process the dielectric-semiconductor interface directly. Pulse power density was varied in the range 0-20 J/cm² with a pulse duration $10^{-3}$ s. Irradiation was from the direction of the dielectric film. It was found that with annealing energies E ≤ 10 J/cm² the volt-Faraday and volt-Siemens characteristics are shifted into the region of lesser enriching potentials. With E > 10 J/cm² there is an inversion of the behavior of the volt-ampere and volt-Faraday characteristics. Changes in the electric characteristics of MDS structures after laser annealing are related to transformations occurring at the dielectric-semiconductor interface. Figures 3; references 11: 8 Russian, 3 Western.

## Long-Range Interaction Effect in Semi-Insulating GaAs and InP Semiconductors After Irradiation by Argon Ions

[Article by P. V. Pavlov, Ye. S. Demidov and V. V. Karzanov, Nizhegorod Physical Technical Research Institute]

[Abstract] Experimental data are given indicating the possibility of improving the homogeneity of monocrystals of already prepared ingots of semi-insulating GaAs and InP after their irradiation by argon ions. A study was made of the dependence of the Hall constant $R_x$ and resistivity ρ in semi-insulating GaAs and InP samples on temperature. Samples measuring 5 x 10 mm were cut from different sectors of a plate of the corresponding material. The

plates were oriented in the plane (100) and were 500-700 µm thick. A scatter of the measured parameters from sample to sample was observed which evidently is attributable to a nonuniform distribution of impurities in the initial plates. The monocrystals were irradiated by 40-keV argon ions, resulting in an evening-out of the electric properties of samples cut from the very same plate. it was found that the evening-out of properties of the samples as a result of ion irradiation is intensified with an increase in the dose and intensity of bombardment. Successive etching of the layers revealed that the electric parameters of the irradiated samples are virtually not dependent on depth. In the case of GaAs, in addition to an improvement in homogeneity, in some cases there was an increase in the Hall mobility of electrons. The observed effect is attributable to the dissolving of defect-impurity aggregates in the volume of the samples as a result of the long-range influence of ion bombardment, similar to that already observed in silicon and germanium. Figures 1; references 5: 4 Russian, 1 Western.

## Anisotropy of Optical Reflection of Gallium Arsenide in Fundamental Absorption Edge Region

[Article by V. L. Berkovits, A. O. Gusev and T. V. Lvova, Physical Technical Institute imeni A. F. Ioffe, Russian Academy of Sciences, St, Petersburg]

[Abstract] A study was made of the effect of polarization anisotropy of optical reflection of GaAs crystals of the orientation (110) in the region of the fundamental absorption edge. The effect involves essentially the following: the parallel and perpendicular light reflection coefficients, plane polarized along the two axes [110] and [001], lying on a given plane, are different. The effect was studied using the method of modulation of the polarization of incident radiation. The experiments were carried out on surface-barrier structures based on slightly alloyed GaAs with the imparting of a displacement stress, and also with samples having a different alloying level. It was found that the part of the reflection anisotropy dependent on the near-surface field can be analyzed within the framework of electric reflection theory. Franz-Keldysh oscillations are observed in the absorption edge region. However, in the region of transitions above the absorption edge ($E_1$, $E_1 + \Delta_1$ no oscillations are observed, as is consistent with theory. The experiments show that a near-surface electrical field, associated with curvature of the zones, causes an anisotropy of reflection in the absorption edge region. The shape of the anisotropy field signal is described well within the framework of electric reflection theory. Figures 5; references 13: 3 Russian, 10 Western.

## Laser-Stimulated Diffusion of Gold in Silicon

[Article by A. S. Zakirov, Kh. T. Igamberdyyev, A. T. Mamadalimov and P. K. Khabibullayev, Thermal Physics Department, Tashkent]

[Abstract] The diffusion of gold in silicon under continuous laser processing with the use of a scanning device was investigated. With a power of laser radiation $10^5$ $cm^2$ the introduction of gold into silicon occurs in a temperature gradient field in which a penetration depth attaining > 100 µm is observed. A mechanism of laser-stimulated diffusion of gold in silicon is proposed on the basis of the determined diffusional and electrophysical characteristics which takes photoionization processes and high-temperature heating into account. Among the findings from this research are the following: 1) diffusion is observed when there is an adequately high laser radiation intensity, and accordingly, high temperatures; 2) the concentration distribution profiles are described by an erfc function and attain quite deep layers; 3) the rate of introduction of donors into p-Si exceeds the rate of introduction of acceptors into n-Si, but the concentration of active centers with deep levels in n-Si is greater than in p-Si; 4) the photosensitivity of silicon alloyed by laser radiation is greater than for thermally alloyed samples; 5) diffusion during laser processing is not accompanied by the formation of vacancy complexes (vacancy-oxygen, vacancy-small impurity). These regularities give evidence that with the employed laser processing conditions gold is diffused into silicon, as a result of which there is a substantial change in the electrophysical and capacitive properties of the initial silicon. Figures 3; references: 12 Russian.

## Passivation of Radiation-Induced Defects in Hydrogenized Silicon Layers With Neutron Irradiation

[Article by V. V. Volotov, G. L. Plotnikov, V. M. Emeksuzyan and K. Shmalts, Physics of Semiconductors Institute, Siberian Department, Russian Academy of Sciences, Novosibirsk]

[Abstract] A study was made of the influence of preliminary hydrogenization and thermal processing on defect formation in silicon of the n- and p-type with irradiation by fast neutrons. Hydrogenization was carried out by two methods: from hydrogen plasma and in boiling distilled water. The processing in hydrogen plasma was at temperatures 100 and 150°C for one hour. The plasma was ignited periodically for 45 ms, after which the chamber with the plates was evacuated to an intense vacuum for 250 ms and then hydrogen was again admitted and the plasma was ignited. Processing in boiling distilled water was for 3.1 and 30 hours. After hydrogenization some of the samples were annealed in a furnace at 240°C for two hours in an atmosphere of dry nitrogen. This, together with other procedures, made it possible to determine the profiles of the concentrations of centers with shallow and deep levels and the distribution of generation times after irradiation. Passivation effects were established for both individual radiation defects and radiation defects in the disordered region due to the formation of atomic hydrogen from bound forms under the influence of neutron irradiation

factors. A decrease in the rate of degradation of generation times in hydrogenized silicon layers during irradiation was discovered. There is a greater efficiency of passivation of radiation defects in n - Si than in p - Si. Figures 5; references 18: 6 Russian, 12 Western.

## Photoelectric Method for Determining Optical Absorption Coefficient and Its Application to Semi-Insulating GaAs

[Article by I. A. Karpovich and S. M. Plankina, Nizhegorod State University imeni N. I. Lobachevskiy]

[Abstract] A new variant of the photoelectric method is described which makes it possible to eliminate the inadequacies of variants previously employed. The method was developed applicable to semi-insulating materials and was tested using semi-insulating GaAs. The proposed method, like in the research of T. S. Moss, et al., PHYS. REV. LETT., Vol 1, No 4, pp 129-131, 1958), is based on measurement of the spectral dependence of relative photosensitivity, but in contrast to the earlier study the latter is measured in a transverse photoconductivity mode and in the entire volume of the sample. The normalization of photosensitivity, making it possible under definite conditions to exclude its dependence on a number of electrophysical parameters of the material, is accomplished using the maximum of characteristic photosensitivity. Additional illumination of the sample by penetrating radiation is ensured in order to ensure a constancy of the lifetime and mobility of the charge photocarriers with a change in wavelength and intensity of the exciting light. Two possible ways for applying the method are described. The experimental method is described in detail. The possibility of determining not only the photoactive, but also the nonphotoactive part of the absorption coefficient, is demonstrated. Figures 2; references 10: 4 Russian, 6 Western.

## Modification of Spectrum of Fine States of Gallium Arsenide Under Influence of Pulsed Laser Radiation

[Article by P. K. Kashkarov and V. Yu. Timoshenko, Moscow State University imeni M. V. Lomonosov]

[Abstract] It was established earlier (A. I. Yefimova, et al., (POVERKHNOST. FIZIKA, KHIMIYA, MEKHANIKA, No 8, pp 94-100, 1990) that pulsed laser irradiation with an energy not exceeding the fusion threshold results in the formation of defects in the near-surface region of GaAs crystals. The forming defects are manifested at 300 K, predominantly as centers of nonradiative recombination of charge carriers. Continuing this research, in this article an attempt is made to obtain information on the nature of laser-induced defects using the low-temperature (T = 4.2

K) photoluminescence method. Photoluminescence measurements were made in an apparatus based on an automated spectrometer. The radiation of an argon laser with $\lambda$ = 488 nm and an intensity about 50 mW/cm$^2$ was used for excitation. The spectral resolution was 0.1 meV. The samples used were epitaxial layers of n - GaAs (Si) 0.1 $\mu$m thick, grown on a backing of a semi-insulating GaAs material. The use of such samples made it possible to bring the thickness of the layer to be analyzed by the photoluminescence method to the postulated depth of localization of laser-induced defects. In this study for the first time a change in the spectral composition of the photoluminescence of GaAs under the influence of subthreshold laser irradiation was registered. Only states associated with small defects are subject to modification. The registered data are evidence of the restructuring of defects participating in both radiative and nonradiative recombinations. Figure 1; references: 3 Russian.

## Model of Radiation-Induced Accumulation of Defects in Silicon-Silicon Oxide System

[Article by D. G. Krylov, Ye. A. Ladygin and A. P. Galeyev, Moscow Institute of Steel and Alloys]

[Abstract] Under the impact of high-energy particles a number of processes occur in the silicon-silicon oxide system in an oxide film obtained by thermal oxidation and at the silicon-silicon oxide interface. Under the influence of these particles there is an impact displacement of atoms at the interface and in the dielectric with the formation of surface states and positively charged centers respectively. The kinetics of the accumulation of surface states at the silicon-silicon oxide interface and positively charged centers in the silicon oxide was computed. A model of these processes was constructed and its validity was demonstrated. Two mechanisms are taken into account: impact displacement of atoms by high-energy particles and the breaking of stressed bonds with capture of a hole. The formation of surface states at the interface and positively charged centers in the volume of the dielectric is examined simultaneously, which makes it possible to compare the experimental data and to estimate the depth of distribution of the elastic stresses in the volume of the dielectric. Generation of defects both during the time of irradiation and afterwards is postulated and the duration of the second stage (time of hole resorption in the dielectric) is determined. Figures 2; references 3: 2 Russian, 1 Western.

## Study of Laser Interferometry in GaAs With Methods of Photoluminescence and Disruption of Total Internal Reflection

[Article by Ya. V. Bobitskin, A. I. Bercha, N. L. Dmitruk, D. V. Korbutyak, N. A. Fidrya, Institute of Semiconductors, Ukrainian Academy of Sciences]

[Abstract] Methods of photoluminescence and disruption of total internal reflection are used to study laser gettering of structural and doping defects in single-crystal GaAs. This is done by scanning the back surface with a high-power laser beam, creating a diffraction grating. The width of the lines of disrupted total internal reflection measured in the plasmon-phonon interaction and the intensity of lines of low-temperature photoluminescence are used to establish the total reduction of the defectiveness level and redistribution of the contents of the doping agent Si over the thickness and the surface of samples. The methods showed that laser-processed GaAs regions (especially when a sructural lattice if formed) are effective getters of doping and intrinsic structural defects. Figures 3; table 1; references 7: 4 Russian, 3 Western.

## Degradation Mechanism of a (GaAs/AlGaAs)-Laser With a Quantum Well

[Article by M. M. Sobolev, A. V. Gittsovich, M. I. Papentsev, I. V. Kochnev, and B. S. Yavich, A. F. Ioffe Physicotechnical Institute, Russian Academy of Sciences, St. Petersburg]

[Abstract] This article resports on the use of volt-farad measurements and the DLTS method to study the processes of degradation of laser double heterostructures in GaAs/AlGaAs with a separate limit and with a quantum well. Two types of laser structures were studied. Type I was a p-n junction near the $p-Al_{0.5}Ga_{0.5}As/n-Al_{0.3}Ga_{0.7}As$ boundary and with a quantum well which does not fall in the layer of the space charge at a back bias voltage $V_0 = 0$. Type II has a quantum well in the layer of the space charge at $V_0 = 0$. It is found that the main mechanism leading to the degradation of both structures in the process of recombination is stimulated dislocations creep, which is associated with the absorption of point defects at the heteroboundary. The process of dislocation creep is accompanied (in type-I structures) by the generation of $As_{Ga}$ and $V_{Ga}$ defects. In type-II structures only $V_{Ga}$ defects accompany this process. In type-II structures one apparently observes dislocation creep from the p-emitter into the n-waveguide, which is accompanied by the generation of an MES defect whose concentration decreases as the dislocation moves. In dislocation creep there is also generation of deep states in the quantum well. In type-I structures, dislocation creep occurs from the n- and p-emitters, which leads to degradation of the laser. Figures 4; tables 2; references 17: 1 Russian, 16 Western.

## Toward a Theory of the Capture of Holes of a Quantum Well in GaAs Semiconductors

[Article by M. V. Vergeles, I. A. Merkulov, A. F. Ioffe Physicotechnical Institute, Russian Academy of Sciences, St. Petersburg]

[Abstract] A decisive factor in the dependence of the probability of capture of charge carriers in a quantum well on its parameters (width and depth) is the localization of particles due to the presence of a fine level in the well (real, vitual, or quasi-steady-state). In semiconductors with a complex structure, a fine-level theoretical description of the valent zone is constructed in a rectangular quantum well, and the dependence of its energy on the wave vector of a hole in the plane of the well is found. The magnitude and shape of peaks are found in relation to the probability of capture of particles from different subzones and the valent zone. It is shown that for an equilibrium distribution of carriers between subzones of light and heavy holes the main role in capture is played by heavy holes. Attention is focused on a new effect, the delaying of a heavy hole due to scattering on a quasi-steady-state which is genetically associated with a subzone of light holes. Figures 4; references 8: 4 Russian, 4 Western.

## Photoluminescence in Carbon δ-Doped GaAs Superlattices

[Article by V. Ya. Aleshkin, A. V. Anshon, L. M. Batukova, Ye. V. Demidov, Ye. R. Demidova, B. N. Zvonkov, N. I. Lobachevskiy Nizhegorod Research Physicotechnical Institute at Nizhegorod State University]

[Abstract] This article studies the features of photoluminescence in carbon δ-p-doped GaAs superlattices. Irradiation was done with a HeNe laser (10 mW) or a Ar (1 W) laser at 77 K. In homogeneously carbon doped layers of p-GaAs the maximum photoluminescence is shifted toward lower energies, compared to the maximum of photoluminescence in an undoped n-layer. Its position is independent of the doping level, indicating the dominance of radiative recombination through the carbon layer. When the concentration of holes increases, the maximum photoluminescence shifts to lower energies due to the formation of a doped zone. In a superlattice with a minimum level of δ-doping the maximum shift in the maximum photoluminescence toward lower energies is observed. A further increase in the elvel of δ-doping, in contrast to the case of homogeneous doping, leads to a shift in the maximum photoluminescence toward higher energies. This shift is accompanied by a severalfold decrease in the intensity of photoluminescence. A substantial shift in the maximum photoluminescence toward lower energies in a superlattice is associated with the spatial separation of electrons and holes in the periodic field of the superlattice and tunnel recombination of electrons with holes through the barrier into the δ layer. The shift in the maximum as the level of δ-doping increases may be due to a shift down of the hole subzone due to dimensional quantization of the energy spectrum of holes in the quantum well of the δ layer and a contribution to photoluminescence of

regions separating the δ layer. In a superlattice with a relatively low level of δ doping one observes a shift in the maximum photoluminescence toward high energies as the level of photoexcitation increases. This effect occurs in individual δ-p layers. This shift is probably associated with a decrease in the height of δ barriers. Figures 2; references 5: 2 Russian, 3 Western.

### Effect of a Rapid Increase in Plasma Concentration on the Propagation Dynamics of an Electromagnetic Wave Through Plasma

[Article by L. G. Glazov, A. A. Rukhadze, Institute of General Physics, Russian Academy of Sciences, Moscow]

[Abstract] This article examines the dynamics of an electromagnetic wave passing through a plasma layer with an exponentially increasing concentration (on the order of $e^{\gamma t}$) where $\gamma$ is on the order of the wave frequency. These ionization frequencies are found in SHF breakdown of gases of moderate pressure in superstrong fields. This article corrects an error in a previous article regarding the asymptotics of large distances from the interface between the plasma and vacuum. A detailed description of wave dynamics is obtained. The wave is a plane monochromatic linearly polarized wave with normal incidence on the plasma layer. Two simple models are used to obtain an analytical solution and to qualitatively examine the passage of the wave through this plasma. First the passage of a wave through a spatially homogeneous layer is examined. The case of a semi-infinite layer is examined in more detail. The qualitative effects associated with the increase in plasma concentration are quantitatively demonstrated by the time dependences of the reflected wave. As $\gamma$ approaches the wave frequency a significant part of the wave strength is not reflected. The second model is one in which the ionizing capability of a superstrong wave of particles moving in a field is independent of their velocity (at each point the plasma concentration is increasing exponentially over time). Figures 7; references: 9 Russian.

### Super-Radiative Instability in the Movement of an Electron Cluster in an Undulator Field or an Electromagnetic Pump Wave Field

[Article by N. S. Ginzburg, Institute of Applied Physics, Russian Academy of Sciences, Nizhi Novgorod]

[Abstract] A super-radiative instability is examined in the movement of an electron cluster of finite length in the field of an undulator or an electromagnetic pump wave. It is shown that the instability has no threshold and its increments are determined. As a result of the development of instability there is bunching of clusters of particles and coherent radiation at frequencies near the frequencies of the individual radiation (scattering) of particles. When a

cluster is advancing at a speed close to the speed of light, the frequency of the high frequency component of radiation (in the direction of advance) may substantially exceed the frequency of particle oscillations. The linear stage of super-radiative processes is studied. The thresholdless character of the instability in the presence of radiative loss is due to the infinite lifetime of the electron in the region of interaction with the high-frequency field. Increments are estimated from data from an experiment conductred at the Stanford Linear Accelerator. References 8: 5 Russian, 3 Western.

### Excitation of Hollow Infrared Waveguides

[Article by V. G. Artyushenko, K. I. Kalaydzhyan, M. M. Mirakyan, Institute of Radio Physics and Electronics, Armenian Republic, Ashtarak]

[Abstract] The excitation of hollow metal waveguides in the middle infrared range is examined. This article determined the theoretical and experimental dependences of the effectiveness of excitation of these waveguides (when they are operating in a low-mode state) on the parameters of pump radiation and the parameters of possible mismatches at the waveguide-waveguide or laser-waveguide junction. The effectiveness of excitation of a waveguide TE mode in relation to the parameters of the waveguide and excited radiation is examined. Excitation of a waveguide by a Gaussian beam is considered. The total losses and the field distribution at the output of the waveguide (as well as the power density in the zone of effect) depend on how the power supplied to the waveguide is distributed among the modes. The dependence of effectiveness of mode excitation on the ratio of the width of constriction of the beam to the height of the waveguide in ideal excitation shows that only odd modes are effectively pumped. If the vector of the electron pump field is not parallel to the plane of the reflecting plates (δ is nonzero) the effectiveness of excitation of TE modes falls as δ rises according to a $\cos^2 \delta$ law. Figures 5; references: 4 Western.

### Effect of Initial Formation Dynamics of a Plasma Conductor on the Effectiveness of Electrodynamic Accelerator Operation

[Article by V. V. Zhelezniy, M. F. Zhukov, A. D. Lebedev, A. V. Plekhanov, Institute of Thermal Physics, Siberian Division, Russian Academy of Sciences, Novosibirsk]

[Abstract] This article presents the results of an experimental study of the dynamics of a plasma cluster in a track accelerator. It is shown that the initial stage of formation of a plasma conductor has a substantial effect on the effectiveness of the operation of these devices. The predominance of gas kinetic pressure over magnetic pressure at this stage causes the free expansion of the conductivity channel. A subsequent transition to a plasma piston mode

becomes problematic and predetermines the low efficiency of a track accelerator. It is shown that when this transition occurs it is possible to increase the effectiveness of accelerator operation and achieve a rather good agreement with calculations. Comparison of model experiments with experiments at track accelerators made it possible to conclude that in most cases a compact plasma conductor mode is not realized. It was found that the majority of failures in the acceleration of large bodies in a long channel is associated with a lack of consideration of the initial phase of formation, and leads to the development of a distributed discharge. Figures 7; table 1; references 43: 36 Russian, 7 Western.

## Focusing of a Relativistic Beam of Particles in a Wiggler Magnetic Field

[Article by N. V. Smolyakov, I. V. Kurchatov Institute of Atomic Energy, Moscow]

[Abstract] The focusing of a relativistic beam of particles in the magnetic field of a plane wiggler of arbitrary shape is examined. Analytical expressions are obtained for the horizontal and vertical focal lengths of the wiggler. It is shown that the sum of the inverse focal lengths of the wiggler is virtually independent of the transverse breakdown of the field (caused by the finite width of magnetic poles). The effect of a strong-field superconducting wiggler is calculated at the frequency of betatron vibrations of the Sibir-2 electron collector. The case of a laminar beam of relativistic particles in a plane magnetic field is considered. It is found that the shape of the wiggler magnetic field must be carefully considered in the analysis of the focusing properties of the wiggler and the selection of an optimal design. Figures 2; references 21: 8 Russian, 13 Western.

## Use of an Explosive-Emission Cathode With a Conical Surface To Form a High-Current Thin-Walled Tubular Microsecond Relativistic Electron Beam

[Article by A. F. Aleksandrov, V. L. Vesnin, S. Yu. Galuzo, M. V. Karavichev, M. V. Lomonosov Moscow University]

[Abstract] An important problem in the use of coaxial magnetically-insulated diodes with explosive emission cathodes to form tubular electron beams is insuring stable spatial and temporal characteristics of the relativistic electron beam. Means of eliminating the instabilities which arise are discussed. This article examines the formation of microsecond high-current tubular relativistic electron beams with increased wall thickness using explosive-emission cathodes with a conical emitting surface. It also studies the effect of cathode plasma on the stability of the radial profile of current density in a thick-walled relativistic electon beam. Experiments were conducted in the Tandem-1 high-current electron accelerator. Regulation of

beam expansion is discussed. The critical magnetic field above which instability has no significant effect on relativistic electron beam behavior is calculated. It is shown that the movement of cathode plasma has a substantial effect on the distribution of current density of a tubular relativistic electron beam with an inreased wall thickness. As time goes on the existence of a homogeneous current density distribution and the dispersion of cathode plasma leads to redistribution of current in the cross section of the beam and formation of a thick-walled tubular beam with a wall thickness of about 1.5 mm. The diameter is determined by the diameter of the external boundary of the expanding cone of cathode plasma. Figures 6; references: 13 Russian.

## Spatial-Temporal Evolution of an Electric Discharge Controlled by a Laser Spark

[Article by E. I. Asinovskiy, L. M. Vasilyak, S. Yu. Unkovskiy, Institute of High Temperatures, Russian Academy of Sciences, Moscow]

[Abstract] This article reports on the results of electronic-optical studies of the generation and movement of luminescent ionization wave fronts in an electric discharge when it is initiated by a single plasma source or by a long laser spark with a large number of laser sources. Results are presented from studies of discharge stability when current is passed for a long period of time. The experimental set-up is described. Analysis shows that breakdown along the long laser pulse occurs in the form of ionizing waves which reach a speed of $0.3 \times 10^9$ - $20 \times 10^9$ cm/s. Optimal delay length between pulses is determined. Nonoptimal behavior is described. Self-propagation of the ionization wave (for up to 10 cm) is observed after voltage is removed from the high-voltage electrode. Various situations are studied, i.e., simultaneous emission of a voltage pulse from two electrodes, and the creation of controlled discharges more than a meter long. The behavior of the discharges is described. Figures 3; references 9: 7 Russian, 2 Western.

## Generation of Coherent Radiation on n-n Boundary in GaInAsSb DGS Lasers

[Article by A. N. Baranov, S. Yu. Belkin, T. N. Danilova, O. G. Yershov, A. N. Imenkov and Yu. P. Yakovlev]

[Abstract] This article is a continuation of earlier research by the authors on heterolasers based on GaInAsSb and is devoted to investigation of interface recombination and its influence on the threshold characteristics of such lasers. Two types of laser structures were studied: so-called DGS lasers with an active laser $Ga_{0.9}In_{0.1}As_{0.09}Sb_{0.91}$, positioned between AlGaAsSb limiting layers, and lasers for which between the AlGaAsSb layers, in addition to the narrow-band GaInAsSb layer, GaSb was introduced into the waveguide, with the GaInAsSb active layer forming a

heterojunction. The laser structures were fabricated by the liquid-phase epitaxy method. The thickness of the narrow-band region was 0.25-3 μm. The research was at 77 K in a continuous mode and at 295 K in a pulsed mode with a pulse duration 100 ns and a pulse repetition rate 5 kHz. A study was made of the spectra of coherent and spontaneous radiation of these heterolasers, as well as the dependence of the current $I_{th}$ on the width d of the active region. Lasers with the minimum levels of threshold currents were selected. The experimental data are presented and ana-lyzed for lasers with both thick and thin active regions and their relative merits are compared. Figures 3; references 16: 11 Russian, 5 Western.

## Surface Electromagnetic Waves: Microscopy of Intermediate IR Range

[Article by A. K. Nikitin and A. A. Tishchenko]

[Abstract] Optical microscopy is a new field of application of surface electromagnetic waves (SEW). The use of SEW in optical microscopy makes it possible to increase its vertical resolution to 0.3-0.1 nm. In earlier studies SEW microscopy was used in studying microinhomogeneities on the free surface of thin metal (Ag, Cu, Au) films with SEW excitation using a scheme proposed by E. Kretschmann (Z. PHYSIK, Vol 241, pp 313-324, 1971). Although appli-cable in both the visible and IR ranges, it does not make it possible to excite SEW on the surface of thick (opaque) films or massive samples. However, using the A. Otto scheme (Z. PHYSIK, Vol 216, pp 398-410, 1968) it is possible to use SEW microscopy without damaging the sample surface and a number of other advantages are evident. In this study, in the example of a specific struc-ture, an examination was made of the possibilities of SEW microscopy with the generation of SEW in the interme-diate IR range by application primarily of the Otto scheme, but invoking the Kretschmann scheme where advantageous. The computations were made for a struc-ture consisting of a prism, air gap and silver sample. The wavelength of the exciting SEW radiation was 5.80 μm. It was found that the choice of the particular method applied (amplitude or phase) is without importance. The experi-ment revealed that amplitude and phase SEW microscopy research carried out using the Otto and Kretschmann schemes is mutually complementary. Figures 3; references 11: 1 Russian, 10 Western.

## Completely Optical Dynamic Fiber Ring Memory

[Article by M. P. Petrov, Ye. A. Kuzin, V. I. Belotitskiy and V. V. Spirin]

[Abstract] Published research in which a study was made of the circulation of optical pulses in a completely optical fiber circuit indicates that the circulation time was in the range from several milliseconds to several seconds. This article gives the results of experimental study of a com-pletely optical dynamic fiber ring memory with a virtually unlimited storage time. The system is based on use of a logic inverter involving use of the stimulated Raman scattering (SRS) effect for the regeneration of optical signals. The pulse repetition rate in the circuit was 100 MHz with a pulse duration 70-100 ns. Figure 1 is a diagram of the completely optical dynamic ring memory system. The latter includes an SRS amplifier, filter ensuring suppression of radiation at the Stokes wave-length, SRS generator, fiber delay line and variable delay line. The source of pumping radiation was an Nd:YAG laser operating at a wavelength 1.064 μm. The length of the fiber in the SRS amplifier was 22 m. The SRS generator and the fiber delay line were made of a single segment of fiber 840 m long. The experiment is described. It is shown that for operation of the memory the pumping power must be close to the SRS threshold level. For the first time it was possible to demonstrate experimentally a completely optical dynamic fiber memory with a virtually unlimited data storage time. The pulse repetition rate in the fiber circuit was $10^8$ Hz. Circuit capacity was 500 bit. Pulse circulation in the fiber circuit was observed for about 10 minutes. Figures 4; references 8: 3 Russian, 5 Western.

## Phase Inverter Based on Superconductor Film Controllable by Temperature Change

[Article by O. G. Vendik and T. B. Samoylova]

[Abstract] Estimates of the principal parameters of a temperature-controllable phase inverter based on a super-conducting microstrip delay line are presented. Specific variants with different superconductors at a frequency 10 GHz are examined. Both traditional superconductors (Nb, NbN) and new high-temperature superconducting mate-rials (Y-Ba-Cu-0) are considered. A table gives typical values for the principal materials and the values of the pertinent coefficients making it possible to convert to the absolute phase shift and quality values for such phase inverters. These coefficients were computed for lines with $Z_0 = 50$ ohm and $\omega = 50$ μm realizable for a LTSC, such as when using mica sheets as a substrate. For lines of HTSC a thin film of metallized organic material, to which is mechanically pressed a HTSC film precipitated onto an $LaAlO_3$, MgO substrate, can be used as the dielectric, or it is possible to use a three-layer structure with a thin epitaxial layer of dielectric between the HTSC films. In an optimal mode the quality for phase inverters based on LTSC films and Y-Ba-Cu-O epitaxial films is identical. The results of the analysis of phase inverters based on semiconducting microstrip delay lines make it possible to choose the appropriate materials and operating modes for a temperature-controllable phase inverter for ensuring the required parameters. Figures 2; references 11: 2 Russian, 9 Western.

## Use of Antimatter for Indirect Compression and Heating of Thermonuclear Targets

[Article by M. L. Shmatov]

[Abstract] A thermonuclear reactor with inertial retention of plasma has been proposed in which the energy released during the annihilation of matter and antimatter would be used for the continuous compression and heating of plasma. This article is essentially a review of the published literature on this subject with brief commentaries on the weakness or strength of different proposals, roadblocks on the path to their realization and possible approaches for overcoming them. The importance of such research is attributable to the fact that an antimatter generator would make it possible to develop a relatively inexpensive engine convenient for spacecraft use. When using antimatter it is theoretically possible to attain a maximum (in comparison with other solutions) ratio of the released useful energy to the total mass of the apparatus, which is of great interest in space applications. The use of antimatter also would make it possible to develop an energy source with a zero or at least a relatively small neutron yield. The principal obstacle to use of antimatter is its very high cost. The mass of the equipment for storing antimatter considerably exceeds its own mass, which is manifested in the relatively small quantity of antimatter which can be stored. Massive shielding is required against radiation from $\gamma$ quanta forming as a result of the decay of neutral pions generated during annihilation. It is necessary to convert the energy of the products of annihilation into radiation in a quite small volume of matter for the energetically advantageous inducing of thermonuclear microexplosions (several possible variants have been proposed). The conversion of the energy released during annihilation into photons also is of interest for the use of antimatter for the pumping of SW lasers. Figure 1; references 22: 5 Russian, 17 Western.

## Boundary Integral Equations Method in Shortwave Diffraction Problems

[Article by N. V. Boyev, I. I. Vorovich, M. A. Sumbatyan, Rostov-on-Don; UDC 539.5]

[Abstract] This article presents a modification of the boundary integral equations method for the study of two-dimensional problems of shortwave diffraction on objects with an arbitrary smooth contour in an acoustic medium. The method is physically based on a consideration of the specifics of interaction of the incident field with convex and concave portions of the object boundary. Rays incident on convex parts of the boundary may not participate in secondary re-reflection. Conversely, rays incident on concave parts may be re-reflected only at points of these sections which are not on the convex part of the contour. Thus, due to the separation of diffraction effects on convex and concave parts of the boundary, one can reduce the size of systems in the boundary integral equations method. This method substantially reduces computation time. Figures 4; references 6: 4 Russian, 2 Western.

## Hyperexponential Spectra of Explosive Destruction of Metal Cylinders

[Article by V. A. Odintsov, Moscow; UDC 539.5]

[Abstract] The distribution laws of fragments obtained in the explosive destruction of metal cylinders are in general bimodal, which is due to the presence of two different morphological sets of fragments (semiregular large fragments containing both initial surfaces of the cylinder, and small fragments containing one initial surface). A statistical model is proposed to describe the bimodal spectra. The model is a hyperexponential distribution function. A good agreement between the proposed model and experimental spectra of fragments of steel cylinders is confirmed. Analysis of experimental results showed that the main determining dimensionless parameters in the fragmentation of cylinders are the relative thickness of the wall, the elongation of the chamber, and the dimensionless fragmentation parameter (which involves the density of the explosive material, the speed of detonation, the internal radius of the cylinder, the shear modulus of the metal, and the specific energy of destruction). Tables list fragmentation results for various parameter values and types of explosives. Figures 3; tables 3; references 10: 9 Russian, 1 Western.

## Flattening of Cylindrical Shells Due to External Evenly Distributed Pressure in Creep Conditions

[Article by A. M. Lokoshchenko, S. A. Shesterikov, Moscow; UDC 539.376]

[Abstract] Cylindrical shells are widely used in machines when an external evenly distribued pressure is applied at high temperature. If this shell is affected by external pressure for a long time with intense development of creep deformations, the problem is one of determining the change in tensions and deformations over time and calculating the lifetime of this cylinder before it flattens. In any real shell the middle line of the cross section in the initial state is, to some degree, a nonideal circle. In most cases, when one considers the effect of initial imperfection of the cross section on the behavior of the shell, one usually assumes that the initial cross section has a slightly oval form characterized by two axes of symmetry. The quantitative character of initial ovalness is usually the ratio of the difference of the maximum and minimum diameters of the cross section to their sum. The coefficient of initial ovalness has a substantial effect on the lifetime of the shell.

Three testing series of shells in conditions of steady-state creep are analyzed. The geometric method of approximating the middle line of the cross section of the shell in the form of two joined arcs leads to theoretical results which agree well with experimental data. Tables are presented which give parameter values and the results obtained from different theoretical models. While the results of all three models fall within the scatter of experimental data, the advantages of the arc model over the others are explained. Figures 2; tables 3; references 14: 10 Russian, 4 Western.

## Matching the Plane of an Elastic Axisymmetrical Membrane by Uniform Stretching

[Article by N. V. Zvolinskiy, B. S. Chekin, Moscow;
UDC 539.4]

[Abstract] This article examines the stretching of an elastic film (which has the shape of a rotation surface) on a plane. Depending on forces which are uniformly distributed over a circle lying in some plane, and which are stretching the film, either the entire film will be stretched on the plane, or only part of it. The results of the study are used in the ophthamological problem of designing an artificial crystalline lens. The natural crystalline lens is in a capsule. After removal of the natural lens, peripheral muscles stretch the capsule, and its diameter, which was initially equal to the diameter of the natural lens, increases. Knowledge of this increase is important for accurate sizing of the artificial lens. The increase in the diameter is addressed. It iniitally has the shape of a spherical segment. Graphs are presented which permit a surgeon to determine the amount of stretching of the capsule for a given initial diameter and thickness of the capsule. Figures 4; reference: 1 Russian.

## Results of First Experiments With Thermonuclear Targets for Powerful 'Iskra-5' Laser Outfit

[Article by A. V. Bessarab, V. A. Gaydash, G. V. Dologoleva, N. V. Zhidkov, V. M. Izgorodin, G. A. Kirillov, G. G. Kochemasov, A. V. Kunin, D. N. Litvin, V. M. Murugov, G. F. Nasyrov, V. T. Punin, V. G. Rogachev, A. V. Senik, N. A. Suslov, G. V. Tachayev and V. I. Shemyakin (deceased)]

[Abstract] At the All-Union Experimental Physics Scientific Research Institute the first experiments were carried out with thermonuclear targets using the powerful "Iskra-5" 12-channel iodine laser outfit. The intensity of the radiation at the laser output was about 12 kJ with a pulse duration 0.25 ns and a beam divergence less than $10^{-4}$. Thin-walled thermonuclear targets with an internal input of laser radiation (inverted corona target—ICT) were developed and fabricated. Experiments were carried out with irradiation of an ICT by a laser radiation pulse with an energy up to 10 kJ. A yield 5 x $10^9$ of D-D neutrons was obtained in targets containing polydeuteroethylene as the working substance. The measured temperature of the ionic component of plasma attains 10 keV. The experimental results are in satisfactory agreement with computed-theoretical evaluations. These computations show that with a changeover to a working substance containing deuterium and tritium in an equimolar ratio the yield of D-T neutrons increases by a factor of approximately 70. Research on nonequilibrium processes accompanying ICT use makes it possible to obtain necessary physical information on the properties of high-temperature plasma and proceed on a sound basis to a study of more complex structures intended for obtaining spark ignition. Figures 6; references 10: 5 Russian, 5 Western.

## Self-Focusing and Relativistic Guidance of Ultrashort Laser Pulse in Plasma

[Article by L. A. Abramyan, A. G. Litvak, V. A. Mironov and A. M. Sergeyev, Applied Physics Institute, Russian Academy of Sciences]

[Abstract] One of the promising methods for generating strong electric fields in plasma for accelerating high-energy particles involves the excitation of plasma waves using ultrashort laser pulses. However, there is still no quantitative theory of this process. This article gives a detailed study of the processes of dynamic self-focusing of an ultrashort laser pulse during propagation in rarefied plasma. The research revealed that a strong ultrashort relativistic laser pulse during propagation in plasma experiences a considerable structural deformation, acquiring a hornlike shape with strong longitudinal intensity modulation. The leading edge of the pulse, as a result of inertia of the nonlinear response, experiences linear diffractional dispersion; however, most of the pulse is captured in a nonlinear guidance mode in which the region of the strong Langmuir track left by the pulse is substantially lengthened. There is an appreciable strengthening (in comparison with a linear case) in the intensity of the plasma wave and an increase in the longitudinal dimension of the region in which this effect is observed. The self-similar solutions obtained in this study for dynamic self-focusing of a pulse therefore make it possible to determine the amplitude of the so-called wake wave and the extent of the region of its effective excitation. Figures 4; references 14: 4 Russian, 10 Western.

## Research on Surface Debye Waves on Facets of GaAs Monocrystals by Molecular Light Scattering Spectroscopy Method

[Article by V. V. Aleksandrov, T. S. Velichkina, Yu. V. Potapova and I. A. Yakovlev, Moscow State University imeni M. V. Lomonosov]

[Abstract] Mandelstam-Brillouin (MB) light scattering is an effective method making possible a detailed study of equilibrium surface phonon spectra of opaque crystals. In addition to a surface wave of the Rayleigh type (or so-called generalized surface wave (GSW)) with a real value of the wave vector lying in the plane of this surface, there may be two additional pseudosurface waves characterized by a complex wave vector deflected in the depth of the crystal. These waves, in contrast to the GSW, attenuate along the surface because the tangential component of their wave vector has an imaginary part. One of them is the pseudo-surface mode (PSM) and the other is the high-frequency pseudosurface mode (HFPSM). With these considerations taken into account, an experimental study was made of surface excitations in the hypersonic range in the case of a cubic GaAs crystal (planes (001) and (111)) by the MB spectroscopy method because in these crystals a unique possibility is afforded for observing both PSM and HFPSM and the crystals themselves are characterized by a quite high anisotropy parameter. The light scattered from the GaAs crystal surface was observed at an angle 180°. The observations were made at room temperature; in all the experiments the electric vector E of the light wave incident on the crystal was parallel to the incidence plane. The radiation source used was the light of a single-frequency argon laser with wavelengths 514.5 or 488.0 nm and a power of about 100 mW in each line. The phenomena observed under the mentioned conditions are analyzed. Figures 5; references 19: 1 Russian, 18 Western.

## Magnetic Structures and Properties of States in Highly Frustrated Heisenberg Antiferromagnetic Materials

[Article by R. S. Gekht; Physics Institute imeni L. V. Kirenskiy, Siberian Department, Russian Academy of Sciences]

[Abstract] The magnetic structures and properties of states in frustrated Heisenberg antiferromagnetic materials are discussed. It is shown that the frustrations induced in the system due to additional spins result in a great diversity of phases with commensurable and incommensurable periods and also in the appearance of aperiodic phases. The possible states in two-dimensional lattices were investigated for a new frustrated system consisting of spins of two types. The additional frustrations induced in such a system cause a strong degeneration of the fundamental state for large spins. The energy spectrum of the different phases was computed. It was found that in the phase with a commensurable period $(0, 2\pi)$ the lower branch of the $\varepsilon_k$ excitation spectrum exhibits additional softening with approach to the boundary with the incommensurable phase $(0, Q)$. In the same phase $(0, Q)$ the energy of the spin waves along definite directions k may become equal to zero regardless of the value of the wave vector modulus. This circumstance is attributable to the presence of local degeneration in the system. The various corollaries of

these findings are examined. A phase diagram of states is constructed and the region of local degeneration of individual structures is defined. Figures 7; references 21: 4 Russian, 17 Western.

## Protection of Mirror of Short-Wave Laser by Destructible Screen

[Article by M. L. Shmatov, Physical Technical Institute imeni A. F. Ioffe, Russian Academy of Sciences, St. Petersburg]

[Abstract] The protection of the mirror of a short-wave laser by a screen which can be destroyed at the time of approach of the principal reflected stream of induced radiation is proposed. A rapid increase in screen transparency can be accomplished by its transformation into plasma. In many cases the screen will reduce the energy load on a unit area of the mirror surface by at least several times. Screens can be used simultaneously with massive diaphragms or soluble collimators for protecting the mirrors or the screens themselves. It is possible to use a design containing several destructible layers between which additional elements are placed. Protection can be provided for the unused mirror surface. The optimal variant would be screen ionization solely due to the plasma effect of the active medium, and in part, the induced radiation. It would also be possible to feed a part of the stream of pumping radiation to the screen, but this would increase the energy load on the mirror. Thin destructible multilayer mirrors, successively entering into play, would make it possible to realize two additional passages of radiation through the active medium. Such a system also could be used for the reflection of a prolonged radiation impulse, including an incoherent impulse. The active medium of a short-wave laser has longitudinal inhomogeneities caused by the nonuniformity of pumping, which in the considered case results in a lengthening of the main induced radiation impulse. In conducting the experiments proposed in this study it is therefore desirable that the pumping be highly uniform. The use of the screens and the destruction of the mirrors will be effective only with a high reproducibility of the properties of the active medium, making it possible to optimize the structural elements. Figures 2; references 20: 7 Russian, 13 Western.

## Simulation of High-Velocity Penetration Problems in Lagrangian Coordinates

[Article by V. V. Bashurov and S. K. Buruchenko, All-Russian Technical Physics Scientific Research Institute; UDC 539.3]

[Abstract] The finite elements method, widely used in solving problems in the mechanics of continuous media, was used in simulating problems related to high-velocity

penetration of a projectile into a target in Lagrangian coordinates. A package of practical programs was prepared for numerical simulation of these problems with allowance for large elastico-plastic deformations. An explicit Lagrangian finite elements method was applied using a program applicable for the case of two space variables. The geometry of the problem is described using triangular elements with a constant field of rates of deformations within an element. Each element point of intersection was assigned some constant mass and the equivalent force for it was determined from the stresses in adjacent elements, after which the velocities and movements of the points of intersection were determined by integrating the equation of motion with the imparted force. The velocities and movements were used in determining new volumes and stresses in the elements. (All the features of explicit finite-difference schemes are characteristic for the used finite elements method.) The Prandtl-Reuss rheological model with the Mises flowability condition was applied. Examples of the computations are given, for example, for the penetration of a zirconium jet into a semi-infinite barrier and the penetration of a tungsten rod into an aluminum plate. The described method with a good accuracy makes it possible to simulate the size of the crater in a barrier in the case of normal incidence of such jets or rods, with allowance for the strength properties of the pertinent materials. Figures 2; references: 3 Western.

## Simulation of Dynamics of Multicomponent Schroedinger Solitons

[Article by V. A. Vysloukh, Ye. A. Kolomiytseva and I. V. Cherednik, Moscow State University imeni M. V. Lomonosov]

[Abstract] The procedures of direct numerical integration of the nonlinear Schroedinger equation have been well developed and progress has been made on methods based on the inverse scattering problem approach, but a number of timely problems in nonlinear waveguide optics, such as study of the propagation of optical pulses in two-mode waveguides, necessitates a more complex model: a vectorial nonlinear Schroedinger equation, as proposed by G. P. Agrowal in Nonlinear Fiber Optics, N. Y., Academic Press, 1988. In order to make effective use of the vectoral variant a method was developed for computing the parameters of two-component solitons based on the inverse scattering approach. The dynamics of multicomponent Schroedinger solitons is investigated by mathematical simulation methods. The possibility of control of soliton parameters by its mixing with a nonsoliton low-amplitude pulse in an orthogonal mode is demonstrated. The dynamics of femtosecond two-component solitons is analyzed within the framework of the adiabatic approximation of the theory of perturbations. The numerical methods outlined at the beginning of the article and the inverse scattering approach developed thereafter mutually supplement one another, making possible an adequate description of both the initial stages in the propagation of ultrashort optical pulses along

the fiber waveguide and their asymptotic behavior over great distances. Allowance for the multicomponent character of solution of the vectoral nonlinear Schroedinger equation results in the detection of new effects absent in a scalar case and affords new possibilities for their practical use. Figures 4; references 16: 9 Russian, 7 Western.

## Characteristics of Application of X-Ray Computational Tomography in Research on Composite Materials

[Article by V. I. Barakhov, V. A. Chernyayeva and V. S. Kiselev; UDC 541.18+539.217.1]

[Abstract] Various aspects of the use of X-ray computational tomography in the study of composite materials are discussed. The method affords possibilities for evaluating the density of each fundamental element of a material without impairing its intactness. The short wavelength of the X-radiation makes it highly penetrable and even at low energies it is possible to study samples of virtually all modern composite materials. Research on two important characteristics is emphasized: the specifics of the method itself and its metrological possibilities. The following are examined: interaction between X-radiation and matter, registry of photons before and after passing through matter; mathematical processing of scanning data related to image retrieval from projections. Three principal effects arising with the incidence of X-rays on matter are analyzed: photoelectric effect; photon scattering; formation of electron-positron pairs. The special features of the tomographic method for composite materials related to the interaction between X-radiation and matter, retrieval of images from projections and random errors in determining the linear attenuation factors are examined on the basis of research carried out using a SOMATOM DR-2 tomograph. The transformation from linear attenuation factor matrices to density matrices, with a description of one of the possible methods for evaluating the true values of the linear attenuation factors of matter and a representation of the correlations between density and attenuation, and also the linear attenuation factors for some composite materials, are then discussed. The complex interaction between X-radiation and matter, the special mathematical processing of scanning data and the random errors in estimating the linear attenuation factors constitute special features of application of X-ray computational tomography in an investigation of composite materials and dictate that they all be taken into account in such research. Figures 4; references: 8 Russian.

## Nonstationary Motion of Superconducting Cylinder in Uniform Magnetic Field

[Article by N. V. Derendyayev and V. A. Senyatkin, Applied Mathematics and Cybernetics Scientific Research Institute, Nizhegorod University imeni N. I. Lobachevskiy]

[Abstract] The motion of an infinitely long cylindrical superconductor in an external constant uniform magnetic field was investigated within the framework of the London equations. The problem of finding the electromagnetic field outside the superconductor is reduced to solution of a hyperbolic second-order differential equation with boundary conditions at the surface of the superconductor and on one of its characteristics. The condition for solvability of this boundary problem is written in the form of a Volterra integral equation of the second kind. By solving this equation it is possible to compute the electromagnetic field in the entire space, the electric current in the super-conductor and the force acting on such a superconductor moving in a magnetic field. The force operative on the superconductor, as well as the electric current flowing through the cross section, are ascertained. A method for solving the problem of radiation of waves with a condition at the wave front is proposed. Both stationary and nonstationary cases are considered and appropriate algorithms are written for determining the distribution of the electromagnetic field during motion of a superconducting cylinder in an external constant uniform magnetic field. Figures 5; references: 3 Russian.

## Relaxation Processes in MDS Elements of Integrated Circuits Caused by Ionizing Radiation and Pulsed Magnetic Field

[Article by A. G. Kadmenskiy, S. G. Kadmenskiy, M. N. Levin, V. M. Maslovskiy and V. Ye. Chernyshev]

[Abstract] The relaxation processes in MDS elements of integrated circuits induced by exposure to radiation and a pulsed magnetic field were investigated. The radiation used was soft X-radiation with a quantum energy up to 20 keV, a power of the exposure dose 50 R/s and an exposure dose D up to $10^5$R. The pulsed magnetic field was unidirectional, had a maximum strength $5 \times 10^5$ A/m and a pulse duration 30 $\mu$s. The duration of the exposure was 2 s with a pulse repetition rate 50 Hz. The results of exposure of p-MDS transistors to X-radiation and a pulsed magnetic field are represented in Figs. 1 and 2 as a function of time. For example, exposure to a pulsed magnetic field resulted in the generation of surface states and a negative charge in the oxide. The energy distribution of surface states coincided with the spectrum of radiation-induced surface states. The generation of a negative space charge and surface state occurred more slowly than their subsequent relaxation to the initial levels. The relaxation of surface states and the charge in the oxide occurred synchronously. The influence of a pulsed magnetic field may lead to the dynamic polarization of the nuclei of $Si^{29}$ atoms. After exposure to a magnetic field the polarization of electron spins is caused by a superfine interaction with the polarized nuclei. These findings, as well as others developed in the study, can be regarded as the first step in clarifying the interrelationship between the mechanisms of long-term relaxations in the base elements of microelectronic systems

when they are exposed to ionizing radiations and a pulsed magnetic field. Figures 2; references 9: 6 Russian, 3 Western.

## Thin Antenna With Plasma Load

[Article by G. A. Markov, A. L. Umnov and M. V. Likhodeyev, Nizhegorod State University imemi N. I. Lobachevskiy]

[Abstract] In order to increase the efficiency of electric dipoles there is a possibility of routine control of their input and radiative characteristics by means of the plasma formations generated by the antenna field. The results of experimental research on the influence of a stationary plasma load formed by the field of the working signal at the end of a thin antenna are presented. Figure 1 is a diagram of the experiment. The investigated antenna was an asymmetric metal dipole situated over a metal plate; the end of the dipole was placed in a discharge tank in which the necessary pressure was established by the continuous evacuation of air. The emitter had an inductive coupling with a HF generator whose signal generated and supported the plasma around the end of the antenna. The influence of the plasma load on the characteristics of the thin antenna could be judged from the current distribution along the antenna. The signal from a transducer was registered on an oscillograph and the plasma parameters were measured using a Langmuir probe. The influence of the end load on the antenna current was studied with a constant output voltage of the HF generator at three fixed frequencies (50, 180, 230 MHz) with different pressures in the discharge tank. A diagram of the experiment accompanies the text. A somewhat different picture was observed at each of the frequencies. A study of these experimental variants revealed that in an antenna with a plasma load at the end by the proper choice of discharge conditions it is possible to control the distribution of the radiating current, and therefore its input impedance and radiation power as well. Figures 2; references 7: 4 Russian, 3 Western.

## Selective Polarimetric Effect in Au-n-GaAs Structures

[Article by S. G. Konnikov, G. D. Melebayeva, D. Melebayev, V. Yu. Rud, Yu. V. Rud and M. Serginov, Physical Technical Institute imeni A. F. Ioffe, Russian Academy of Sciences, St. Petersburg]

[Abstract] The results of experiments carried out for the first time on the polarimetric effect in Au-n-GaAs structures in which the free surface of a crystal of gallium arsenide opposite the barrier contact is used as the receiving plane are given. The observations made it possible to proceed to a narrow-band photoanalyzer mode without any changes in instrument design. The surface

barrier structures were created by the ordinary method of precipitation of thin palladium-gold layers on a mirror smooth surface of epitaxial GaAs layers with a concentration of free electrons $n = 10^{15} - 10^{16} \text{ cm}^{-3}$ which were grown on substrates of semi-insulating GaAs. Figures 1-3 give typical experimental results of measurements of the photosensitivity of Au-n-GaAs structures in plane-polarized radiation with its slant incidence from the direction of the GaAs layer. The typical spectral dependence of the maximum azimuthal photosensitivity of the investigated structures gives evidence of their effective applicability as selective polarimetric photodetectors with illumination from the direction of the semiconductor, or with allowance for other experimental results, as broadband polarimetric photodetectors with illumination from the direction of the barrier contact. Figure 3; references 12: 10 Russian, 2 Western.

## Volumetric Character of Hardening of Martensite Under Influence of Megavolt Highly Precise Electron Beam

[Article by A. M. Yefremov, Yu. V. Ivanov, V. I. Itin, B. M. Kovalchuk, I. S. Kashinskaya, S. V. Lykov, A. B. Markov, D. I. Proskurovskiy and V. P. Rotshteyn, Highly Precise Electronics Institute, Russian Academy of Sciences, Tomsk]

[Abstract] The behavior of martensite under the influence of powerful shock waves induced by a highly precise electron beam is examined. The propagation of such waves results in intensive deformation processes, including splitting off of the rear part of the sample. A study was made of the hardening, as well as the phase and structural transformations in martensite steel 45 with exposure to the powerful shock waves excited by a megavolt highly precise electron beam with a power density up to $10^{11}$ W/cm$^2$. Irradiation was accomplished using a highly precise electron accelerator in the following mode: beam current—65 kA, maximum electron energy—1.5 MeV, pulse duration—50 ns. The samples with a diameter 20 mm and a thickness 5-10 mm were irradiated by the paraxial part of the beam with a diameter 12 mm. After irradiation the samples were investigated by optical metallography, examination under an electron microscope and microhardness measurements. The target thermal regime was found by numerical solution of the thermal conductivity equation. Under the influence of shock waves there is evidently a

blockage of such known channels for the dissipation of its energy as an increase in the density of defects and fragmentation of crystals. The influence of shock waves results in the development of volumetric processes of the movement of dislocations and reorganization of the defect structure in macrovolumes of the material. This, in turn, results in the accumulation in the material of additional elastic energy up to the level corresponding to its tensile strength. It is evident that a microstructural state with such a high elastic energy is unstable. Volumetric accumulation and subsequent relaxation of elastic energy results in the formation in the martensite of the experimentally observable periodically hardened structure. Figures 3; references: 6 Russian.

## Strength and Longevity of Light Conductor Fibers

[Article by V. S. Kuksenko, U. Sultonov, A. Abdumanonov, M. I. Shamsidinov and S. N. Karimov]

[Abstract] Light conductor fibers are quite complex in chemical composition and structure, but in this study the focus is on the mechanical behavior of these objects and therefore it was sufficient to discriminate the principal parameters and structural elements responsible for the strength and longevity of this construction material. However, the high strength of the light conductor fibers and their brittleness causes definite difficulties in their loading. In the experiment a special loading system with two drums was used (a figure accompanies the text). The sample was clamped to the surface of one of the drums (70 mm in diameter). Both drums were attached to a solid plate, one of them rigidly, whereas the other, through which the sample was loaded, could be rotated. The distances between the drums determined the working length of the sample and could be varied. The longevity of the fibers was determined under different loads and at different temperatures. Emphasis was on low activation energies of the failure process. The results of such a study are presented. Although a polymer film protects the fiber against mechanical damage, it cannot protect it against degradation with exposure to surface-active water and therefore there is a need for seeking those coatings which would make it possible to safeguard the fiber surface from exposure to moisture since this would ensure an increase in longevity by many orders of magnitude, as is essential for light-conducting cables intended for prolonged use. Figures 3; references: 5 Russian.

## Wideband Suppression of Light Noises in Propagation Through a Multiphoton Absorber

[Article by V. N. Gorbachev, A. I. Trubilko, A. I. Herzen Russian State Pedagogical University, St. Petersburg]

[Abstract] Propagation of light with arbitrary statistics is examined in a medium with multiphoton absorption or amplification. The limit level of suppression of shot noise is 33 percent for two-photon absorption and 50 percent for $m$-photon absorption as $m$ goes to infinity. The reduction of noise occurs in a broad band of frequencies. A Langevin approach is used to analyze the transfer equation for the electromagnetic field density matrix. The transfer equation method makes it possible to describe the propagation of light in the medium in the framework of quantum electrodynamics. A test problem is examined, and the change in the statistical properties of light are calculated and numerical estimates given for two-photon interaction (for calssical and sub-Poisson light). Results are presented for an $m$-photon interaction. The Langevin approach makes it possible to avoid explicit calculation of a $P$-function to calculate the observed quantities and to directly obtain normally ordered averages. Figures 2; references 25: 9 Russian, 16 Western.

## Nonlinear Response of a Photorefractive Crystal in an AC Field Affected by a Nonstationary Interference Pattern

[Article by A. V. Dugin, B. Ya. Zeldovich, P. N. Ilinykh, O. P. Nesterkin, Chelyabinsk State Technical University]

[Abstract] This article studies the recording of a static hologram of a moving interference pattern in a photorefractive crystal when an alternating current field is applied to it. The frequency of the field coincides with or is a multiple of the modulation frequency of one of the interacting beams, and substantially exceeds the inverse of the recording time. Phase and amplitude modulation are studied. Theoretical analysis is done on the basis of material equations which describe the process of spatial separation of charge in a photorefractive crystal. The experiment used $Bi_{12}TiO_{20}$ crystals, one with a long electron drift length (compared with the period of the holographic lattice) and one with a small drift length. Monochromatic modulation is studied, as are some special cases of polychromatic modulation. The case of recording of a holographic lattice in a sign-variable field in the form of a meander is discussed. The effectiveness of holographic recording using this mechanism primarily depends on the relation between the electron drift length and the period of the recorded lattice. Figures 8; references 13: 3 Russian, 10 Western.

## Quasi-Two-Dimensionality of a Phonon Subsystem of Bismuth Superconductors

[Article by A. A. Bush, I. N. Goncharuk, Yu. E. Kitayev, M. F. Limonov, Yu. F. Markov, R. A. Evarestov, Moscow Institute of Radio Engineering, Electronics, and Automation, St. Petersburg University, and the A. F. Ioffe Physicotechnical Institute, Russian Academy of Sciences]

[Abstract] To study the vibrational spectra of multicomponent bismuth superconductors, a method is proposed and used to comparatively analyze a number of compounds which are formed by sequential addition of new layers: $(Bi, Ca)O_\delta \rightarrow (Bi, Sr)O_\delta \rightarrow Bi_2Sr_2CuO_6 \rightarrow Bi_2Sr_2CaCu_2O_8 \rightarrow Bi_2Sr_2Ca_2Cu_3O_{10} \rightarrow Bi_4Sr_4CaCu_3O_{14}$. A theoretical group analysis of the symmetry of normal vibrations of bismuth compounds (both isolated layers and three-dimensional crystals) is done using zone representations of three-dimensional groups. A symmetry link between layer and bulk vibrations is determined. It is found that in the transition from one compound to another the frequencies of bulk phonons generated by layer vibrations change insignificantly, that is, predominantly intralayer parameters are determined. This makes it possible to conclude that the phonon subsystems of bismuth superconductors are quasi-two-dimensional. Tables provide data on the chemical composition of the crystals, the phonon symmetry in individual layers, and crystal types. Combination light scattering is used to study optical vibrations of bismuth compounds. Figures 5; tables 8; references 34: 13 Russian, 21 Western.

## Magnetic Phase Diagrams of a $YBa_2(Cu_{1-x}Fe_x)_3O_y$ System

[Article by I. S. Lyubutin, T. V. Dmitriyeva, V. G. Terziyev, Institute of Crystallography, Russian Academy of Sciences]

[Abstract] Mossbauer spectroscopy is used to study magnetically-ordered states in a system of oxygen saturated and oxygen depleted samples of $YBa_2(Cu_{1-x}Fe_x)_3O_y$ at $0.01 \leq x \leq 0.30$. It was found that in the superconductive state, magnetic ordering of Fe ions occurs at Cu1 nodes, probably like spin glass. Losses in superconductivity due to a high degree of doping, as well as when oxygen is driven out, leads to the appearance of magnetic ordering at Cu2 nodes. In samples depleted of oxygen, at low iron concentrations ($x \leq 0.05$) the sublattices of Cu1 and Cu2 are not

magnetically linked and one observes two magnetic phase transitions: a low temperature transition at $T_{m1} \approx 20$ K for sublattice Cu1 and a high temperature transition at $T_{m2} \approx 400$ K for sublattice Cu2. As the iron concentration increases, at $x \geq 0.1$ a strong exchange interaction appears between the Cu1 and Cu2 sublattices, and the entire matrix is ordered antiferromagnetically with a single point of magnetic transition, $T_{m2} \approx 460$ K. Phase diagrams are constructed which define the region of coexistence of magnetism and supercondutivity, as well as regions of various magnetic phases in $YBa_2(Cu_{1-x}Fe_x)_3O_y$ systems saturated with and depleted of oxygen depending on iron content. Figures 9; references 42: 9 Russian, 33 Western.

## Potential Fluctuations and the Structure of Impurity Bands in a Weakly Compensated Semiconductor

[Article by Yu. Ya. Tkach, Ye. V. Chenskiy, Institute of Radio Engineering and Electronics, Russian Academy of Sciences]

[Abstract] A model is developed for a weakly doped and weakly compensated semiconductor. The Markov method is used to calculate the density of potential fluctuation depending on the degree of compensation $K$ of the semiconductor. It is shown that the dependence of the position of the Fermi level on compensation is due to an increase in the amplitude of potential fluctuation as $K$ rises. The density of donor and acceptor states is calculated when there is little compensation. It is shown that both densities have the form of dependences with two maxima. The Fermi level for n-type semiconductors is between the maxima at the minimum of donor density. Acceptor density has a "forbidden" gap with energy on the order of $e^2 N_d^{1/3}/\varepsilon$ ($N_d$ is the average concentration of donors over volume, and $\varepsilon$ is the permittivity of the semiconductor). It is found that studying the spectral density of absorption from the acceptor level makes it possible to determine the density of potential fluctuation in weakly compensated semiconductors. Figures 6; references 7: 5 Russian, 2 Western.

## Magnetic Field Induced Photogalvanic Effect in Hole GaAs

[Article by A. V. Andrianov, Ye. V. Beregulin, Yu. B. Lyanda-Geller, I. D. Yaroshetskiy, A. F. Ioffe Physicotechnical Institute, Russian Academy of Sciences]

[Abstract] Results are presented from experimental and theoretical studies of Hall and non-Hall linear photogalvanic effects in a magnetic field. Results are also presented for magnetically induced circular photogalvanic effects in p-GaAs. The physical nature of the observed phenomena is described. A good qualitative and quantitative agreement is obtained between experiment and theory for effects in the infrared induced by the radiation of a $Co_2$ laser. It is shown that, depending on concentration and temperature, the effect may be associated with the asymmetry of the scattering of holes on phonons or impurities. It may also be associated with the asymmetry of interaction with radiation. It is also shown that the features of the dynamics of particles with spin in crystals without an inversion center leads to a situation where the circular photogalvanic effect (which is absent when $H = 0$) induced by the magnetic field is an order of magnitude greater than Hall and non-Hall currents associated with the turning of the distribution function which causes the linear photogalavnaic effect at $H = 0$. Study of the linear photogalvanic effect in the infrared made it possible to study the effect in the submillimeter range of the spectrum. Study of the mechanisms of the circular photogalvanic effect in a magnetic field led to the prediction of new photogalvanic effects in quantum wells and superlattices. Figures 7; references 16: 13 Russian, 3 Western.

## Semiconductor Structures and Devices on GaAs With Deep Centers

[Article by S. S. Khludkov and O. P. Tolbanov, Siberian Institute of Engineering Physics imeni V. D. Kuznetsov at Tomsk State University; UDC 621.382.2]

[Abstract] Unconventional semiconductor devices built on π-v-n GaAs structures with electron-hole junctions, formation of such structures and their characteristics being analyzed on the basis of available up-to-date research data. The structures are formed by doping GaAs with group-IV transition elements such as Cr and Fe so as to produce deep centers, which then become overcharged in an external electric field or under incident electromagnetic radiation. The structure then has a v-region on an n-type substrate and under a space-charge region separating it from a π-region of a high-resistance layer on top. A review of the technology and the processes involved includes includes a description of two fundamental mechanisms: first the mechanism mechanism by which such a structure acquires an S-type current-voltage characteristic with negative differential resistance upon application of a reverse bias, then the mechanism of high-speed switching. Next is considered absorption of electromagnetic radiation covering the entire spectrum from visible light through X-rays to γ-rays and of high-energy particles by such a structure. On the list of already produced new GaAs devices with deep centers in the π-v-n structure are high-speed electronic switches such as avalanche S-diodes and S-triodes for pulse circuitry capable of switching 20-1000 V within 0.04-0.5 ns, photodetectors of 0.2-10 μm radiation, those of 0.2-0.4 μm ultraviolet light featuring a sensitivity of 0.2-0.5 A/W sensitivity, and detectors of ionizing radiation or of charged particles. Two important advantages of these GaAs devices over conventional Si and Ge devices, in

addition to their much higher speed and radiation sensitivity, are their much higher radiation immunity and that they do not require cryogenic cooling. The detectors also record much more effectively than do GaAs detectors with p-i-n structures or Schottky barriers. Figures 5; references 30.

## Contactless Radio-Wave Methods of Measuring Electrophysical Properties of Semiconductor Materials

[Article by M. V. Detinko, Yu. V. Lisyuk, Yu. V. Medvedev, and A. A. Skrylnikov, Siberian Institute of Engineering Physics imeni V. D. Kuznetsov at Tomsk State University; UDC 621.3.083.2-52:537.311.322]

[Abstract] Inasmuch as radio-wave and microwave methods of measurement are contactless and nondestructive, they are preferred for measurement of electrophysical properties of semiconductor materials with high accuracy and high spatial resolution. These methods also ensure retention of surface sterility. Applications of these methods are first demonstrated on measurement of the electrical resistivity with quasi-steady resonators. Several constructions of quasi-steady microwave resonators acting as transducers are described: toroidal and coaxial ones, also of those utilizing the photoelectric effect. Methods of instrument resonator design are compared, the method of equivalent circuit being the simplest but not sufficiently precise for taking into account the skin effect and quasi-steadiness of the electromagnetic field. The method of partial regions is preferable for calculation of electrodynamic characteristics of a coaxial resonator, solution of the wave equation being reducible to solution of the dispersion equation for the natural complex frequency of such a resonator. Description of contactless diagnostic testing of semiconductor structures by the microwave magnetoresistance method is followed by analytical calculations for a semiconductor plate representing the extreme limit of a flat ellipsoidal one. Calculations of its microwave magnetoresistance in terms of power loss are made for such a plate in a parallel microwave electric field and a perpendicular magnetic one, in a perpendicular microwave electric field and a parallel magnetic one, and in both fields parallel to the plate but crossing at right angles. Different relations are obtained for plates of "low-resistivity" semiconductor materials and "high-resistivity" ones. Next is considered the microwave magnetoresistance of semiconductors in a laid-on coaxial transducer. Another applications of the microwave resonance method include measurement of the mean cavity life of charge carriers, this quantity being determined indirectly upon measurement of the effective time of photoconductivity relaxation following application of square pulses of long-wave radiation to the semiconductor structure. Instruments available for contactless diagnostic testing of semiconductor structures include the IPS-1F/2F for measuring the electrical resistivity of epitaxial semiconductor films on conducting substrate, the VAGA for measuring the surface resistance of and the carrier mobility in thin semiconductor films on insulating substrates, and the TAUM for measuring the mean life of charge carriers. The ARGAL complex is available automatic measurement of both electrical resistivity and carrier mobility distributions in plates of semi-insulating materials. Figures 10; references 52.

## Polarization and Scattering Spectrum Characteristics of Intricate Dynamic Bodies

[Article by A. I. Timoshenko, R. P. Starovoytova, V. S. Kiryanov, G. A. Skorospelov, and V. V. Fisanov; Siberian Institute of Engineering Physics imeni V. D. Kuznetsov at Tomsk State University; UDC 621.371.167]

[Abstract] Scattering of electromagnetic radiation by intricate dynamic bodies is analyzed in the high-frequency approximation on the basis of a physical model representing such a body as an ensemble of "bright" specular scatterers. As specific bodies are selected axisymmetric ones having closed surfaces, surfaces with ribs and smooth segments of large electrical dimensions between ribs. The base lines of the ribs, which break the surface smoothness, are assumed to have radii of curvature sufficiently large to allow replacement of the body with an array of scattering centers located on those lines and having the properties of the equivalent wedge. Each of these centers constitutes both a source of a field subject to the laws of physical optics and a source of edge waves, in accordance with physical theory of diffraction pertaining to inhomogeneities of the "corner" kind excited by surface current segments in the vicinity. The mathematical model in the form an appropriate scattering matrix is constructed so as to facilitate numerical evaluation of the radiation polarization and scattering spectrum characteristics of such bodies. An expression for the coefficient of E or H polarization anisotropy is given for a compound body composed of a narrow-angle conic frustum and a wide-angle nose cone on its smaller base. More general expressions are then given for the complete set of radiation polarization and scattering spectrum characteristics of any ribbed axisymmetric bodies. Calculations have been made accordingly for a plain cylinder, for a consisting of a cylinder and a cone, and for a body consisting of a cone and a conic frustum. An analysis of the results demonstrates that those characteristics are very closely related to the geometrical characteristics of a scattering body and, therefore, contain a great deal of information necessary for identification of a tracked object. Its usefulness may be limited when applied to objects which contain local scatterers not rigidly positioned relative to the center of mass. Figures 4; references 11.

## Ionospheric Perturbations Caused by Strong Explosions

[Article by P. M. Nagorskiy and Yu. Ye. Tarashchuk, Siberian Institute of Engineering Physics imeni V. D. Kuznetsov at Tomsk State University; UDC 550.388.2]

[Abstract] The reaction of the ionosphere to strong chemical and nuclear explosions is analyzed on the basis of scientific research data. Such data were obtained following artificial perturbation of the atmosphere-ionosphere-magnetosphere system with explosions equivalent to hectatons of TNT, triggered on earth rather than on spacecrafts. The energy released by such an explosion was transmitted into the ionosphere by an acoustic wave. Exploding 300 tons of TNT in the lower atmosphere is known to release an energy of the order of 1 TJ, the ionosphere then absorbing a power of the order of 1 GW. The reaction of the ionosphere was monitored by vertical and oblique Doppler sounding on a "grid" of fixed frequencies, the thus obtained data including those from the "Massa" (Mass) research project (L.S. Alperovich, B.O. Burmeyster, M.B. Gokhberg, et al.; DOKLADY AKADEMII NAUK SSSR, Vol 269, 1983). Data were also obtained by monitoring with short-wave signals and mathematically simulating their response to ionospheric perturbations. Powerful explosion are sources of high-energy pulses known to cause three kinds of perturbations in the upper atmosphere including the ionosphere: 1) electrodynamic plasma waves, 2) internal gravitational waves generated by interaction of gravity and buoyancy forces, 3) acoustic waves evolving due to compressibility of the medium. Acoustic plasma perturbations in the ionosphere were generated by three chemical and four nuclear aboveground explosions, the reaction being monitored by vertical sounding from: 1) six ground stations (Almaty, Tashkent, Karaganda, Novosibirsk, Irkutsk, Volgograd) respectively 60-650-750-1400-2200-2300 km away from the explosion site on 28 November 1981; 2) one ground station (Irkutsk) 90 km away from the explosion site on 25 April 1982; 3) two ground stations (Novokazalinsk, Tbilisi) respectively 460 km and 1300 km away from the explosion site on 26 December 1982. Internal gravitational waves in the upper atmosphere and particularly in its ionospheric F-layer were generated during the "Massa" project, the reaction being monitored in six ground stations (Almaty, Novosibirsk, Tomsk, Irkutsk, Moscow, Yakutsk) respectively 60-1400-1600-2200-3100-3950 km away from the explosion sites. An analysis of the data identifies electrodynamic plasma waves and internal gravitational waves as large-scale perturbations focusing at distances up to 3000 km from the epicenter, their characteristic dimensions reaching the megameter range. Acoustic shock action on the upper atmosphere and particularly the ionosphere was generated by a powerful explosion equivalent to 1300 tons of TNT on 26 December 1982 in Nikus, the reaction being monitored by both vertical and oblique sounding along the Ashkhabad-Tomsk line with 15.8 MHz and 19.6 MHz signals and along the Tegeran-Tomsk line with 15.1 MHz signals. The response of these signals to transient processes taking place in the ionospheric communication channel following this explosion was simulated in numerical experiments based on the physical model (P.M. Nagorskiy; IZVESTIYA AKADEMII NAUK SSSR: FIZIKA ZEMLI, No 11, 1989) which takes into account all factors influencing the evolution of acoustic shock perturbation and the electron concentration distribution. The results have facilitated solution of problems regarding propagation of short radio waves through the ionospheric communication channel, validation and refinement of the physical perturbation model, and synthesis of the response of a sounding signal during several transient processes simultaneously taking place in the ionospheric plasma. The results indicate that acoustic shock perturbation scatters short radio waves while it enters the E-layer, a negative frequency shift attending their refraction within the perturbed region and a positive frequency attending their refraction by the second shock wave (which evolves from the rarefaction wave). Figures 4; references 13.

## Study of Communication Network Satellites by Method of Mathematical Modeling

[Article by A. A. Nazarov and S. B. Pichugin, Siberian Institute of Engineering Physics imeni V. D. Kuznetsov at Tomsk State University; UDC 519.2]

[Abstract] A geostationary satellite communication network covering a large number of subscriber stations distributed over a large territory is analyzed by the method of mathematical simulation for probabilistic time characteristics, throughput capacity of the communication channel, and mean message delay time. The model selected for this purpose represents such a network as a queuing system, its facilities representing the network resources and its tasks representing the responses to an incoming demand flux. Sharing of the resources is effected in accordance with a random multiple-access protocol, which includes repeated transmission of messages until their distortion-free reception has been achieved and a "dynamic" algorithm of conflict resolution whose manner of execution depends on the current network conditions. A one-line queuing system is considered which receives a most simply structured flux of calls with a characteristic parameter $\gamma$. When a facility is free, then it immediately attends to an incoming call for a length of time within a B(s) distribution. If no other call has subsequently come in, then the the incoming one will have been completely attended to by the time it is abandoned. When another call comes in while the first one is being attended to, then both become distorted so that a conflict arises and there follows an inaccessibility period of a duration within an A(s) distribution. Calls coming in during an such a period are distorted and proceed to a device which generates repeated calls until achievement of a successful reception by the facility. A call from this generator arrives at the facility for attendance after a random delay of a duration within an exponential distribution characterized by the parameter $\sigma/i$ (gs - dispersion, i - number of incoming calls to a generator of repeated ones). Calculations made on the basis of this model in accordance with the "dynamic" random multiple-access protocol have yielded the throughput capacity S of such a satellite communication network, the distribution of the

necessary number of devices generating repeated calls for exponentially distributed incoming distorted calls, and the mean message delay time. The distribution of active subscriber stations is shown to be asymptotically exponential. The results indicate the range of network parameters within which this "dynamic" protocol is more effective than a "static" one such as the "Aloha" protocol whose manner of execution does not depend on the current network conditions. References 5.

## Disorder and Order in Long-Wave High-Temperature Acoustics, Part 2: Dielectrics, Semiconductors, Conductors

*937J0042A Moscow USPEKHI FIZICHESKIKH NAUK in Russian Vol 162 No 11, Nov 92 pp 43-110*

[Article by M. B. Gitis, Kishinev Polytechnic Institute imeni S. Lazo]

[Abstract] The term "order" in the Russian language is clarified as one which refers to: 1) a sequence of objects, 2) a layout or arrangement of objects, 3) a sequence of actions. Inasmuch as none of these three definitions implies how order can be measured, it has been accepted in physical sciences to rather measure the departure from order and thus the degree of disorder. Sources of disorder are classified into "natural" and "artificial" ones, in crystals thermal or athermal point defects (interstitial atoms, vacancies) being natural ones and implanted impurities being artificial ones. A discussion of direct and indirect methods of disorder measurement is followed by a review and analysis of up to date theoretical and experimental research data pertaining to acoustic effects at temperatures up to 1700°C in solid media with locally broken crystallographic order: crystalline dielectrics, crystalline semiconductors, conductors (metals), and superionic conductors. First are considered crystalline dielectrics with local disorder, of concern having been its direct effect on the acoustic properties of these materials. When disorder carriers in such a crystal also carry an electric charge and a sound wave propagating through it is accompanied by an electric field, then processes which take place have been found to be analogous to those taking place in the absence of electric charge and electric field but not to require a similar disorder symmetry. Next are considered crystalline semiconductors (Si, Ge, $A^{III}B^V$ and $A^{II}B^{IV}$ compounds), of particular concern being extrinsic semiconductors: heavily doped ones being characterized by a high electron mobility and lightly doped ones being characterized by an only small or hardly any overlap of electronic states in different impurities. Manifestations of local disorder in the form of point defects are not as diverse in metals as they are in semiconductors, most thoroughly having been studied acoustic effects in metals with a b.c.c. crystal lattice (V, Fe + 3% Si, Nb, Mo, W). Superionic crystalline conductors have an electrical conductivity higher than 0.1 S/cm but a low activation energy of about 0.1 eV, therefore electrically do not stand quite apart from ionic ones and thus are acoustically similar to them. Structurally, however, they differ significantly from plain ionic ones by containing a phase with many more minima in the spatial distribution of potential energy in one of its ionic components than

there are ions in that component. Consequently, the mobility of one of the ionic components in a superionic crystal is higher than in a plain ionic one while its other components form a stable lattice. Disorder here is of a peculiar nature: the more mobile ions of one kind moving within the periodic lattice formed by the less mobile ions of the other kind. This disorder thus also peculiarly influences acoustic effects in such crystals. Figures 12; references 160.

## Order and Disorder in Long-Wave High-Temperature Acoustics, Part 2: Monatomic Liquids

*937J0042B Moscow USPEKHI FIZICHESKIKH NAUK in Russian Vol 162 No 11, Nov 92 pp 111-181*

[Article by M. B. Gitis, Kishinev Polytechnic Institute imeni S. Lazo]

[Abstract] The effects of disorder in amorphous materials and in melts on their acoustic characteristics at high temperatures are reviewed on the basis of up to date theoretical and experimental research. Disorder in these media is topological rather than local, owing to its high concentration in them, and crystallographic order does not exist even in the zeroth "solvent" approximation. Following a general interpretation of data with clear distinctions drawn between amorphous materials and melts, amorphous compounds and elements (Si) are considered first. Acoustic effects due to disorder in them are related to the thermoacoustic characteristics of these materials, particularly to their temperature coefficient of acoustic velocity and its transition from a positive to a negative one. For an adequate interpretation of sound velocity and absorption measurements, these materials are compared with crystalline ones. Next are considered monatomic melts, here the temperature coefficient of their bulk modulus being particularly important. Four groups of melts are distinguished: 1) melts of close-packed metals (Pb); melts of metals with a strongly nonlinear temperature coefficient of acoustic velocity (Zn,Cd,Hg); 3) melts of semimetals (In,Sb,Tl,Bi) and elemental semiconductors Si,Ge); 4) melts of monatomic dielectric materials (Se). This classification is based on similarities and differences, respectively, in the temperature dependence of the acoustic velocity and of the acoustic absorption coefficient covering the 500-1100 K (up to 1800 K for silicon) range. The key role in revealing the effect of melting on the acoustic velocity and the acoustic absorption coefficient of melts has been assigned to the bulk modulus, this parameter characterizing liquids as well as solids and having been used as criterion for comparison of molten monatomic materials close to the melting point with amorphous materials during melting. The effect of the chemical short-range order on the acoustic has been revealed by a comparative study of polyatomic systems, of key significance being the dependence of both the acoustic velocity and its temperature coefficient on the concentration of one of the components in an amorphous compound or alloy melt. The results of this research indicate that high-temperature acoustic measurements can be useful in several practical

areas such as in technical quality control of crystals or amorphous devices and also in metallurgy. Figures 14; tables 5; references 155.

## Influence of Motion of Optical Medium During Sounding

[Article by V. P. Vasilyev, V. A. Grishmanovskiy, L. F. Pliyev and T. P. Startsev, Precision Instrument Making Scientific Research Institute]

[Abstract] In the optical sounding of spacecraft which carry prism retroreflectors it is essentially a Fizeau experiment (in a somewhat modified variant) which is replicated. The prism reflector usually has the configuration of a tetrahedron with three mutually orthogonal surfaces (a corner reflector). A phenomenon is observed which has never been described in the literature: dependence of the angle of deflection of the reflected radiation on the refractive index of the material of the prism. The research was carried out on three days in June 1989 during which more than 60 reflected signals were received. It revealed that with identical mean ranges and identical observation conditions the signals from a quartz reflector were on the average an order of magnitude stronger than from a hollow reflector. The computed absolute quantity of received signal energy differed from the observed energy by not more than a factor of 2-3 in all observation sessions (computations for the quartz reflector were made on the assumption that the Bradley effect is compensated by the Fizeau effect). All evidence indicates. that there is a strengthening (rather than a weakening) of the real signal from a prism reflector. Figure 1; references 7: 5 Russian, 2 Western.

## 'Plasmon' Mechanism of Superconductivity: Possible Cause of Increase in Critical Temperature in Multilayer Cuprate Metal Oxide Compounds

[Article by E. A. Pashitskiy, Physics Institute, Ukrainian Academy of Sciences]

[Abstract] In layered cuprate metal oxide compounds (MOC) there is a tendency to an increase in $T_c$ with an increase in the number n of $CuO_2$ layers. In this study it is shown that such a dependence of $T_c$ on n in multilayer cuprate MOC may be related to an inhomogeneous (along the z-axis) distribution of the density of "light" current carriers in a broad 2D zone localized in the planes of conducting $CuO_2$ layers or to Coulomb interaction among charges in layers, which lies at the basis of electron-plasmon interaction with low-frequency collective excitations of charge density of "heavy" carriers in a narrow 2D zone—acoustic plasmons, as well as polar electron-phonon interaction with dipole-active oscillations of ions—optical

phonons, which are hybridized with the acoustic plasmons. A review of this problem shows that the plasmon mechanism of superconductivity in a layered metal with a narrow 2D zone near the Fermi level results in an increase in the critical temperature $T_c$ with an increase in the number n of conducting layers in a primitive element with a tendency to saturation with large n, which qualitatively agrees with the experimental dependencies of $T_c$ on n in cuprate metal oxide compounds of the type $Bi_2Sr_2Ca_{n-1}Cu_nO_x$ and $Tl_mBa_2Ca_{n-1}Cu_nO_x$. Figures 3; references 9: 3 Russian, 6 Western.

## Anisotropy of Fluctuation Contribution to Depth of Penetration of Magnetic Field in Exotic Superconductors

[Article by Yu. S. Barash, A. S. Melnikov and A. I. Yukhimets, Physics Institute imeni P. N. Lebedev]

[Abstract] Exotic superconductors should manifest specific anisotropic magnetic properties. Since such anisotropic properties differ qualitatively from those observed in the case of superconductors described by the Ginzburg-Landau theory with an anisotropic mass tensor, their study may play an important role in identifying the type of superconducting pairing. A study was made to determine whether measurement of the anisotropy of magnetic field penetration depth $\lambda$ makes it possible to distinguish a superconductor with nontrivial pairing from an ordinary superconductor with an anisotropic mass tensor. This investigation revealed that such a specific $\lambda$ anisotropy in an exotic superconductor may occur due to fluctuation corrections even in those cases when without allowance for fluctuations $\lambda$ anisotropy has no specific peculiarities. A temperature dependence for the relative anisotropy of depths of magnetic field penetration near $T_c$ would be indicative of exotic superconductivity. The fluctuation contribution to the depth of penetration has never been studied experimentally. A small temperature dependence of relative anisotropy is more easily determined in an experiment than specific temperature corrections to the absolute penetration depths. This gives hope that such experiments can be used for identifying exotic superconductors. References 10: 6 Russian, 4 Western.

## Scattering for a Nonlinear Schroedinger Equation: A Near-Soliton State

[Article by V. S. Buslayev and G. S. Perelman]

[Abstract] For a general nonlinear Schrodinger equation the Cauchy problem is examined with near-soliton initial data. Assuming that the spectrum of the linearized equation for the initial soliton is constructed simply, it is shown that the asymptotics of the solution for long times is given by a soliton with slightly displaced parameters and a small dispersion term which is described by a free Schrodinger

equation. The solution method used has a number of similarities with the article by Soffer and Weinstein (Comm. Math. Phys. Vol 133 No 1, 1990). The article has two parts. The first contains a complete proof of the result with reference to specific estimates for linearized evolution. The second section contains a systematic examination of the spectral properties of linearized evolution, and proof of the estimates made in the first part. A brief form of the article containing a description of the main results can be found in the authors' article in the proceedings of the Nantes conference in J. Asterique. Figures 2; references 14: 3 Russian, 11 Western.

## Interaction of an Electromagnetic Wave With the Field of a Plane Gravity Wave

[Article by A. I. Akhiyezer, N. P. Merenkov, Kharkov Physicotechnical Institute, Ukrainian Academy of Sciences; UDC 539.12]

[Abstract] This article studies the effect of the field of a plane monochromatic gravity wave on an electromagnetic wave. No assumptions are made about the directions of propagation or the polarizations. A solution is obtained to Maxwell's equation in a linear approximation in the gravitational field for various polarizations of the electromagnetic wave and the gravity wave. The situation where the direction of propagation of an unperturbed electromagnetic wave coincides with the direction of propagation of the gravity wave is studied. The limit case corresponding to geometric optics is studied. The structures of the amplitudes of satellite electromagnetic waves which arise are analyzed in terms of dependence on polarizations, directions of propagation, and frequencies of interacting gravity and unperturbed electromagnetic waves. The amplitudes of the satellites are proportional to the amplitude of the gravity wave. Their frequencies are respectively equal to the sum and difference of the frequencies of the initial electromagnetic wave and the gravity wave. Linear and circular polarization of the electromagnetic wave are considered. Elliptical polarization of the gravity wave is considered. References 11: 7 Russian, 4 Western.

## Toward a Theory of Two-Beam Acceleration of Charged Particles in a Corrugated Waveguide

[Article by A. O. Ostrovskiy, Kharkov Physicotechnical Institute, Ukrainian Academy of Sciences; UDC 537.532.4:621.384.6]

[Abstract] Results of a theoretical study of two-beam acceleration of charged particles in a corrugated waveguide with ideally conducting walls are presented. The case is examined where a high-current relativistic electron beam is in Cherenkov synchronism with the first spatial field harmonic and the accelerated beam is in Cherenkov synchronism with the fundamental harmonic (a two-resonance acceleration scheme). Numerical methods are used to study the excitation by a high-current beam. System parameters are determined for which the highest rate of acceleration is possible. The effect of forces of a spatial high-frequency charge of a high-current beam on the generation of accelerating high-frequency fields is discussed. The process of excitation of electromagnetic waves by a high-current relativistic electron beam accelerating the particles of a secondary beam is described. It is shown that in this two-beam acceleration scheme, the use of a high-current relativistic electron beam can provide (in technically acceptable conditions) a maximum strength of excited high-frequency fields on the 1.5 MV/cm level and rates of accumulation of the energy of accelerated particles of T = 0.3-0.35 MeV/cm. The dynamics of the formation of a cluster of accelerated particles is examined. It is found that for steady-state generation of high-frequency electron fields the increase in energy is monotonic. The number of accelerated particles is about 20 percent of the total number of particles in the secondary beam. As the length of the electrodynamic structure increases, the steady-state generation mode loses its stability and an automodulation mode is estblished in the system. This leads to a nonmonotonic increase in the electron energy and a decrease in the rate of acceleration. Figures 7; references: 20 Russian.

## Possible Mechanism of Formation of Rare Tautomeric Forms of Nucleotide Basis in UV Irradiation of DNA

[Article by Ye. A. Grebneva, Donets Physicotechnical Institute, Ukrainian Academy of Sciences; UDC 541.571.9;547.963.32;575.24]

[Abstract] When DNA is in solution or vacuum, cases arise where adenine may join with cytosine (instead of thymine) and thymine may combine with guanine (instead of adenine). This incorrect pairing may explain chemical mutagenesis. It has been proposed that UV irradiation may cause the protons of hydrogen bonds to be transferred to partner atoms (tunneling). A mechanism is proposed for the transfer of protons to partner atoms along a hydrogen bond using the example of these transitions in paired guanine-cytosine bases in UV irradiation of DNA. The transfer of protons is caused by a change in the shape of the proton potential due to excitation of an electron subsystem and strong forced vibrations. In this case the proton may do one of eight things. The most likely are the transfer of excitation energy into heat or radiation, but the other options, which may be unstable, involve the transfer of protons along hydrogen bonds to partner atoms. Two-proton transfers indicate the transformation of G-C pairs into rare tautomeric forms. The difference in the tautomery of nucleotide pairs is interpreted as a potential mutation of base change. Figure 1; references 14: 10 Russian, 4 Western.

## Influence of High-Order Dispersion on the Dynamics of a Dark Soliton of a Nonlinear Schroedinger Equation

[Article by F. G. Bass, V. Ye. Vekslerchuk, V. V. Kono-top, S. A. Puzenko, Institute of Radio Physics and Electrons, Ukrainian Academy of Sciences; UDC 535.2:621.373.8]

[Abstract] While the nonlinear Schroedinger equation adequately describes the dynamics of picosecond pulses, the dynamics of femtosecond pulses must include consideration of the effect of third-order linear dispersion and nonlinear dispersion on wave evolution. This article examines the dynamics of a dark soliton (a drop in intensity on the background of a constant pedestal) in the framework of a nonlinear Schroedinger equation that includes terms which describe the effect of linear and nonlinear high-order dispersion on wave evolution. The distortion of soliton shape by perturbations is also considered. Assuming that the dispersion effect is small, the changes in amplitude and speed of the initial soliton are calculated. One can predict in the first order of perturbation theory the probability of generation of new solitons in the system. However, it is not certain that these new solitons will be stable formations, because the results hold only over limited distances, and solitons with a small amplitude appear in an asymptotic region where solitons and qua-silinear modes separate. This examination adds to the information available on the dynamics of femtosecond optical pulses in a nonlinear waveguide. References 13: 3 Russian, 10 Western.

## Electrode SHF-Heating of Plasma

[Article by V. P. Kovalenko, A. V. Stefanovskaya, Institute of Physics, Ukrainian Academy of Sciences and T. Shevchenko Kiev University; UDC 533.9]

[Abstract] Using a simplified model, the collisionless interaction of plasma electrons with a strong SHF field is studied in the electrode layer. The model and the simplifying assumptions are described (i.e., secondary electron emission from the collector is ignored). Based on a numerical solution of the equation of motion for electrons, a conclusion is reached on the possibility of transferring the energy of an oscillating field to plasma electrons. For the steady-state case an electron current at the SHF probe is calculated and the floating potential acquired by the electrode is found. The individual trajectories of electrons in the electrode layer are calculated. It is found that the constant component of the collector is important in the energy exchange between the plasma and the field. It is shown that when an electromagnetic HF field does not penetrate into the plasma, this is an effective plasma heating mechanism. This mechanism is associated with the transfer of HF energy to electrons leaving the plasma in the boundary layer and then returning to it. Figures 3; table 1; references 9: 6 Russian, 3 Western.

## Formation of Photosensitivity Spectra of Injection Graded Photodiodes Based on Irradiated AlGaAs

[Article by M. P. Verkhovodov, G. P. Peka, D. A. Pulemetov, T. Shevchenko Kiev University; UDC 621.315.592]

[Abstract] An experimental mechanism is proposed and confirmed for the formation of spectral characteristics of injection graded photodiodes. These photodiodes are $p^+$-p-n structures with a graded n-base of AlGaAs, obtained by liquid-phase epitaxy compensated by the effect of radiation (neutrons, electrons). Low-dosage irradiation leads to the formation of selective spectral characteristics with a half-width of 20-30 meV and of increasing photosensitivity to $10^2$ - $10^3$A/W. Irradiation by optimal doses of electrons makes it possible to form controlled spectra with a transition from selective to wideband photosensitivity (a change in the region of spectral sensitivity by more than a factor of 20). The formation of these spectra is associated with the existence (in the n-base of the initial structures near the p-n transition) of a narrow compensated region formed in the process of growth and resistance modulation of this region by the injection current. The calculated characteristics obtained describe all experimentally observed behavior. Figures 5; table 1; references: 8 Russian.

## Coding System Constructed on the Basis of Generalized Reed-Solomon Codes

[Article by V. M. Sidelnikov, S. O. Shestakov]

[Abstract] Other publications have proposed methods of constructing an open coding system based on theoretical code constructions. They were based on a generally known matrix of dimension $s + 1$ x $N$ with elements from a finite field $F_q$ in the form $B = H$ x $A$, where $A$ is some unknown matrix which is the calibrating matrix of the $q$-significant generalized Reed-Solomon code, in particular, the Hopp code. The quantity $H$ is an unknown nondegenerate matrix of dimension $s + 1$ x $s + 1$. This article presents a method of finding unknown matrices $A$, $H$ with elements from the field $F_q$ which define the matrix $B$ in $O(s^4 + sN)$ operations. Thus, the unreliability level of the examined systems of open code are establihsed. Another article finds that the system of "open coding" presented here has a rather high resistance to infiltration. References 4: 1 Russian, 3 Western.

## Probabilistic and Statistical Methods for Predicting Reliability of Complex Software

[Article by V. Yu. Korolev, Mathematical Statistics Department, Computational Mathematics and Cybernetics Faculty, Moscow University]

[Abstract] At the present time in the CIS there are no standards for evaluating the reliability of software and reconciling the methods for evaluating the quality of software and other documentation. This situation makes it imperative to rectify this important deficiency. This review and analysis, although quite extensive, makes no pretense at an all-inclusive exposition of this highly complex problem. Only probabilistic-statistical methods for its solution are examined. The emphasis is on work done during recent years at Moscow University. The point of departure in this research has been a so-called mosaiced model, which makes it possible to formulate a unified and flexible approach to evaluation of software reliability indices. In addition to known mathematical models for analyzing the reliability of software the article discusses new models which in the last analysis are based on the mosaiced approach. Particular attention is given to so-called scale mixtures of exponential distributions, with evaluations of the stability of the exponential law when there is a random perturbation of the scale parameter and other properties of mixtures of exponential distributions. Methods for the statistical analysis of experimental data are proposed for the purpose of predicting the reliability of software on the basis of debugging tests. The described methods are suitable for predicting the reliability of arbitrary complex systems. References 61: 22 Russian, 39 Western.

## Numerical Simulation of Problem of Computing Signal Trajectory in Ionosphere

[Article by V. I. Dmitriyev and T. Yu. Shameyeva, Mathematical Physics Laboratory, Computational Mathematics and Cybernetics Faculty, Moscow University]

[Abstract] Some problems arising in the theory of electromagnetic sounding of the ionosphere are examined. The electron concentration is related to medium permittivity and in the considered ionospheric model completely determines the ionospheric radio wave propagation process. The point of departure in this study is a method for solving the inverse problem of retrieval of ionospheric parameters using limited sounding data and a known initial model of state of the ionosphere as proposed earlier by the authors in MATEM. MODELIR. I RESHENIYE OBRATNYKH ZADACH MATEM. FIZIKI, Moscow, 1992. This is now supplemented by numerical simulation of the problem of computing the signal path for a modified state of the ionosphere. Traditional solution of the inverse slant sounding problem makes possible retrieval of the parameters of such a modified ionosphere, but in solving the inverse problem the direct problem must be solved repeatedly and therefore the path is computed repeatedly. Computing the signal path again and again for a modified ionosphere using a particular initial model is an extremely unwieldy and time-consuming process. Procedures are therefore proposed making it possible to solve the direct problem more rapidly, and even when doing this repeatedly a substantial amount of time is saved. The full algorithm for computing the path on the basis of the proposed linearization procedures is presented. This has made possible a closer approach to preparation of a graphic package of practical programs for modeling data on the state of the ionosphere. References: 5 Russian.

## Problem of Evasion From Four Pursuers

[Article by N. V. Lagunova, Optimum Control Department, Computational Mathematics and Cybernetics Faculty, Moscow University]

[Abstract] The problem of escape of one evader from a group of pursuers has been well studied in the theory of differential games. Recently the more general problem has been investigated: study of the game of pursuit-evasion of groups of pursuers and evaders. Some conditions were defined by A. A. Chirkiy, et al. in KIBERNETIKA, No 5, pp 58-63, 1989 under which at least one evader can avoid capture whatever may be the strategy and tactics of the pursuers. However, these conditions are not always satisfied for a game of four pursuers and two evaders making simple movements, although Chirkiy demonstrated that the evasion problem for such a game is always soluble. His proof of this assertion encountered difficulties in at least one respect: the assumption that the pursuers are striving for a simultaneous capture of the evaders. This article gives a detailed examination of such a situation and presents a full proof of solubility of the evasion problem for a four-against-two game. A complete algorithm is presented for step-by-step solution of this problem with proofs being given for each successive step. References: 8 Russian.

## Theory of Transversely Inhomogeneous Highly Precise Beam-Plasma Amplifier in Collective Cerenkov Effect Mode

[Article by M. V. Kuzelev and V. A. Panin, Physical Electronics Department, Moscow University; UDC 533.9:537.5]

[Abstract] Amplification of plasma electromagnetic waves occurs in a collective Cerenkov effect mode when the beam and plasma are adequately far separated in the waveguide cross section. Precisely this situation was examined in greater detail than in earlier studies. The case of a circular metal waveguide with a thin tubular beam and plasma was investigated. It is shown that depending on the beam current the nonlinear stabilization mechanism is determined by a number of factors. A general analytic solution of the problem was obtained (for arbitrary currents) and the most important characteristics of the amplifier were defined. Both linear and nonlinear theories of the amplification of an electromagnetic plasma wave in a transversely inhomogeneous beam-plasma system are examined. The study begins with examination of a waveguide of arbitrary section in which thin beams of electrons and plasma with undisturbed densities, completely magnetized by a longitudinal magnetic field, are present, after which a number of variants of different complexity are examined. Analytic and numerical methods are used in computing the optimum length and efficiency of amplification and the output power of electromagnetic radiation. The use of transversely inhomogeneous beam-plasma waveguides in a collective Cerenkov effect mode will make it possible to develop efficient microwave-range amplifiers. Figure 1; references: 11 Russian.

## Influence of Transverse Inhomogeneity of Pumping Field on Motion of Electrons in Nonadiabatic Magnetic Undulators With Guiding Magnetic Field

[Article by V. A. Kubarev, Physical Electronics Department, Moscow University; UDC 621.385.6]

[Abstract] In order to obtain optimum modes of helical beams of relativistic electrons there must be a definite value of their pitch factor. The presence of a transverse inhomogeneity of the pumping field in real undulators has two principal results: broadening of nonlinear resonance and drift of the guiding centers of particles. A theory of these effects is proposed for symmetric and asymmetric undulators with a uniform guiding magnetic field. The theory is progressively developed with an examination of the following: equations of motion in a drift approximation (symmetric undulators); nonlinear resonance without allowance for transverse inhomogeneity; influence of transverse inhomogeneity on dynamics of electrons. It is shown that the influence of transverse inhomogeneity of the undulator field is important in modes with high values of the pitch factor of electrons and for beams of a great (at the scale of the inhomogeneity) thickness. Symmetric undulators with respect to the scatter of the velocities of electrons and their transverse drift have substantially better characteristics than asymmetric undulators. Figures 2; references: 3 Western.

## Characteristics of Striction Coupling Between Modes in Spherical Electroacoustic Resonators

[G. V. Belokopytov, N. P. Pushechkin and V. N. Semenenko, Physics of Oscillations Department; UDC 537.868:531]

[Abstract] The integral coefficients of the striction coupling between modes in spherical dielectric resonators were computed and experimentally determined. A unique circumstance is that for an isotropic spherical resonator there is an analytical representation for the fields of characteristic electromagnetic and acoustic oscillations. This makes it possible to simplify the expressions for the integral coefficients, to formulate selection rules for effectively interacting combinations of modes and to prepare an efficient computation program. The selection rules are defined and the integral coefficients of the striction interaction are computed with allowance for the vectorial character of the interacting fields and the anisotropy of the electrostriction tensor. There is a good correspondence between the results of computations and experimental data on the striction parametric excitation of radial elastic oscillations in dielectric resonators of potassium tantalate with microwave pumping. The research demonstrated the possibility of computing the integral characteristics of spherical nonlinear electroacoustic resonators. The accuracy in the computations makes it possible to obtain a qualitative explanation of the experimentally observed regularities of striction excitation and also to obtain a quantitative agreement. This affords a possibility for predicting the threshold of striction parametric excitation in other materials and frequency ranges. References 10: 6 Russian, 4 Western.

## Polarization Effects During Light Transmission Through Acoustic Field in Isotropic Medium

[Article by V. I. Balakshiy and D. A. Khasan, Physics of Oscillations Department, Moscow University; UDC 535.241.13]

[Abstract] A theoretical study was made of the change in light polarization in the Bragg optoacoustic interaction process. With transmission of plane polarized light through an acoustic field excited in an isotropic medium the light radiation becomes elliptically polarized. By changing the power or frequency of the ultrasound it is possible to control the degree of polarization. A study also was made of the effect of polarization nonreciprocity for two light waves passing through an acoustic field in mutually opposite directions. The research indicated that the change in light polarization in the optoacoustic interaction process has a complex character. An isotropic medium with an acoustic wave excited in it behaves like an anisotropic crystal with optical activity: elliptical polarization

appears in transmitted light and, in addition, rotation of the ellipse axes occurs. The degree of the effect is dependent on the parameters of the acoustic wave, which affords possibilities for developing light modulation devices of a new type. In a Bragg diffraction mode such a complex change in light polarization is fully manifested only in the zero order. However, in an intermediate diffraction mode, which is usually embodied in optoacoustic devices, this effect also should be observed at the maxima of other orders. Figures 3; references 7: 4 Russian, 3 Western.

## Z-Parameters of Piezoelectric Transducer for Solid-State Gravitational Antennas

[Article by A. V. Gusev and A. V. Tsyganov, State Astronomical Institute imeni P. K. Shternberg; UDC 550.34.052]

[Abstract] The most general analysis of the dynamic and noise characteristics of solid-state gravitational antennas with a piezoelectric transducer can be made on the basis of the theory of linear quadripoles. A system of equations is given for describing such a transducer as a linear quadripole with Z-parameters. The primary noise parameters of such a transducer, governed by losses in the piezoelectric material, were determined earlier on the basis of the fluctuation-dissipative theorem. On this basis the objective of the study was computation of a system of Z-parameters of the transducer as a sensor of gravitational antenna displacements. The simplest model of a solid-state gravitational antenna is a homogeneous rod of the length L at whose midpoint there is a piezoelectric element rigidly coupled to the rod. The inverse influence of the transducer on the solid-state antenna is taken into account by the introduction of "volumetric" forces. The derivation of the fundamental relations for solving the problem is given. Proceeding on this basis, the system of Z-coefficients was computed for such a transducer as a sensor of small displacements of a solid-state gravitational antenna of the Weber type. The pertinent computations are illustrated in the example of the solid-state gravitational antenna at the State Astronomical Institute. References: 7 Russian.

## Modeling and Analysis of Energy Spectra of δ-Electrons Formed by Ultrarelativistic Hadrons

[Article by B. I. Goryachev and N. V. Linkova, Nuclear Physics Scientific Research Institute; UDC 539.14:539.124]

[Abstract] In an earlier study (YADERNAYA FIZIKA, 54, No 6, p 1663, 1991) the authors proposed a method for studying the electromagnetic structure of hadrons by an analysis of the energy spectra of δ electrons formed by ultrarelativistic hadrons. In principle the method makes it possible, together with the charge rms radius $r_0{}^*$ also to determine the dimensionless factor M characterizing the compactness of the electric charge distribution in the hadron. An analysis has now been made to determine the mean energy and rms energy Q for the measured energy spectrum of δ electrons. The article gives the results of computations for determining the accuracy in measuring the mean energy and rms energy. The energy spectra of the δ electrons were determined by the Monte Carlo method. The differential section of formation of δ electrons was described by an expression correct for spin-free relativistic hadrons. A table gives the relative errors in determining these parameters, as well as $r_0$ and M for a given volume of statistics; a rule is given for determining these parameters for any volume of statistics. The final formulas give estimates consistent with the results of computations made using the Monte Carlo method. A systematic underestimate (overestimate) of Q results in an increase (decrease) in $r_0$ and M because it would be equivalent to a more rapid (slower) dropoff of the electric form factor with an increase in the transmitted energy Q. Figures 2; references 2: 1 Russian, 1 Western.

## Visualization of Spatial Distribution of Output Radiation of Cerenkov Microwave Generator in Relativistic Electron Beam

[Article by A. F. Aleksandrov, S. Yu. Galuzo and A. M. Kuznetsov, Physical Electronics Department, Moscow University; UDC 537.56.533.9]

[Abstract] A successful attempt was made to determine the spatial distribution of microwave radiation using the microwave breakdown of air in a dielectric chamber with reduced pressure with small dimensions of the breakdown space. The thin-walled chamber was formed by the surface of two dielectrics. The chamber measured 27 x 23.5 cm with a space between the plates 1 cm. The experiments were made using a highly precise electron accelerator with a Cerenkov generator as the source of microwave radiation. The wavelength of the generated microwave radiation was about 5.5 cm. An annotated diagram of the experiment is given and explained in the text. With chamber pressures greater than 400 mm Hg air breakdown was not observed. By changing pressure in the direction of a decrease it was possible to obtain time-integrated photographs of luminescent gas regions. Examples of such photographs are given for pressures in the dielectric chamber 250, 100 and 50 mm Hg. At a pressure 250 mm Hg the air breakdown has a "focal" character, whereas with an air pressure decrease to 100 mm Hg it is possible to discriminate two concentric annular luminescent regions on the photographs. One of the shortcomings of the proposed method for visualization of the spatial distribution of microwave power is an uncertainty of its sensitivity. Figures 3; references: 8 Russian.

## Highly Invariant Sets Relative to Differential Inclusion and Convergence Problem for Discontinuous Control Systems

*937J0073A Minsk DIFFERENTSIALNYYE URAVNENIYA in Russian No 9, Sep 92 pp 1490-1498*

[Article by Kh. G. Guseynov, Baku State University; UDC 517.911]

[Abstract] The properties of strong invariance of a closed set relative to a differential inclusion were investigated. Although the properties of strong invariance of sets have been studied under different conditions, in this study the problem is reexamined in terms of the derivatives of set valued mapping, thereby providing the adequate condition for strong invariance of closed sets relative to a differential inclusion whose right-hand side is semicontinuous upward for a set of arguments. The results are used in investigating the convergence problem for controllable systems with discontinuous right-hand sides. So-called position strategies (N. N. Krasovskiy, et al., Pozitsionnyye differentsialnnye igry [Position Differential Games], Moscow, 1974) are used as the method for forming a controlling effect. It is assumed that in the realization of the controlling effect in the form of a position strategy the phase states may be measured with some error. Using the theorem of strong invariance of sets relative to a differential inclusion an adequate condition is obtained for a strategy for solving the convergence problem for control systems with discontinuous right-hand sides. References 16: 11 Russian, 5 Western.

## Tests of Strong Orbital Stability of Trajectories of Dynamic Systems. I

*937J0073B Minsk DIFFERENTSIALNYYE URAVNENIYA in Russian No 9, Sep 92 pp 1507-1520*

[Article by A. Yu. Kravchuk, G. A. Leonov and D. V. Ponomarenko, St. Petersburg University; UDC 517.925]

[Abstract] The orbital stability process is an important characteristic of periodic motions in dynamic systems. A number of tests are discussed with whose satisfaction a particular periodic motion will be orbitally stable. The point of departure in this study is an initial system defining orbital stability for an arbitrary trajectory. A parametrization is found for this initial system from the class T, naturally arising in a study of smooth dynamic systems. The introduction of this parametrization makes it possible for the initial system to write an analogue of the system in variations and to reduce the strong orbital stability problem to the Lyapunov stability problem. The use of this procedure, rather widely employed in stability theory, makes it possible to formulate the conditions for strong orbital stability and instability of an arbitrary solution of a nonlinear autonomous system in terms of Lyapunov stability of the zero solution of an auxiliary linear or quasilinear lesser-order system. This information is used in obtaining adequate conditions for strong orbital stability and instability of solutions of smooth autonomous systems of differential equations. [The article represents a continuation and some generalization of earlier studies, including several by G. A. Leonov, one of the authors of this research]. References 15: 11 Russian, 4 Western.

## Optimal Control in Nonlinear Stationary System With Nonmonotonic Operator

*937J0073C Minsk DIFFERENTSIALNYYE URAVNENIYA in Russian No 9, Sep 92 pp 1579-1587*

[Article by S. Ya. Serovayskiy, Kazakh State University; UDC 517.977]

[Abstract] Although optimum control problems for systems described by nonlinear equations of an elliptical type with monotonic operators have been well studied, in the absence of monotonicity conditions significant difficulties arise which are attributable in large part to the unsatisfactory properties of the equations. Several proposals have been made for overcoming these difficulties, but they have serious shortcomings. In order to remedy this situation a study was made of a nonlinear fourth-order elliptical equation with a nonmonotonic operator allowing a nonunique solution. In studying the extremal problem related to it use is made of the most natural method for obtaining optimality conditions, assuming direct finding of the minimizable functional derivative. A determination of the functional derivative in nonlinear infinite dimensional systems usually requires differentiability of the control state function; this can be established using the inverse (or implicit) function theorem, although the conditions of the inverse function theorem are in this case violated. The difficulties which arise are overcome by introduction of the concept of an expanded solution of the equation and proof of its existence is demonstrated by means of the Schauder fixed point theorem. Expanded differentiability of the control solution is established, which makes it possible to find the functional derivative and obtain the necessary optimality conditions in the form of variational inequalities by the classical method. References: 9 Russian.

## Asymptotic Form of Solution of Spectral Problem of Transport of Neutrons Using Small Mean Free Path Parameter

*937J0073D Minsk DIFFERENTSIALNYYE URAVNENIYA in Russian No 9, Sep 92 pp 1587-1599*

[Article by V. A. Tupchiyev, Obninsk Atomic Energy Institute; UDC 517.95]

[Abstract] A study was made of the spectral problem of a one-velocity equation for the transport of neutrons with an adsorption boundary condition and with a small parameter: mean free path in the medium. This problem was examined most fully by V. S. Vladimirov in TR. MAT. IN-TA im. V. A. STEKLOVA AN SSSR, No 59, pp 1-158, 1961, but without any assumptions concerning the smallness of the indicated parameter. Accordingly, the objective of this study is to construct and validate asymptotic expansions of the eigenvalues and eigenfunctions of this problem with respect to this small parameter applying the ideas of the limiting functions method. Such a problem was considered earlier, but not in the spectrum, and a one-dimensional and isotropic case of this spectral problem has been examined. Results obtained earlier by C. Bardos, et al. and A. Bensoussan, et al. were used in finding an asymptotic form of solution of the spectral problem in $R_3$ and related problems for the limiting functions were examined. The asymptotic form was validated in $R_3$ for an isotropic case and for any eigenvalue and eigenfunction, but a general anisotropic case

required further substantiation. Such a validation is based on the Kellogg method and an important lemma defined by M. I. Vishik, et al. By establishing uniform asymptotic expansions for the eigenfunctions and the corresponding expansions of the high-order eigenvalues for the small parameter it was thereby possible to solve the problem of rigorous validation of the diffusional approximation and introduction of further asymptotic corrections of any order relative to the mentioned small parameter. References 13: 11 Russian, 2 Western.

### Diffusion of a Turbulent Spot in a Problem of a Singularly-Perturbed Initial Turblulence Energy

*937J0075A Moscow ZHURNAL VYCHISLITELNOY MATEMATIKI I MATEMATICHESKOY FIZIKI in Russian Vol 32 No 12, Dec 92 pp 1916-1928*

[Article by V. N. Grebenyev, Novosibirsk; UDC 517.958:532.5]

[Abstract] Turbulence in a stratified ocean is of a mottled nature. The generation of points of turbulence is associated with bursts of turbulence when internal waves collapse, or when there is a local loss in stability in a shear current in the ocean with subsequent remixing of liquid. This problem, the evolution of a turbulent spot, is examined in this article in the framework of an $(e, L)$ model of the semi-empirical theory of turbulence. This model is based on the balance equation of turbulent energy, which is a nonlinear degenerating parabolic equation. It is also based on the Kolmogorov hypothesis on the self-modeling of a field of turbulent eddies and the development of a turbulent flow. The existence of a generalized solution of the problem with the initial condition in the form of a $\delta$ function is proven. It is also established that in the asymptotic stage of the process the spreading of the turbulent spot becomes the origin of energy dissipation. References 16: 10 Russian, 6 Western.

### Transfer of a Boundary Condition Through a Vacuum in Axisymmetrical Problems

*937J0075B Moscow ZHURNAL VYCHISLITELNOY MATEMATIKI I MATEMATICHESKOY FIZIKI in Russian Vol 32 No 12, Dec 92 pp 1929-1939*

[Article by K. V. Brushlinskiy, V. S. Ryabenkiy, N. B. Tuzova, Moscow; UDC 519.63]

[Abstract] In a number of problems in mathematical physics in a finite space the statement of a boundary condition requires solution of an external Dirichlet problem with a Laplace-like equation in the vacuum surrounding the region. A nonlocal boundary condition is constructed for differential analogs of these problems in the case of a square region in a plane $(r, z)$ of cylindrical coordinates. This construction is based on the theory of differential potentials. The method is implemented in a numerical solution of the problem of the evolution of a magnetic field in a conducting ring with current in a homogeneous external field. Figures 2; references: 7 Russian.

### Use of Recognition Methods in Medical Diagnosis Problems

*937J0075C Moscow ZHURNAL VYCHISLITELNOY MATEMATIKI I MATEMATICHESKOY FIZIKI in Russian Vol 32 No 12, Dec 92 pp 1956-1971*

[Article by O. I. Beryezkin, A. V. Serolapkin, N. L. Chenskikh, Cheboksary; UDC 519.714]

[Abstract] Similarities between the mathematical methods of recognition theory and medical diagnosis are indicated. For example, the theory evaluates the information contained in a knowledge table and its potential usefulness (in part and as a whole) in solving a recognition problem. However, there are features of diagnosis which require special consideration. The care which must be taken by a doctor in developing a knowledge table for a patient and the case of ongoing and progressive illness are addressed. Guidelines for the implementation of the system (hardware, user interface) are discussed. The universal automated diagnostic expert system developed from this work is described. Table 1; references: 10 Russian.

### Geometric Approach to Classification-New Model of the Work of a Neuron

*937J0075D Moscow ZHURNAL VYCHISLITELNOY MATEMATIKI I MATEMATICHESKOY FIZIKI in Russian Vol 32 No 12, Dec 92 pp 1972-1980*

[Article by A. N. Teterin, Izhevsk; UDC 519.7]

[Abstract] Rosenblatt's 1962 model of the perceptron and more complex later models from Minsky and Nilsson do not satisfactorily match current notions about the neuron derived from neural physiology. The recognition of a decrease in brightness, a moving edge, shadowing, and moving small objects occurs in structures which have little in common with the three-layer perceptron. Even viruses and amoebae are capable of classification. Algorithms show that two types of neuron operation are possible, one consisting of a body with one or more dendrites, or one output dendrite, which may branch (axons). In the first type, when the dendrites are "queried" in parallel, all dendrites form an "electrochemical medium" to compare values for one indicator. Its presence determines the goal of subsequent chemical changes, with a consideration of signals coming from the dendrites. This "chemical reaction" will be directed toward refining the classification object. In the second model, the neuron is "tuned" to reception of a signal from one dendrite and, depending on this signal, switches to some state in the path of a decision tree with querying of another dendrite. It is possible that in addition to an information signal a braking signal from another dendrite is needed to return the neuron to its initial state. Neither option rules out a learning mode (in a network of neurons). This article propsoes a theorem of separability of limited sets and theorems to verify the algorithms which are developed. These algorithms make it possible to express the method of approximation of a separating surface in terms of the division of sets into nonintersecting subsets and their projections in a space of lower dimension. This makes it possible to speak of a new geometric approach to the solution of classification problems. This method clarifies and proves the possibility, in principle, of one neuron classifying a sample represented by limited sets. References 5: 2 Russian, 3 Western.

NTIS
ATTN PROCESS 103
5285 PORT ROYAL RD
SPRINGFIELD VA

Foreign Broadcast Information Service (FBIS) and Joint Publications Research Service (JPRS) publications contain political, military, economic, environmental, and sociological news, commentary, and other information, as well as scientific and technical data and reports. All information has been obtained from foreign radio and television broadcasts, news agency transmissions, newspapers, books, and periodicals. Items generally are processed from the first or best available sources. It should not be inferred that they have been disseminated only in the medium, in the language, or to the area indicated. Items from foreign language sources are translated; those from English-language sources are transcribed. Except for excluding certain diacritics, FBIS renders personal names and place-names in accordance with the romanization systems approved for U.S. Government publications by the U.S. Board of Geographic Names.

Headlines, editorial reports, and material enclosed in brackets [ ] are supplied by FBIS/JPRS. Processing indicators such as [Text] or [Excerpts] in the first line of each item indicate how the information was processed from the original. Unfamiliar names rendered phonetically are enclosed in parentheses. Words or names preceded by a question mark and enclosed in parentheses were not clear from the original source but have been supplied as appropriate to the context. Other unattributed parenthetical notes within the body of an item originate with the source. Times within items are as given by the source. Passages in boldface or italics are as published.

## SUBSCRIPTION/PROCUREMENT INFORMATION

The FBIS DAILY REPORT contains current news and information and is published Monday through Friday in eight volumes: China, East Europe, Central Eurasia, East Asia, Near East & South Asia, Sub-Saharan Africa, Latin America, and West Europe. Supplements to the DAILY REPORTs may also be available periodically and will be distributed to regular DAILY REPORT subscribers. JPRS publications, which include approximately 50 regional, worldwide, and topical reports, generally contain less time-sensitive information and are published periodically.

Current DAILY REPORTs and JPRS publications are listed in *Government Reports Announcements* issued semimonthly by the National Technical Information Service (NTIS), 5285 Port Royal Road, Springfield, Virginia 22161 and the *Monthly Catalog of U.S. Government Publications* issued by the Superintendent of Documents, U.S. Government Printing Office, Washington, D.C. 20402.

The public may subscribe to either hardcover or microfiche versions of the DAILY REPORTs and JPRS publications through NTIS at the above address or by calling (703) 487-4630. Subscription rates will be provided by NTIS upon request. Subscriptions are available outside the United States from NTIS or appointed foreign dealers. New subscribers should expect a 30-day delay in receipt of the first issue.

U.S. Government offices may obtain subscriptions to the DAILY REPORTs or JPRS publications (hardcover or microfiche) at no charge through their sponsoring organizations. For additional information or assistance, call FBIS, (202) 338-6735,or write to P.O. Box 2604, Washington, D.C. 20013. Department of Defense consumers are required to submit requests through appropriate command validation channels to DIA, RTS-2C, Washington, D.C. 20301. (Telephone: (202) 373-3771, Autovon: 243-3771.)

Back issues or single copies of the DAILY REPORTs and JPRS publications are not available. Both the DAILY REPORTs and the JPRS publications are on file for public reference at the Library of Congress and at many Federal Depository Libraries. Reference copies may also be seen at many public and university libraries throughout the United States.